TRANSPORTATION RESEARCH
RECORD

No. 1431

Bridges, Other Structures, and Hydraulics and Hydrology; Soils, Geology, and Foundations

Culvert Distress and Failure Case Histories and Trenchless Technology

A peer-reviewed publication of the Transportation Research Board

TRANSPORTATION RESEARCH BOARD
NATIONAL RESEARCH COUNCIL

NATIONAL ACADEMY PRESS
WASHINGTON, D.C. 1994

Transportation Research Record 1431
ISSN 0361-1981
ISBN 0-309-05509-1
Price: $24.00

Subscriber Categories
IIC bridges, other structures, and hydraulics and hydrology
IIIA soils, geology, and foundations

Printed in the United States of America

Sponsorship of Transportation Research Record 1431

GROUP 2—DESIGN AND CONSTRUCTION OF TRANSPORTATION FACILITIES
Chairman: Charles T. Edson, Greenman Pederson, Inc.

Structures Section
Chairman: David B. Beal, New York State Department of Transportation

Committee on Culverts and Hydraulic Structures
Chairman: A. P. Moser, Utah State University
Kenneth J. Boedecker, Jr., Dennis L. Bunke, Bernard E. Butler, Darwin L. Christensen, Jeffrey Enyart, James B. Goddard, James J. Hill, Paige E. Johnson, Iraj I. Kaspar, Michael G. Katona, Carl E. Kurt, Bryan E. Little, Timothy J. McGrath, John J. Meyer, John C. Potter, Edward A. Rowe, Jr., James C. Schluter, David C. Thomas, Corwin L. Tracy, Robert P. Walker, Jr.

Soil Mechanics Section
Chairman: Michael G. Katona, Air Force Civil Engineering Laboratory

Committee on Subsurface Soil-Structure Interaction
Chairman: Thomas D. O'Rourke, Cornell University
Arnold Aronowitz, Timothy J. Beach, Jeffrey Enyart, Lester H. Gabriel, James B. Goddard, William A. Grottkau, John Owen Hurd, D. T. Iseley, Jey K. Jeyapalan, Michael G. Katona, Salah Y. Khayyat, Kenneth K. Kienow, Steven R. Kramer, John M. Kurdziel, Michael C. McVay, Samuel C. Musser, Priscilla P. Nelson, Thomas C. Sandford, Shad M. Sargand, James C. Schluter, Allen L. Sehn, Ernest T. Selig, Sunil Sharma, Mehdi S. Zarghamee

Geology and Properties of Earth Materials Section
Chairman: Robert D. Holtz, University of Washington

Committee on Soil and Rock Properties
Chairman: Mehmet T. Tumay, National Science Foundation
Robert C. Bachus, Dario Cardoso de Lima, Umakant Dash, Don J. De Groot, Eric C. Drumm, David J. Elton, Kenneth L. Fishman, Paul M. Griffin, Jr., Robert D. Holtz, An-Bin Huang, Mary E. Hynes, Steven L. Kramer, Rodney W. Lentz, Emir Jose Macari, Paul W. Mayne, Kenneth L. McManis, Victor A. Modeer, Jr., Priscilla P. Nelson, Peter G. Nicholson, Norman I. Norrish, Samuel G. Paikowsky, Sibel Pamukcu, Carl D. Rascoe, Kaare Senneset, Sunil Sharma, Timothy D. Stark

Transportation Research Board Staff
Robert E. Spicher, Director, Technical Activities
G. P. Jayaprakash, Engineer of Soils, Geology, and Foundations
Daniel W. Dearasaugh, Jr., Engineer of Design
Nancy A. Ackerman, Director, Reports and Editorial Services
Norman Solomon, Assistant Editor

Sponsorship is indicated by a footnote at the end of each paper. The organizational units, officers, and members are as of December 31, 1993.

Transportation Research Record 1431

Contents

Part 2—Trenchless Technology

Foreword

The 10 papers in this volume are presented in two groups. The first eight papers relate to culvert distress and failures, whereas the last two papers relate to trenchless technology.

The first group of papers presents information on structural distress or failures of in-service culverts. The papers describe failure mechanisms of culvert pipe materials that were identified from laboratory investigations.

The second group introduces the transportation industry to the existing and developing techniques for trenchless installation of utility systems. These papers provide information on performance evaluations that are based on case histories.

PART 1

Culvert Distress and Failures

Investigation of Large Deformations of a Corrugated Metal Pipe in Silty Soil

ALLEN L. SEHN AND J. MICHAEL DUNCAN

A 1.83-m-diameter corrugated metal culvert was installed as part of a flood control project in West Williamson, West Virginia. The culvert was installed in a 3.35-m-wide trench, and its crown was up to 9 m below grade. By the end of construction, the culvert experienced deformations that decreased its vertical diameter by as much as 15 percent and increased its horizontal diameter by as much as 10 percent. On the basis of the magnitude of the observed deformations, the owner decided to replace the culvert and to commission a study to determine the cause of the deformation of the pipe. The study was conducted in two phases. The first involved finite element analyses using soil properties based on conventional laboratory tests. The results indicated that the soils in the field must have been considerably more deformable than indicated by the results of the conventional tests. It seemed likely that the deformability of the in situ silty soils at the site might have been increased as a result of the vibratory compaction used to compact the soil around the culvert. The second phase involved finite element analyses using soil parameters from special vibratory loading tests on undisturbed specimens. The laboratory testing program indicated that vibratory loading can cause a significant reduction in the stiffness of silts. The finite element analyses indicated that such a loss of soil stiffness during construction could result in deformations similar to those observed in the field. On the basis of the laboratory test data and the agreement between the results of the analyses and the measured field deformations, it appears that some silts are subject to considerable softening under the influence of vibratory loads. In cases like the one described, where silts are subjected to static loads during vibration, deformations may be considerably larger than those that would occur under the influence of static loads without vibrations.

A corrugated metal pipe was installed as part of the West Williamson L.P.P. Pump Station in West Williamson, West Virginia. The 1.83-m-diameter culvert was constructed in a trench that extended as much as 9 m below the original ground surface into very soft to medium sandy and clayey silts. In some sections of the trench, steel sheet piling was required for stability of the trench walls, and a concrete mud slab was required at the bottom of the excavation over the full length of the culvert to stabilize the bottom of the trench during construction.

The culvert was installed between February 1984 and May 1985. In May 1985, before the installation of the culvert had been completed, large deformations of the culvert were noticed. The vertical diameter of the originally round pipe had decreased by as much as 27 cm, and the horizontal diameter had increased by as much as 19 cm. The deformations were so large that the culvert was considered to have failed, and it was replaced.

The investigation described in this paper was undertaken to determine the cause of the large deformations of the pipe. The investigation was conducted in two phases. In Phase I, finite element analyses were performed using soil properties derived from conventional laboratory tests performed by the Ohio River Division Laboratory of the Army Corps of Engineers. The results of these analyses indicated that the soils in the field had to be considerably more deformable than indicated by the results of the conventional test to explain the large deformations of the culvert. It seemed likely that the deformability of the natural soils at the site might have been increased by the vibrations associated with compaction of the soils around the pipe and removal of the piling at Section 4. Phase II of the investigation was undertaken to investigate this possibility.

Phase II of the study involved (*a*) obtaining undisturbed samples from the site, (*b*) conducting vibratory loading tests on these samples in the laboratory, and (*c*) performing additional finite element analyses using soil properties based on the new laboratory test results and simulating the earth pressures due to compaction in the analyses. Although the laboratory tests did not replicate exactly the type of vibratory loading imposed on the in situ silts, they showed that vibratory loading can have a deleterious effect on the stiffness and strength of silts. The Phase II studies indicated that the vibratory loading could have caused a considerable degree of disturbance in the silty soils. This disturbance is believed to have resulted in significant loss of stiffness of the natural soils adjacent to the trench, thus permitting the excessive deformation of the pipe during backfilling.

This experience affords an important lesson concerning the behavior of silty soils under the action of vibratory loadings. Although many of the details concerning this behavior are not understood yet, it seems clear that silty soils are subject to considerable softening under the action of vibratory loads. In cases where silts are subjected to static loads during vibration, deformations may be considerably larger than those that would occur under the influence of static loads without vibration.

SITE CONDITIONS

At the West Williamson L.P.P. Pump Station project, a 1.83-m-diameter corrugated metal culvert extends a distance of about 83 m from pump house to a manhole. Within 30 m of the manhole, sheet piling was used to support the trench walls. PZ-38 steel sheet piles were driven in interlocked pairs with a gap of about 30 cm between pairs. On the right side of the culvert, most of the sheet piles were removed when the trench was backfilled. Some of the sheet piles on the right side, and all of the sheet piles on the left side, were not removed.

Four sections across the trench and culvert were identified as representative of the varying conditions along the length of the culvert. At Sections 1 and 2, the backfill around the culvert was compacted against natural soils on the right side of the trench and

A. L. Sehn, Department of Civil Engineering, University of Akron, Akron, Ohio 44325-3905. J. M. Duncan, Department of Civil Engineering, Virginia Polytechnic Institute and State University, Blacksburg, Va. 24061-0105.

against previously placed and compacted fill on the left side of the trench. Section 1 is shown in Figure 1. Section 2 is similar to Section 1 except that random fill was used in place of the impervious fill used at Section 1, and the top of fill at Section 2 was approximately at an elevation of 196.7 m.

At Sections 3 and 4, the trench extended about 9 m below the top of natural ground, and sheet piles were used to support the trench walls. The cross section at Station 3 is shown in Figure 2. At this section, the PZ-38 piling remained in place on both sides of the culvert after backfilling. Section 4 is similar to Section 3 except that at Section 4 the piling on the right side of the culvert was removed during backfilling.

CULVERT PROPERTIES

The culvert was a 1.83-m-diameter corrugated steel circular pipe with 1.27-cm by 6.77-cm corrugations and 8 gauge (4.27-mm) metal thickness. Under normal conditions, this pipe would be considered adequate to withstand as much as 27 m of cover. The maximum cover thickness at the West Williamson project was only about 5 m. The pipe would also be considered capable of withstanding the H-20 highway loading with as little as 0.30 m of cover over the crown.

The 27-m maximum and 0.30-m minimum cover depths are based on analytical and empirical data and are consistent with standard practice. Typical specifications for design of such culverts require that deflections be no larger than 5 percent of the diameter, and standard designs meet this requirement under normal conditions of backfilling and loading. The deflections of the culvert at the West Williamson project were as much as 14 percent of the diameter. These large deformations indicate that the loading

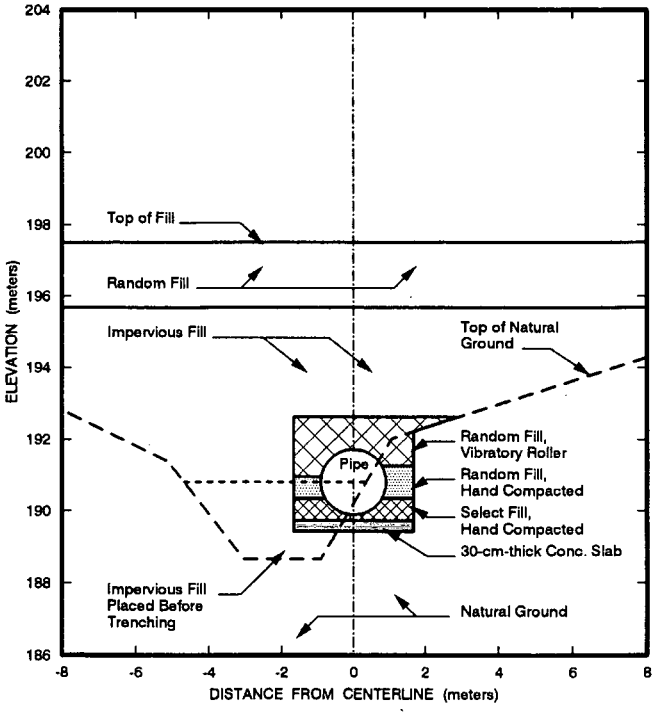

FIGURE 1 Section 1, West Williamson 1.83-m-diameter culvert.

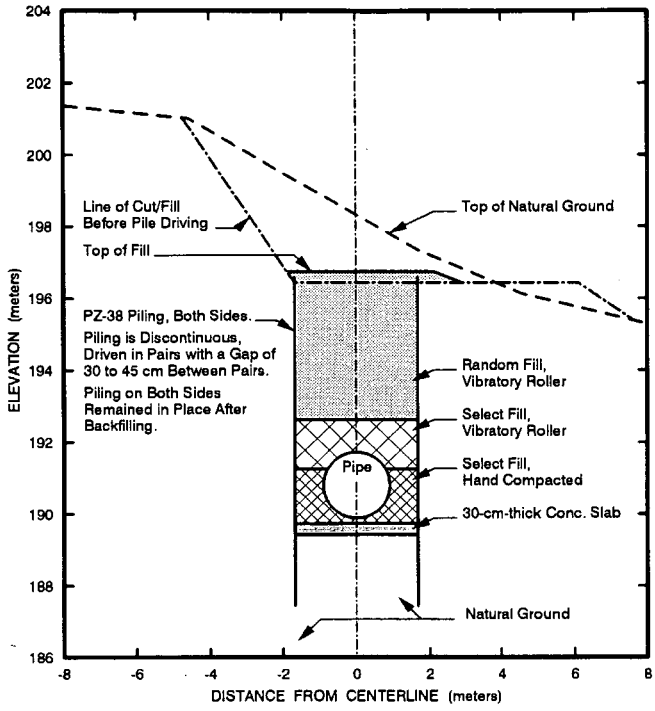

FIGURE 2 Section 3, West Williamson 1.83-m-diameter culvert.

on the pipe exceeded normally encountered loadings in some way or that the support provided by the surrounding soil was less effective than normal.

CULVERT DEFORMATIONS

The culvert deflections measured in May 1985 are summarized in Table 1. The vertical diameter of the culvert decreased as much as 26.7 cm, and the horizontal diameter increased as much as 19.0 cm. At Section 3, where the piling remained in place on both sides, the horizontal and vertical diameters changed by more than 15 cm. At Section 4, where the deformations were the largest, detailed measurements revealed a noticeable bias in the horizontal movements, with a shift of the culvert to the right. This bias may be due to the sloping ground surface or the removal of the piling on the right side at this section, or both.

SOIL CONDITIONS

From the ground surface down to approximately the elevation of the culvert, the natural soil is a dark brown sandy silt with low to medium plasticity and very soft to medium consistency. Underlying the brown silt is a gray to dark gray sandy silt with low plasticity and very soft to medium consistency. Observations of the position of the groundwater level in July 1985 indicated that the phreatic surface was about 0.5 m below the invert elevation of the culvert.

Plasticity, water content, and consistency data for the natural soils from the site are summarized in Table 2. A total of 14 samples of brown silt were classified. Of these, 10 were plastic and 4 were nonplastic. For most of the plastic samples, the plasticity

TABLE 1 Deflections of 1.83-m-Diameter Corrugated Metal Culvert at the West Williamson L.P.P. Pump Station (Measured May 1, 1985)

Station (meters)	Change in Diameter† (cm)		Note
	Vertical	Horizontal	
71.0	-6.4	-7.6	Pump plant
74.1	-14.0	2.5	
77.1	-10.2	7.6	
80.2	-17.8	7.6	Section #1
83.2	-16.5	8.9	
86.3	-20.3	10.2	
89.3	-11.4	10.2	
92.4	-20.3	10.2	
95.4	-17.8	11.4	
98.5	-16.5	8.9	Section #2
101.5	-6.4	3.8	
104.5	-6.4	1.3	
107.6	-1.3	1.3	Open end
--	--	--	No pipe
132.6	-15.2	15.2	Section #3
135.6	-15.2	15.2	
138.7	-22.9	17.8	
141.7	-20.3	15.2	
144.8	-26.7	19.1	Section #4
147.8	-17.8	15.2	
150.9	-20.3	8.9	
153.9	0.0	0.0	Manhole

† Based on initial horizontal and vertical diameters equal to 1.83 meters. Measurements were reported to the nearest 1.3 cm (0.5 inch).

data plotted above the A-line on the plasticity chart, resulting in a classification of CL according to the USCS. This classification may be somewhat misleading because the observed behavior of the soils was more "silty" than "clayey." The samples were less sticky than many CL materials and were more easily disturbed during trimming and handling. In addition, they contained layers of fine sands and nonplastic silts. Laboratory tests on four samples of the gray silt, summarized in Table 2, indicate that it is slightly less plastic than the overlying brown silt and that it has a slightly higher average water content in situ. The gray silt also contained layers of fine sand.

Even though many of the samples of the natural soils at this site are classified as clays of low plasticity, the writers believe that the engineering behavior of the soils differs appreciably from the be-

TABLE 2 Plasticity, Water Content, and Consistency of Brown and Gray Silt, West Williamson L.P.P. Pump Station (from Army Corps of Engineers, Ohio River Division Laboratory Tests)

Soil	Property	Minimum	Maximum	Average
Plastic Brown Silt (10 samples)	Liquid Limit	27	44	35
	Plastic Limit	17	25	22
	Plasticity Index	10	19	13
	Water Content	18.2	37.5	28.3
	Consistency	very soft to medium		
Non-Plastic Brown Silt (4 samples)	Water Content	18.2	27.4	23.9
Plastic Gray Silt (4 samples)	Liquid Limit	26	42	32
	Plastic Limit	17	28	21
	Plasticity Index	7	14	11
	Water Content	23.8	43.2	29.1
	Consistency	very soft to medium		

havior of typical CL soils and that they are in fact properly called silts. Accordingly, they are called silts throughout this paper.

The backfill materials are zoned as shown in Figures 1 and 2 and consist of the following:

- Select granular backfill (SM-SC): At all sections, this material was placed and hand-compacted beneath the invert and the haunches of the pipe. At Sections 3 and 4, this material also was compacted over the crown of the culvert using a small vibratory roller.
- Random backfill (CL): When used to fill over the crown of the pipe, this material was compacted using a small vibratory roller. When placed further from the pipe, it was compacted using a sheepsfoot roller.
- Impervious backfill (CL): This material was used at Section 1 and was compacted using a sheepsfoot roller.
- Unreinforced concrete: A 30.5-cm-thick unreinforced concrete slab was placed at the base of the excavation throughout the length of the culvert.

The concrete slab was used to provide a working surface. This was necessary because the slit at the bottom of the excavation was easily disturbed and quickly became muddy as it was traversed by men and machines.

PHASE INVESTIGATION

The first phase of the investigation began in September 1985. The culvert was inspected before removal, and soil samples were obtained for testing. Laboratory testing was done by the Ohio River Division Laboratory in Cincinnati. The results of the tests were used to obtain soil parameters for use in finite element analyses that were undertaken to determine the cause of the large deformations of the culvert.

Soil Properties for Phase I Finite Element Analyses

Several laboratory tests were performed on the natural soils and the compacted backfill materials to evaluate the strength and modulus parameters needed for the finite element analyses. The testing program included: (*a*) unconsolidated undrained (Q) triaxial tests on samples of the brown silt, (*b*) consolidated undrained (R) triaxial tests on samples of the gray silt, (*c*) consolidation tests on samples of the gray silt, (*d*) consolidated drained (S) triaxial tests on recompacted samples of the select backfill material, and (*e*) classification tests. Detailed test results are presented by Duncan and Sehn (*1*).

On the basis of the results of the laboratory consolidation tests and construction records, it seems likely that the gray silt would have sufficient time for dissipation of excess pore pressures and should be modeled using strength and stiffness parameters based on data from drained tests. With the data available during Phase I of the investigation, it was believed that the brown silt would probably experience undrained loading, and strength and stiffness parameters for this material were based on data from undrained laboratory tests.

No laboratory test data were available for the impervious backfill or the random backfill. For these materials, the parameters needed for the analyses were estimated on the basis of typical hyperbolic parameters for compacted soils reported by Duncan et al. (*2*). The typical values reported by Duncan et al. (*2*) are based on the analysis of several hundred triaxial tests on various types of soil and, in the absence of laboratory data, provide a reasonable means of estimating the hyperbolic parameters for a soil based on soil classification and relative compaction.

The finite element analyses performed during this investigation used hyperbolic stress-strain relationships (*2,3*) to model the nonlinear stress-strain and volume change behavior of soils. On the basis of the data available during Phase I, the parameters given in Table 3 were believed to represent the best estimate of the material properties. The information used to derive these parameter values is summarized below the table.

The deformations calculated using the parameters in Table 3 were considerably smaller than the observed deflections. For this reason, a second set of parameters, intended to represent the weakest and most deformable possible behavior of the soils at the site, was selected for use in further analyses. These properties are summarized in Table 4 and are termed "softened" soil properties. The properties selected for the backfill materials were chosen to represent the possible existence of very poorly compacted backfill adjacent to the culvert, even though none was found. The basis of selection of these parameter values is summarized below the table.

Phase I Finite Element Analyses Procedures

The Phase I finite element analyses simulate the placement of backfill around and above the culvert and the loadings imposed on the culvert by compaction equipment. In the finite element mesh used for the analyses, the culvert was represented by 12 beam elements, and the soil was represented by 156 two-dimensional quadrilateral or triangular elements. At sections where piling was present, the piling was modeled by beam elements. Each analysis began with the culvert in place and the backfill up to the springline. The analysis then proceeded in a number of steps to simulate placement of the remaining backfill and application of equipment loads over the culvert. The equipment loads were represented by vertical nodal point forces, and no changes were made in the soil properties to represent the effects of vibrations during compaction. This is one of the major differences between the Phase I and the Phase II analyses.

Cases Analyzed in Phase I

The finite element analyses performed during Phase I are summarized in Table 5. A total of 22 cases were analyzed. The cases include study of (*a*) the four sections described previously, (*b*) the effects of the strength and stiffness of the soil on the calculated deflections, (*c*) the influence of the concrete slab on the calculated deflections, and (*d*) the effects of equipment loading and backfill cover depth on the deflections and bending moments in the culvert.

Two types of equipment loads were investigated. One was a 15.4-Mg crawler tractor, represented by a load of 6.37 Mg per meter of length of the culvert. This load was divided among four nodes to represent the loads from two tracks of the tractor. In all cases, twice the actual load was applied to study the possible

effects of load concentration on the calculated values of deflection and bending moment in the culvert wall.

The second type of equipment loading was used to model the vibratory compactor used to compact the backfill around the culvert and was modeled by a line load of 2.23 kg per meter of length of culvert to represent its static weight. Studies by D'Appolonia et al. (*4*) indicate that the loads applied by vibratory compactors are higher than the static weight of the compactor. For the size of the compactor being modeled here, it is likely that loads as high as three to four times the static weight may be produced. Loads as high as five times the static weight were used in the analyses.

Results of the Phase I Analyses

The results of the Phase I analyses are summarized in Table 5. The largest calculated deflections (Anal. 7) were a 3.3-cm decrease in vertical diameter and a 3.8-cm increase in horizontal diameter. These deflections are for the full fill loading at Section 4 with the softened soil properties. The calculated deflections are only about one-sixth to one-seventh of the observed deflections. The heaviest roller load (Anal. 16) caused only about 2.3 cm of vertical deflection and 1.8 cm of horizontal deflection. Even if these values are added to those calculated in Anal. 7, the resulting deflections would be only about one-fourth as large as those measured.

The results of the Phase I analyses indicate that the finite element analyses did not adequately represent the field behavior. It was concluded that the silty soils in the field may have deformed under the combination of static and vibratory loads imposed on them during the backfilling operations or during the removal of piling at Section 4. Under the influence of the vibratory loads, the silts might have become even softer than modeled by the "softened" soil parameters. The Phase II investigation described subsequently was undertaken to investigate this possibility.

PHASE II INVESTIGATION

The objectives of the Phase II investigation were to develop a better understanding of the behavior of silts when they are subjected to static and vibratory loads and to use this information in

TABLE 3 First Estimate of Material Properties

Parameter	Material Number					
	1	2	3	4	5	6
	Gray Silt (ML)	Concrete (24 MPa)	Select Backfill (SM-SC)	Brown Silt (ML)	Random Backfill (CL) (RC = 90)	Imperv. Backfill (CL) (RC = 95)
K, modulus number	250	326,200	145	65	90	120
n, modulus exponent	0.75	0.00	0.60	0.00	0.45	0.45
R_f, failure ratio	0.70	0.55	0.45	0.75	0.70	0.70
ϕ_o, friction angle	35	40	44	0	30	30
$\Delta\phi$, friction increment	0	0	7	0	0	0
c (kPa), cohesion	0	11,975	0	115	9.6	14.4
K_b, bulk mod. number	230	155,300	100	1,150	80	110
m, bulk mod. exponent	0.5	0.0	0.5	0.0	0.2	0.2
ρ (Mg/m^3) density	2.08	2.40	2.24	2.00	2.00	2.08

Notes:
Material 1 - K, n, R_f, ϕ_o, $\Delta\phi$, c, and ρ from lab tests on "undisturbed" samples; K_b and m estimated.
Material 2 - Estimated properties for 24 MPa compressive strength concrete.
Material 3 - K, n, R_f, ϕ_o, $\Delta\phi$, and c from lab tests on lab-compacted samples; K_b and m estimated.
Material 4 - K, n, R_f, ϕ_o, $\Delta\phi$, c, and ρ from lab tests on "undisturbed" samples; K_b and m estimated.
Material 5 - Estimated density and properties.
Material 6 - Estimated density and properties.

conjunction with finite element analyses to explain the large deformations of the culvert.

To study the behavior of the silts, high-quality samples were obtained from the site using a 12.7-cm-diameter fixed-piston thin-walled sampling device. The samples were tested in the soil mechanics laboratory at Virginia Tech. On the basis of the information from the laboratory tests, soil parameters were selected for use in the analyses of the culvert. During the Phase II analyses, the effects of compaction were included in two ways. The effects of the vibrations during compaction were represented by using information from special vibratory loading triaxial tests in evaluating the soil properties, and the effects of compaction on the stresses and deformations were represented using the analytical methods developed by Duncan and Seed (*5*).

Phase II Laboratory Tests and Material Properties

Laboratory testing during Phase II of the investigation included (*a*) classification tests, (*b*) unconsolidated undrained (Q) triaxial tests on undisturbed specimens of the gray and brown silts, (*c*) unconsolidated undrained (Q) triaxial tests on remolded specimens of the brown silt, (*d*) a consolidation test on a specimen of the brown silt, and (*e*) special vibratory load triaxial tests on specimens of the gray silt. Details of the testing program and the test results were reported by Duncan and Sehn (*1*).

The purpose of the vibratory load triaxial tests was to investigate the effects of vibration loading on the strength and deformation characteristics of the natural silt soils from the project site. The vibratory triaxial testing consisted of (*a*) applying a static deviatoric stress, equal to about 50 percent of the expected undrained strength, at a constant rate of loading; (*b*) holding the load at the 50 percent level for about 5 min, (*c*) applying five sets of cyclic loading, with each set consisting of 10 cycles of loading between 25 and 75 percent of the expected undrained strength of the specimen, followed by 5 min at the 50 percent load level; and (*d*) constant rate of strain loading to failure or nearly to failure followed by observing creep behavior. The test sequence was not intended to model exactly the field loading conditions, but it provides a reasonable basis for estimating the effects of vibratory loading on the properties of the silts.

TABLE 4 Softened Material Properties

Parameter	Material Number					
	1	2	3	4	5	6
	Gray Silt (ML)	Concrete (24 MPa)	Select Backfill (SM-SC) (RC = 85)	Brown Silt (ML)	Random Backfill (CL) (RC = 85)	Imperv. Backfill (CL) (RC = 85)
K, modulus number	**120**	326,200	**100**	**32.5**	**60**	**60**
n, modulus exponent	0.75	0.00	0.60	0.00	0.45	0.45
R_f, failure ratio	0.70	0.55	**0.70**	0.75	0.70	0.70
ϕ_o, friction angle	35	40	**33**	0	30	30
$\Delta\phi$, friction increment	0	0	**0**	0	0	0
c (kPa), cohesion	0	11,975	**9.6**	115	**4.8**	**4.8**
K_b, bulk mod. number	**115**	155,300	**50**	**575**	**50**	**50**
m, bulk mod. exponent	0.5	0.0	0.5	0.0	0.2	0.2
ρ (Mg/m^3) density	2.08	2.40	2.24	2.00	2.00	2.08

Notes:

Material 1 - K and K_b reduced to 50% of first estimate, other values unchanged.
Material 2 - Estimated properties for 24 MPa compressive strength concrete.
Material 3 - Estimated density and properties.
Material 4 - K and K_b reduced to 50% of first estimate, other values unchanged.
Material 5 - Estimated density and properties.
Material 6 - Estimated density and properties.
Values that differ from the the first estimate presented in Table 3. are in boldface type.

TABLE 5 Summary of Phase I Finite Element Analyses and Results

Anal. No.	Sect. No.	Soil	Loading and Special Conditions	M_{max}/M_p	Change in Horizontal and Vertical Diameters (cm)			
					Calculated		Measured	
					h	v	h	v
1	1	First Est.	Fill loading only	0.136	1.3	1.5	7.6	17.8
2	2	First Est.	Fill loading only	0.015	1.5	1.3	8.9	16.5
3	3	First Est.	Fill loading only	0.300	2.0	2.3	15.2	15.2
4	4	First Est.	Fill loading only	0.300	2.0	2.3	19.0	26.7
5	1	Softened	Fill loading only	0.265	2.3	2.5	7.6	17.8
6	2	Softened	Fill loading only	0.226	2.0	2.3	8.9	16.5
7	4	Softened	Fill loading only	0.492	3.3	3.8	19.0	26.7
8	1	First Est.	Fill loading only, no conc. slab	0.207	1.5	1.8	7.6	17.8
9	2	First Est.	Fill loading only, no conc. slab	0.145	1.3	1.3	8.9	16.5
10	4	First Est.	Fill loading only, no conc. slab	0.380	2.8	3.0	19.0	26.7
11	4	First Est.	Crawler, 2X static, symmetric, 25 cm of cover	0.349	1.3	0.5	19.0	26.7
12	4	First Est.	Crawler, 2X static, load at right, 25 cm of cover	0.426	1.3	1.8	19.0	26.7
13	4	First Est.	Crawler, 2X static, symmetric load, no cover	0.345	1.3	0.5	19.0	26.7
14	4	First Est.	Crawler, 2X static, load at right, no cover	0.544	1.0	1.8	19.0	26.7
15	4	First Est.	Vib. Comp., 5X static, load at left, no cover	1.350	1.3	0.8	19.0	26.7
15	4	First Est.	Vib. Comp., 4X static, load at left, no cover	1.080	1.0	0.5	19.0	26.7
15	4	First Est.	Vib. Comp., 3X static, load at left, no cover	0.804	.08	0.3	19.0	26.7
15	4	First Est.	Vib. Comp., 2X static, load at left, no cover	0.530	.05	0.3	19.0	26.7
16	4	Softened	Vib. Comp., 5X static, load at left, no cover	1.520	2.3	1.8	19.0	26.7
16	4	Softened	Vib. Comp., 4X static, load at left, no cover	1.210	2.0	1.3	19.0	26.7
16	4	Softened	Vib. Comp., 3X static, load at left, no cover	0.903	1.5	1.0	19.0	26.7
16	4	Softened	Vib. Comp., 2X static, load at left, no cover	0.595	1.0	0.8	19.0	26.7

The results of a test on a specimen of the gray silt are shown in Figure 3. For this specimen, the axial strain increased from about 5.0 percent to about 7.8 percent during the vibratory loading portion of the test.

The results of another vibratory load triaxial test on the gray silt are shown in Figure 4. In this figure, the inset is an expanded view of the cyclic load portion of the test. For each cycle of load, there is an increment in the permanent deformation of the specimen, and although the incremental deformation caused by each successive load cycle decreases, the 50th load cycle still produced a small increment of permanent deformation.

On the basis of the results of the laboratory testing program, the idealized behavior shown in Figure 5 was developed. The solid lines show the general relationship between typical laboratory test

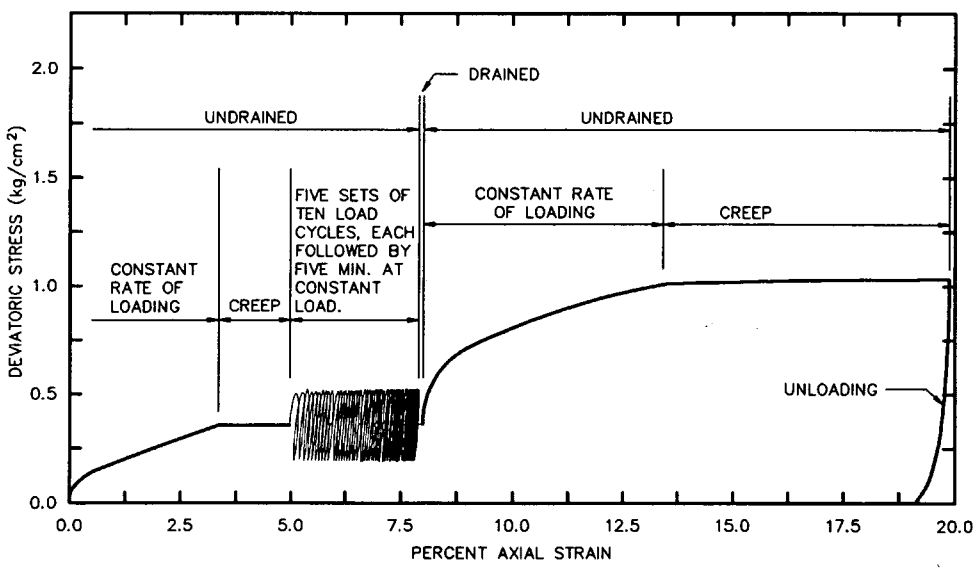

FIGURE 3 Vibratory loading triaxial test on gray silt, West Williamson L.P.P. Pump Station (Sample UD-101-S2-C1).

results from triaxial testing on undisturbed and disturbed or remolded specimens. The line from Point A to Point B represents the axial deformation of an undisturbed specimen due to the cyclic loading portion of a vibratory load triaxial test. The dashed stress-strain curve represents the idealized response of a specimen subjected to static and vibratory loads and is, qualitatively, the type of response used in the finite element analyses to model the effects of vibratory loads on the soil properties.

The material properties used for the Phase II finite element analyses are given in Table 6.

Phase II Finite Element Analyses Procedures

The Phase II finite element analyses modeled the conditions at Section 4, where the largest deformations occurred. The Phase I analyses showed that for a given set of soil properties, the calculated deformations at Sections 3 and 4 were always equal and were larger than those calculated for Sections 1 and 2. These relative magnitudes are consistent with the field measurements.

Since the Phase I analyses showed that the unsymmetric ground conditions were not a significant factor in the calculated distortion of the culvert, the Phase II analyses used a mesh representing one half of the culvert and the backfill. This models the culvert as symmetrical about the centerline and allows a finer mesh to be used. The culvert was represented by eight beam elements, and the soil was represented by 125 two-dimensional elements.

In addition to the factors considered in the Phase I investigation, the Phase II investigation includes the effects of compaction on the properties of the silt, as explained earlier, and the effects of earth pressures induced by compaction.

Analyses were performed using both Properties 4a and 4b in Table 6 to represent the brown silt.

Results of the Phase II Analyses

The results of the Phase II finite element analyses are summarized in Table 7. The calculated deflections for all of the cases are in reasonable agreement with the values measured at Section 4. For the three cases analyzed, the calculated vertical deflections ranged from 58 to 73 percent of the measured values, and the calculated horizontal deflections ranged from 80 to 96 percent of the measured horizontal deflection.

On the basis of the agreement between the measured and calculated deflections, it appears that the analyses performed reflect the actual behavior of the culvert. Since the major difference between the Phase I analyses and the Phase II analyses was in the simulation of the effects of vibration on the stiffness and strength of the silt, it seems clear that these effects played a major role in the large deformations suffered by the culvert during construction.

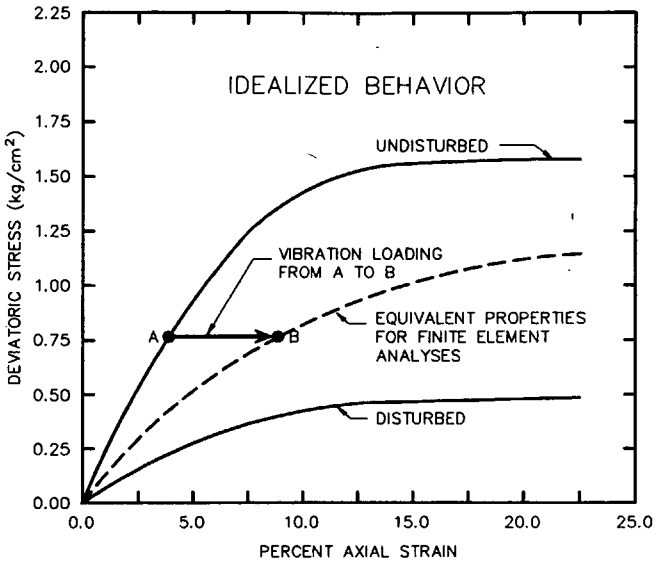

FIGURE 5 Effect of vibratory loading on stress-strain behavior.

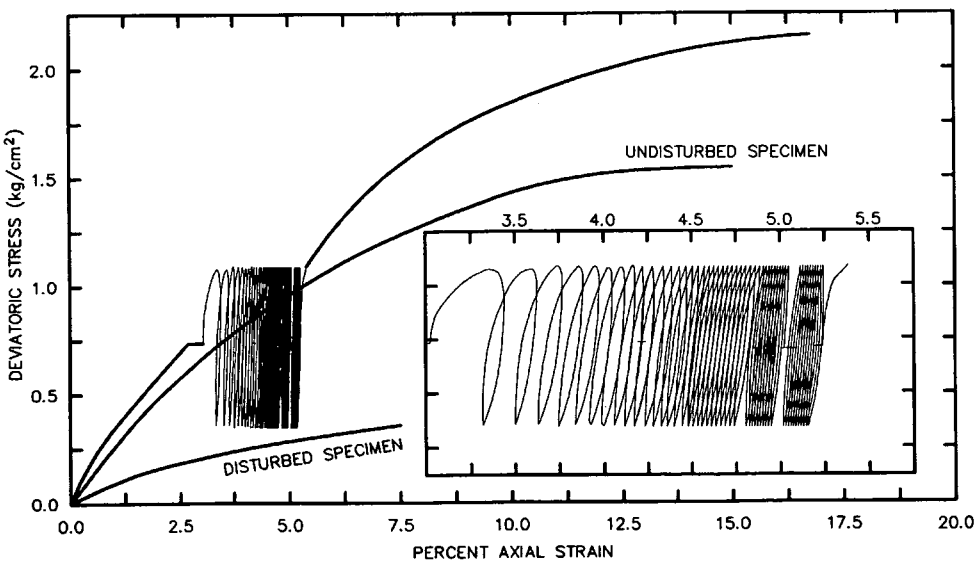

FIGURE 4 Vibratory loading triaxial test on gray silt, West Williamson L.P.P. Pump Station (Sample UD-100-S4-A3).

TABLE 6 Material Properties Used for Phase II Finite Element Analyses

Parameter	Material Number					
	1	2	3	4a	4b	5
	Gray Silt (ML)	Concrete (24 MPa)	Select Backfill (SM-SC)	Brown Silt (ML)	Brown Silt (ML)	Random Backfill (CL) (RC = 90)
K, modulus number	**14**	326,200	145	**50**	**30**	90
n, modulus exponent	**0.00**	0.00	0.60	0.00	0.00	0.45
R_f, failure ratio	**0.65**	0.55	0.45	**0.90**	**0.80**	0.70
ϕ_o, friction angle	**0**	40	44	0	0	30
$\Delta\phi$, friction increment	0	0	7	0	0	0
c (kPa), cohesion	**57**	11,975	0	**67**	**57**	9.6
K_b, bulk mod. number	**240**	155,300	100	**850**	**510**	80
m, bulk mod. exponent	**0.0**	0.0	0.5	0.0	0.0	0.2
ρ (Mg/m^3) density	2.08	2.40	2.24	2.00	2.00	2.00

Notes:
Values that differ from the the first estimate presented in Table 3 are in boldface type.

TABLE 7 Summary of Phase II Finite Element Analyses and Results

Anal. No.	Sect. No.	Loading and Special Conditions	$\frac{M_{max}}{M_p}$ Note 1	$\frac{M_{max}}{M_p}$ Note 2	Change in Horizontal and Vertical Diameters (cm)			
					Calculated		Measured	
					h	v	h	v
1	4	Compaction-induced earth pressures and loads, Brown silt as material 4a in Table 6	1.45	1.10	17.8	18.3	19.0	26.7
2	4	No compaction-induced earth pressures or loads, Brown silt as material 4a in Table 6	1.22	0.92	15.2	15.5	19.0	26.7
3	4	Compaction-induced earth pressures and loads, Brown silt as material 4b in Table 6	1.78	1.34	18.3	19.6	19.0	26.7

Note: 1) The values of M_{max}/M_p in this column are based on a moment required to form a plastic hinge in the culvert wall, M_p, of 4900 N-m per meter of culvert assuming that the culvert material has a yield stress of 276 MPa.

2) The values of M_{max}/M_p in this column are based on a moment required to form a plastic hinge in the culvert wall, M_p, of 6500 N-m per meter of culvert assuming that the culvert material has a yield stress of 366 MPa.

CONCLUSIONS

On the basis of the results of the investigation of the large deformations of the culvert at the West Williamson L.P.P. Pump Station, the following conclusions were reached:

1. Vibratory loading has a large effect on the undrained stress-stain properties of the silt at the site. The results of unconsolidated undrained triaxial tests with vibratory loading showed that the strains under undrained conditions were increased by about 80 percent by the application of 50 cycles of vibratory loading.
2. The deformations of the culvert calculated in the Phase II finite element analyses are in substantial agreement with the deformations measured in the field. Since the major difference between the Phase I and the Phase II analyses was the fact that the Phase II analyses modeled the effects of vibration on the stress-strain behavior of the silt, it appears that the effects of the vibration on the silt are the principal reason that the deflections of the culvert were so much larger than expected. As the silts deformed because of the vibratory loading, their deformation allowed the compacted backfill and the culvert to spread horizontally, leading to the large deformations that were measured in the field.
3. Since the silts at the West Williamson L.P.P. Pump Station site do not appear to be unusual, similar behavior can be expected in other cases where silts are subjected to vibratory loads.
4. The behavior of silts under vibratory loading is complex, and many aspects of their behavior are still not well understood. Research into the effects of stress conditions during vibration, the effects of vibration frequency, and the effects of the number of load cycles on the stress-strain behavior and strength of silts would be desirable.

ACKNOWLEDGMENTS

The authors acknowledge and appreciate the support of the Huntington District and the Ohio River Division of the U.S. Army Corps of Engineers throughout this investigation. In particular, the assistance and support of David Hammer, Russ Fondelier, Thomas Hugenberg, and Dan Boster are acknowledged. Thomas L. Brandon of Virginia Tech provided valuable suggestions and assistance during the laboratory testing program.

REFERENCES

1. Duncan, J. M., and A. L. Sehn, *Investigation of the Cause of Failure of the Corrugated Metal Culvert at the West Williamson L.P.P. Pump Station, West Williamson, West Virginia.* U.S. Army Corps of Engineers, Huntington, W. Va., 1987.
2. Duncan, J. M., P. Byrne, K. S. Wong, and P. Mabry. *Strength, Stress-Strain, and Bulk Modulus Parameters for Finite Element Analyses of Stresses and Movements in Soil Masses.* Geotechnical Engineering Report UCB/GT/80-01, University of California, Berkeley, 1980.
3. Duncan, J. M., and C. Y. Chang. Nonlinear Analysis of Stress and Strain in Soils. *JSMFD*, ASCE, Vol. 96, No. SM5, 1970, pp. 1629–1653.
4. D'Appolonia, D. J., R. V. Whitman, and E. D'Appolonia. Sand Compaction with Vibratory Rollers. *JSMFD*, ASCE, Vol. 96, No. SM1, Jan. 1969, pp. 263–284.
5. Duncan, J. M., and R. B. Seed. Compaction-Induced Earth Pressures Under K_0 Conditions. *JGED*, ASCE, Vol. 112, No. GT1, Jan. 1986, pp. 1–12.

Publication of this paper sponsored by Committee on Subsurface Soil-Structure Interaction.

Lessons Learned from Culvert Failures and Nonfailures

DAVID C. COWHERD AND IOAN J. CORDA

A study of the deformation (flattening) of a number of flexible metal culverts, including some that collapsed and some that did not, is presented. The deformation measurements of the various arcs of the structure were used to develop a procedure for evaluating the stability of buried flexible structures on the basis of the degree of "flattening." It is a well-known fact that a flexible, buried structure depends not only on its own strength and rigidity but also on the backfill around it for support. Consequently, the importance of good backfill is relatively well understood. It is not apparent, however, how much deformation can be tolerated before flattening becomes a problem. Two failures where measurements were made as the deformation progressed are analyzed, and the degree of flattening at which failure occurred is evaluated. Several structures that have experienced considerable flattening but have not failed are evaluated. In addition to evaluating the degree of flattening that can be tolerated before problems are experienced, a correlation was made between the type of backfill and the potential for structure flattening. Soils data were acquired from project files or subsurface investigations. Charts showing the effect of type of backfill, as well as width of a select backfill envelope on structure flattening, were prepared.

Corrugated metal culverts (and other types of buried structures) are made up of various arcs of circles (Figure 1 shows an arch pipe and the various parts of circles involved). The deflected shape of the pipe reflects the bending moment and plastic hinge formation that can lead to collapse. One method of measuring the degree of flattening of a circular arc is to measure the midordinates and the chord length of the various arcs (Figures 1 and 2). By comparing the actual measurement of the midordinates with the design midordinate, a degree of flattening can be calculated. This study used a calculation of percentage change in midordinate dimension as a measure of the degree of flatness. The percentage of midordinate flattening of the top arc was then evaluated for structures that failed and also for others that did not fail. The shape is an indicator of pressure distribution required for deformation stability. A table of recommendations based on percentage flattening of the top midordinate was developed. A computer program was prepared to analyze the structure's shape and make recommendations based on the amount of flattening defined as a percentage change in midordinate dimension from the design value.

MOVEMENTS IN STRUCTURES THAT FAILED

Two structures that collapsed because of excessive flattening and for which movement data were available were studied. The characteristics of the two structures are given in Table 1.

Bowser-Morner Associates, Inc., 4518 Taylorsville Road, P.O. Box 51, Dayton, Ohio 45401-0051.

Movement data from either direct measurements of midordinates or from hook elevation readings shortly before failure were available. The midordinate flattening was calculated for the structures directly or was indirectly estimated from hook readings. Table 2 gives the top midordinate measurements and the percentage change in dimensions at various stations throughout the structures.

On the basis of the midordinate flattening data, Structure 1 collapsed at a top midordinate flattening of about 48.3 percent, whereas Structure 2 collapsed at a flattening of about 29.5 percent. The data for Structure 1 were taken about 6 months before failure and represent relatively accurate amounts of flattening at the time of failure. The data from Structure 2 represent movements taken near the time of installation of the structure and not movements at failure. On the basis of the degree of compaction and the length of time before failure, it is estimated that the flattening of the midordinates for Structure 2 was about 50 percent at the time failure.

Both of these structures indicate that collapse occurred at a top midordinate flattening of from 45 to 55 percent.

MOVEMENTS IN STRUCTURES THAT DID NOT FAIL

Three long-span structures that experienced considerable flattening, and more than 900 pipe arch structures in Ohio (*1*) installed between 1951 and 1965 that experienced varying degrees of flattening, were studied. These "nonfailure" structures with large amounts of deformation (based on midordinate flattening) were studied to determine the reasonable limits of how flat a structure can become before problems are experienced. Data for the three long-span structures are presented in Table 3.

These structures were evaluated by measuring the actual midordinate and chords of the structures. The measured midordinates were compared with the design midordinate and the percentage of flattening was calculated as indicated in Table 4.

The data for these three structures indicate that midordinate flattening in various locations ranged from 21.2 to 47.4 percent. The structures did not collapse and hence provide some data on how flat (in terms of midordinate shortening) structures can become without collapsing. The 47.4 percent movement in Structure 1 was a very localized condition. Consequently, this station deformation is not a fair assessment of how much average movement can be tolerated. However, movements in the structure in other locations were as high as 21.2 percent. The movements of the top midordinates within the structures without failure varied from about 22 to about 34 percent.

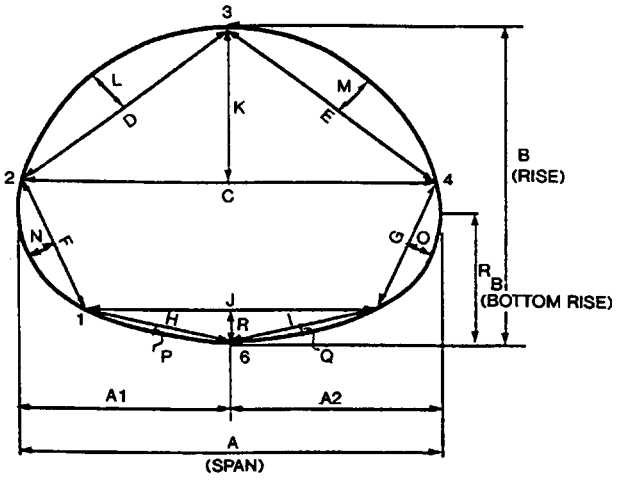

NOTES:

1. A THROUGH R REPRESENT DIMENSIONS MONITORED AT EACH STATION.
2. JOINT LOCATIONS 1,2,4 AND 5 REPRESENT CHANGE IN CURVATURE: 3 IS LOCATED EQUIDISTANT BETWEEN 2 AND 4; 6(IF ACCESSIBLE) IS LOCATED EQUIDISTANT BETWEEN 1 AND 5.
3. DIMENSIONS H,I,J,P,Q, AND R MAY NOT BE ACCESSIBLE FOR MEASUREMENT.

FIGURE 1 Typical measurements for pipe arch structure.

In addition, a study of some 900 pipe arch structures was undertaken in Ohio to evaluate the midordinate flattening. Fifty structures were selected from these 900 for a comprehensive evaluation of the top midordinates. The structures ranged in size from a span and rise of 1.8 by 1.4 m to 5.0 by 3.0 m. Most of the structures were installed between 1951 and 1965. The average age of the structures was 25 years. The percentage shortening of the three top midordinates for these structures is given in Table 5.

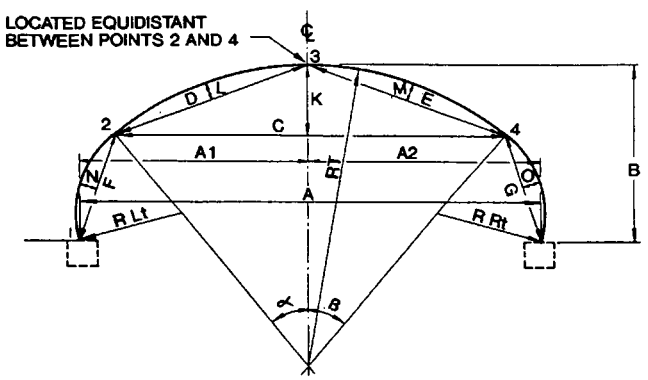

NOTES:

1. A THROUGH L REPRESENT DIMENSIONS MONITORED AT EACH STATION.
2. JOINT LOCATIONS 1 THROUGH 5 REPRESENT CHANGE IN RADIUS.
3. MIDORDINATES ARE: K,L,M,N,O

FIGURE 2 Typical measurements for low-profile arch structure.

One of these structures experienced a top midordinate flattening of 25 to 30 percent. Another experienced a flattening of 20 to 25 percent. Most had less than 20 percent movement. However, one of the structures sustained movements near 30 percent, and no failure occurred.

DEVELOPMENT OF RECOMMENDATIONS

The information from the evaluated structures, both those that failed and those that did not fail, was used to develop a table of movements versus recommendations on the basis of top midordinate reduction (see Table 6). The table was designed to yield recommendations for load derating to closure of a structure on the basis of top circumference flattening. The cessation of deformation with time is a measure of continuing satisfactory performance.

COMPUTER PROGRAM TO ANALYZE FLATTENING

A computer program (referred to as MULTSPAN) was developed to rapidly assess midordinate flattening within structures. A data base of all sizes and shapes of structures with the design values of midordinates, radii, and other pertinent information was prepared. One can enter the program with either the structure designation or with the design rise and span and type of structure, and the program will look up the design midordinates. The data base includes all the standard shapes and types of structures. If the design structure and the field measurements of midordinates and chords are entered, calculations of percentage change in dimension and recommendations (as indicated in Table 6) are output. Table 6 is built into the program, and the output is in the form of a recommendation. Table 7 gives sample input data for the MULTSPAN program. Table 8 gives the summary output data along with the recommendations.

The program will also print out the measurement data for each station measured along the pipe, along with the percentage of movements at each individual station. The program allows computation of the percentage of midordinate change as compared with a set of readings at any given time as opposed to the design data. This feature allows continued tracking of flattening of the structure so that an assessment can be made as to whether the pipe is likely to reach an ultimate failure point, and over what period of time.

TABLE 1 Characteristics of Failed Structures

Parameter	Structure No. 1	Structure No. 2
Type	Pear	Low Profile Arch
Span (m)	8.56	11.58
Rise (m)	8.48	7.16
Thickness (mm)	7.0	6.0
Corrugation (mm)	152 x 51	152 x 51
Fill Over Top (m)	2.74	1.83
Type of Backfill	"On-Site" Soil CL-ML	"On-Site" Soil SP-ML
Degree of Compaction	90%	59% - 89%
Foundation	Soft Soil	Relatively Hard Soil

1m = 3.281 feet
1mm = 0.039 inch

TABLE 2 Midordinate Flattening Before Failure

Structure Station	Top Center Chord (C) Design	Top Center Chord (C) Meas.	Top Midordinates (mm) Center (K) Design	Center (K) Meas.	Left (L) Design	Left (L) Meas.	Right (M) Design	Right (M) Meas.	Critical Diff. %
Structure #1:									
1	6258	6453	844	436	213	192	213	134	+48.3
2	6258	6453	844	463	213	165	213	128	+45.1
3	6258	6447	844	469	213	152	213	152	+44.4
4	6258	6459	844	491	213	165	213	146	+41.8
5	6258	6440	844	521	213	177	213	143	+38.2
6	6258	6428	844	536	213	192	213	140	+36.4
7	6258	6407	844	576	213	213	213	155	+27.6
8	6258	6376	844	680	213	201	213	165	+23.3
9	6258	6343	844	902	213	201	213	171	+20.5
10	6258	6325	844	802	213	219	213	149	+30.4
11	6258	6331	844	792	213	204	213	152	+29.0
Structure #2:									
0	9400	9403	1710	1547	442	466	442	311	+29.5
4	9400	9245	1710	1734	442	475	442	354	+19.9
9	9400	9403	1710	1573	442	405	442	372	+15.7

1mm = 0.039 inches

PREDICTIONS OF MOVEMENT OF STRUCTURE BASED ON BACKFILL DATA

A companion computer program, SOILEVAL, was developed (*2*) to predict the degree of flattening of a structure on the basis of backfill data. For several of the structures studied, soils data were either available or borings were made to obtain soils data. This information was used to correlate the type of soil and degree of compaction with percentage flattening of the structures.

The form of the equation used in the SOILEVAL model to evaluate soil-structure interaction is

$$\Delta y = \frac{A\ \Delta W\ \mathrm{SF}}{I/r_a^3 + B(E'/E)} \leq F_s\ \Delta W\ \mathrm{SF} \qquad (1)$$

where

Δy = maximum expected deflection at the crown of the structure;
F_s = factor of safety to take into account the variability of soil properties, equal to 1.5;
ΔW = potential horizontal movement of one side of the structure due to compression of both backfill and original soil under the stress generated by the pipe;
SF = shape factor, defined as the ratio between the vertical displacement of the structure at the crown and the corresponding maximum movement on one side of the structure;
I = moment of inertia of pipe wall;
E'/E = ratio of modulus of soil and modulus of elasticity of pipe material;
r_a = average radius of the structure, equal to the span plus the rise divided by 4; and
A, B = empirical coefficients statistically determined from field measurements.

The potential horizontal displacement of the structure due to soil compressibility (without any restriction due to structure stiffness) is obtained by summing the displacement calculated for each incremental layer on one side of the pipe. As in the calculation of shallow foundation settlement, the summation is extended to a distance at which the additional stress in the soil generated by the structure is less than 20 percent of the horizontal stress corresponding to the overburden pressure, or to a maximum distance of 2.5 times the rise dimension, whichever is less. The following equations are used:

$$\Delta W = \sum [W\ \Delta e/(1 + e_o)] \qquad (2)$$

TABLE 3 Characteristics of Nonfailed Structures

Parameter	Structure No. 1	2	3
Type	Pipe-Arch	Aluminum Pipe Arch	Low Profile Arch
Span (m)	3.25	3.94	11.56
Rise (m)	2.10	2.29	4.75
Thickness (mm)	3.5	2.5	6.0
Corrugation (mm)	152 x 51	127 x 25	152 x 51
Fill Over Top (m)	7.5	3.4	1.0
Type of Backfill	Cohesive Soil	Silty Clay (ML)	Silty Sand with Gravel (SM)
Degree of Compaction	95%	90%	90%
Foundation	Clayey Sand	Silty Clay	Silty Clay

1m = 3.281 feet
1mm = 0.039 inch

$$\Delta e = C_c \log \frac{K_o P'_v + \alpha P_h}{K_o P'_v} \quad (3)$$

$$\alpha = 10^{(-0.45d/R)} \quad (4)$$

$$P_h = P_v r_t / r_s \quad (5)$$

where

W = initial width of an incremental layer;
Δe = potential decrease in void ratio;
e_o = initial void ratio, not affected by the supplementary pressure induced by the structure;
C_c = compression index of the soil (backfill or original soil beyond the backfill);
K_o = coefficient of earth pressure at rest;
P'_v = effective overburden pressure at the level of calculation (i.e., approximately in the middle of the loaded area by the structure);
α = influence coefficient at the distance from the structure corresponding to the middle of a given incremental layer;
P_h = supplementary pressure on the side plates of the structure induced by the downward movement of the structure's crown;
P_v = total vertical pressure due to the soil dead load on the top of the structure, considered approximately equal to the unit weight of the backfill times the depth of cover;
R = rise of the structure;
r_t = top radius of the structure; and
r_s = side radius of the structure.

TABLE 4 Percentage of Midordinate Flattening of Nonfailed Structures

Structure Station	Midordinate Deformation (mm)								
	Center (K)			Left (L)			Right (M)		
	Design	Meas.	% Diff	Design	Meas	% Diff	Design	Meas.	% Diff
Structure #1:									
0+00	1366	1335	+2.4	387	329	+14.7	387	357	+8.1
0+20	1366	1335	+2.4	387	357	+8.1	387	363	+6.4
0+40	1366	1320	+3.3	387	335	+13.0	387	363	+6.4
0+60	1366	1320	+3.3	387	329	+14.7	387	363	+6.4
0+80	1366	1320	+3.3	387	335	+13.0	387	357	+8.1
1+00	1366	1320	+3.3	387	344	+11.4	387	351	+9.7
1+20	1366	1320	+3.3	387	344	+11.4	387	357	+8.1
1+40	1366	1335	+2.4	387	317	+17.9	387	344	+11.4
1+60	1366	1335	+2.4	387	344	+11.4	387	351	+9.7
1+70	1366	1195	+12.6	387	204	+47.4	387	451	-16.5
1+80	1366	1295	+5.2	387	305	+21.2	387	344	+11.4
2+00	1366	1295	+5.2	387	317	+17.9	387	351	+9.7
2+20	1366	1265	+7.5	387	317	+17.9	387	344	+11.4
2+40	1366	1259	+7.9	387	317	+17.9	387	351	+9.7
2+60	1366	1237	+9.3	387	305	+21.2	387	344	+11.4
2+80	1366	1259	+7.9	387	311	+19.6	387	344	+11.4
3+00	1366	1265	+7.5	387	317	+17.9	387	344	+11.4
3+20	1366	1259	+7.9	387	317	+17.9	387	329	+14.7
3+40	1366	1271	+7.0	387	305	+21.2	387	329	+14.7
3+60	1366	1277	+6.5	387	305	+21.2	387	329	+14.7
3+80	1366	1277	+6.5	387	344	+11.0	387	305	+21.2
Structure #2:									
3+75	594	549	+8.0	152	165	-7.3	152	137	+10.6
4+00	594	539	+9.0	152	162	-5.3	152	143	+6.6
4+25	594	530	+10.5	152	174	-13.3	152	122	+20.5
4+50	594	436	+21.9	152	192	-25.2	152	137	+10.6
4+75	594	424	+28.5	152	171	-11.3	152	101	+34.4
5+00	594	585	+1.3	152	125	+18.5	152	137	+10.6
5+25	594	564	+4.9	152	186	-21.3	152	131	+14.5
5+50	594	558	+5.9	152	168	-9.3	152	128	+16.5
5+75	594	582	+1.8	152	189	-23.2	152	134	+12.5
6+00	594	591	+0.3	152	180	-17.3	152	137	+10.6
6+25	594	579	+2.3	152	192	-25.2	152	134	+12.5
6+50	594	594	-0.3	152	162	-5.3	152	149	+2.6
6+75	594	573	+3.3	152	183	-19.3	152	125	+18.5
7+00	594	555	+6.4	152	189	-23.2	152	119	+22.5
7+25	594	527	+11.1	152	171	-11.3	152	116	+24.5
7+44	594	521	+12.1	152	189	-23.2	152	125	+18.5
Structure #3:									
1+00	1670	1533	+8.2	430	497	-15.4	430	469	-9.0
1+12	1670	1518	+9.1	430	402	+6.5	430	442	-2.7
1+24	1670	1542	+7.7	430	375	+12.9	430	418	+3.0
1+36	1670	1503	+10.0	430	375	+12.9	430	393	+8.7
1+48	1670	1567	+6.2	430	369	+14.3	430	411	+4.4
1+60	1670	1579	+5.5	430	335	+22.1	430	408	+5.1
1+72	1670	1585	+5.1	430	387	+10.1	430	424	+1.6
1+84	1670	1579	+5.5	430	384	+10.8	430	442	-2.7
1+96	1670	1564	+6.4	430	418	+3.0	430	454	-5.5

NOTE: + = Flattening
- = Peaking
1mm = 0.039 inch

TABLE 5 Percentage Shortening of 50 Pipe Arches

Percentage Shortening of Midordinate %	# of Structures
0-10	35
10-15	9
15-20	4
20-25	1
25-30	1

A number of soil properties must be known or properly estimated, both for the backfill and the original soil. They are e_o, C_c, K_o, and the unit weight. The program gives the option of entering these as input data or estimating them on the basis of various levels of knowledge of soil conditions.

Potential backfill and original soils have been divided into seven categories, and the geotechnical parameters have been estimated for each category. These parameters versus soil type have been built into the program so that by choosing a soil category on the basis of simplified soils data, the appropriate geotechnical indexes are automatically used. If more precise data are available, the program allows the direct input of the soil parameters. Table 9 gives the soil categories and corresponding C_c values built into the model.

These soil types were incorporated into the SOILEVAL computer program (*3*) with appropriate shape factors for the structure. The program can predict the degree of flattening that may occur once a type of backfill and compaction are determined. The program was set up to use actual compaction data, standard penetration test data, actual consolidation data, or a default soil (No. 1–7) to analyze the structure. The SOILEVAL program was then tested on various structures for which the vertical movement was known. Computed movements, using the program, were compared with actual movements. Table 10 gives a comparison of the measured vertical movement versus the movement computed by the SOILEVAL program.

Table 10 indicates that relatively close correlation was obtained. In this study, information from previous borings was available, borings were made as part of the study, or initial data were available to categorize the backfill soil and the original soil outside the backfill envelope. The computed and actual values show relatively good correlation, indicating that the SOILEVAL program yields useful information on predicted flattening of structures as a function of backfill condition.

The program can be used to evaluate an in-place structure experiencing movement or various types of possible backfill (being considered during design) to predict the degree of flattening that will occur if a certain type of backfill is used. On the basis of the SOILEVAL program, curves of predicted movement versus degree of compaction for various types of backfill material were prepared (see Figure 3).

Figure 3 allows a quick review of the expected vertical deflection (also in terms of percent change in top midordinate dimension) for various types of backfill at various degrees of compaction for a particular structure.

The material outside the select backfill envelope immediately around the structure also contributes to flattening of the structure by allowing the sides of the structure to move out and the top to move down. SOILEVAL was used to develop graphs of the degree of midordinate flattening on the basis of the type of material outside the select backfill envelope. The soil outside the select backfill may be original soil or embankment fill. Figure 4 was prepared on the basis of the geometry of the selected backfill on one side of the pipe and the type of material for the original soil. The typical culvert installation is shown in Figure 5.

These charts provide a quick reference value for evaluating the type of backfill, the degree of compaction, the width of any select backfill, and the effect of various types of material outside the select backfill on structure movement.

CONCLUSIONS

The technique of measuring midordinates and the evaluation of percentage changes in midordinate dimension of various arcs of the structure provide a relatively simple method of evaluating in-place distortion of flexible metal structures. The allowable midordinate deflections and associated recommendations take into account the failure and nonfailure of actual structures. The recommendations provide a factor of safety in the evaluation process. The overall safety of the structures is generally a function

TABLE 6 Percentage Midordinate Reduction and Remedial Action

Midordinate % Reduction	Depth of Cover (m)	Recommended Action
<15	Any	No action required.
15 - 20	Over 1.8	No action required.
15 - 20	Under 1.8	Monitor on 6-month interval.
20 - 25	Over 1.8	Reduce legal load to 90% of H-20 and monitor on 6-month intervals.
20 - 25	Under 1.8	Reduce legal load to 75% of H-20 and monitor on 6-month intervals.
25 - 30	Over 1.8	Reduce load to 75% of H-20 and monitor on 6-month intervals
25 - 30	0.9 - 1.8	Reduce load to 50% of H-20 and monitor on 6-month intervals.
25 - 30	Under 0.9	Reduce load to 50% of H-20 and do detailed analysis.*
>30	Any	Close road until detailed analysis is done.

*NOTE: Detailed analysis to include soil borings to determine if additional movement of the structure can be expected.

1m = 3.281 feet

TABLE 7 MULTSPAN Sample Input of Chords and Midordinates

	Chords (mm)							
	Top			Side		Corner		Bottom
Station	Center	Left	Right	Left	Right	Left	Right	Center
	(C)	(D)	(E)	(F)	(G)	(H)	(I)	(J)
5	3283	2124	2091	613	610	1326	1341	2649
6	3316	2097	2082	610	610	1332	1338	2655
7	3289	2091	2082	613	613	1323	1335	2649

	Midordinates (mm)							
	Top			Side		Corner		Bottom
Station	Center	Left	Right	Left	Right	Left	Right	Center
	(K)	(L)	(M)	(N)	(O)	(P)	(Q)	(R)
5	1305	381	405	146	143	49	58	110
6	1286	372	372	149	146	52	55	88
7	1301	378	381	143	149	55	58	98

1mm = 0.039 inch

TABLE 8 Summary of Output Data

	Design Value	Avg. Value	Max. At Value Sta.	Min. At Value Sta.	Critical % Diff.
Midordinates (mm)	*				
Top Center	1527	1451	1516	1397	+8.64
Top Left	436	442	473	400	+8.23
Top Right	436	418	446	394	+9.63
Radii (mm)					
Top Center	1783	1859	1909	1760	-7.00
Top Left	1783	1756	1933	1657	-8.41
Top Right	1783	1759	1845	1625	-3.45

* Midordinate design values are computed based on design parameters or estimated based on geometric relationships. A value of zero indicates that a suitable midordinate value could not be computed because the field measurements could not be taken at the major breaks in curvature. Plus means decrease in midordinates or radius. A decrease in midordinates is considered critical.

Recommendation: Pipe shows no serious deformations - no top midordinate deflection is greater than 15% - maintain normal inspection frequency.

1mm = 0.039 inch

TABLE 9 Default Soil Types

Soil Category	Type of Soil	Class (Based on ASTM D-2487 Classification)	C_c Average Values
1	Gravel, Crushed Stone	GW, GP & Assimilated	0.01
2	Silty/Clayey Gravel	GM GC	0.02
3	Well-Graded Sand	SW	0.02
4	Poorly Graded Sand	SP	0.03
5	Silty/Clayey Sand	SM, SC	0.08
6	Silty Soils	ML, MH	0.10
7 (L)	Clayey Soils (Lean)	CL ($W_L < 50$)	0.18
7 (F)	Clayey Soils (Fat)	CH ($W_L \geq 50$)	0.35

TABLE 10 Measured Vertical Movement Versus Computed Movement

Structure No.	Soil Category		Computed Movement (mm)-Horizontal			Measured Vert. Move. (mm)
	Backfill	Original Soil	Backfill	Original Soil	Vertical (total)	
1	7	Rock	152	0	304	286
2	7	Rock	86	0	372	424
3	1	VII	24	155	357	277
4	5	Old Bridge	125	0	250	250
5	4	Rock	06	0	12	06

1mm = 0.039 inch

of the degree of flatness of the various arcs of the structure, not of the ring compression factor of safety. Most structures will in fact show a relatively high factor of safety on the basis of ring compression, although the degree of flatness may be high. This technique, therefore, provides a reasonable and simple method of evaluating structures as to their safety.

The SOILEVAL program allows an evaluation of the potential for additional movement of structures given the soil backfill type and degree of compaction. It also provides a design tool for evaluation of various types of backfill and degree of compaction for prediction of percentage of flattening of the midordinates of the structure.

Both MULTSPAN and SOILEVAL allow an approximate prediction of the life of a structure on the basis of degree of flattening. MULTSPAN accomplishes this by projecting movements on the basis of successive movement readings. One set of readings is compared with the next set some period of time later. When several readings have been made and the amount of flattening over time has been established, a curve of flattening versus time can be plotted and predictions made of when flattening will become a problem. SOILEVAL allows a computation of the time versus flattening and also allows an estimation of the time over which flattening may become a problem. Current methods of predicting structure life on the basis of metal thickness, corrosivity of backfill, degree of corrosion, and metal loss do not take into account problems due to flattening of the arc of the structure. This analytical/empirical computer program, therefore, allows a prediction of the life of the structure on the basis of degree of flattening of the structure with time.

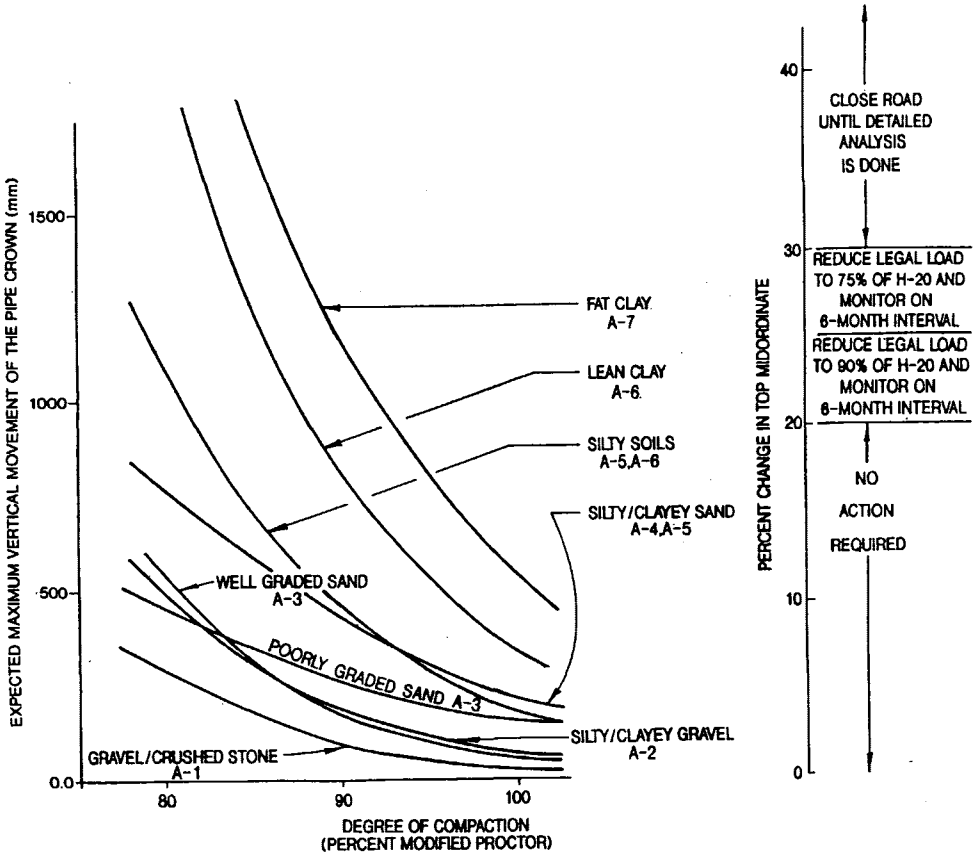

FIGURE 3 Effects of type of backfill at various degrees of compaction.

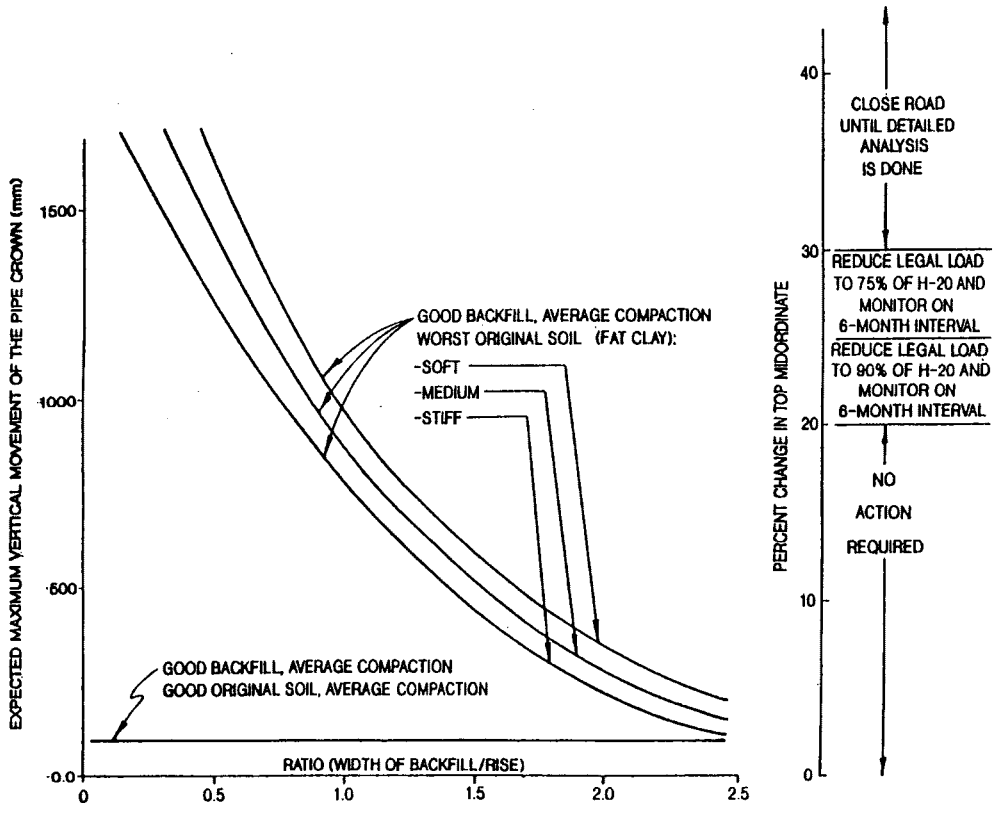

FIGURE 4 Effect of select backfill width.

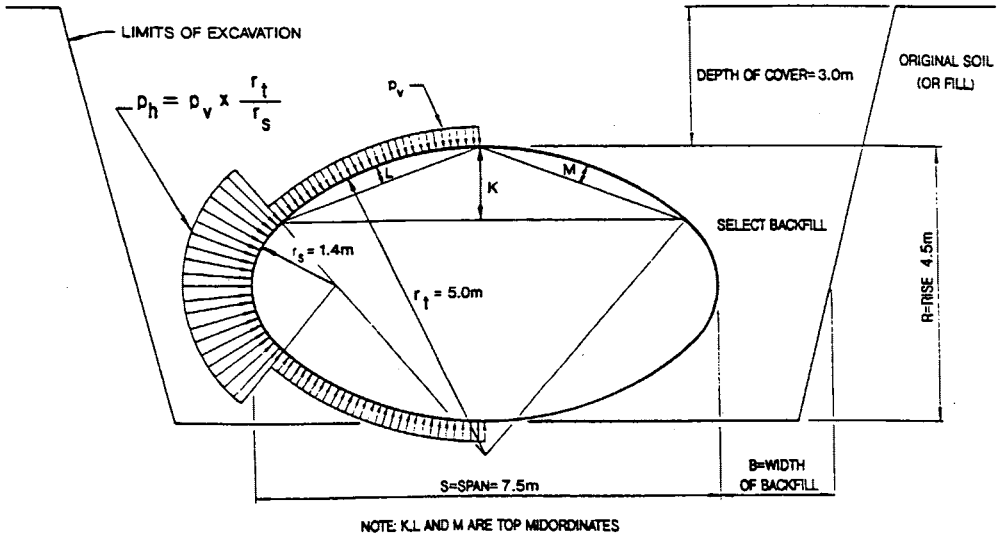

FIGURE 5 Typical culvert installation—trench condition.

The analysis procedure allows an evaluation of potential remedial action for the structure as opposed to removal of the structure. The ability of the structure to carry and transmit load is a function of the radius of the arc and the various section moduli of the corrugated metal plates throughout the structure. The MULTSPAN program calculates the radius of the arcs once the chord and midordinate are calculated. When the radius of the arc is known, the appropriate section moduli for the amount of fill over the structure can be calculated. The structure can then be structurally reinforced to provide the appropriate section modulus for the modified radius or arc of the structure.

REFERENCES

1. Degler, G. H., D. C. Cowherd, and J. O. Hurd. Analysis of Visual Field Inspection Data of 900 Pipe-Arch Structures. In *Transportation Research Record 1191*, TRB, National Research Council, Washington, D.C., 1988, pp. 46–56.
2. Cowherd, D. C., and V. G. Perlea. A Method for Evaluating and Projecting Future Movement of In Situ Pipes. *Proc., First National Conference on Flexible Pipes,* Columbus, Ohio, 1990, pp. 39–50.
3. Perlea, V. G. Predicting Performance of Large-Diameter Buried Flexible Pipes: Learning from Case Histories (discussion). *Proc., Second International Conference on Case Histories in Geotechnical Engineering,* Vol. 2, University of Missouri-Rolla, St. Louis, 1989, pp. 1417–1420.

Publication of this paper sponsored by Committee on Subsurface Soil-Structure Interaction.

Pipe Failure Caused by Improper Groundwater Control

ERNEST T. SELIG AND TIMOTHY J. MCGRATH

A sewer collection system installed in a Middle Eastern city incorporated 11 km of fiberglass reinforced plastic mortar (RPM) sewer pipe 500 to 1100 mm in diameter. A short time after installation it was discovered that the pipelines were highly deflected and that some pipe was cracked at the crown. Subsequently a number of the cracked pipes failed, causing large craters and collapse of the roadway. Inspections showed that more than one-half of the RPM pipe system was deflected well over 5 percent, the limit imposed by the contract documents, with some portions deflected up to about 20 percent of their original diameter, and that numerous sections of pipe were cracked at the crown. Investigation of the conditions at the sites showed that the deflections and failures resulted mainly from inadequate control of the groundwater during construction and improper attention to the grading of the crushed stone pipe embedment relative to the natural sand materials against which it was placed. During construction the dewatering system did not maintain the groundwater level below the trench bottom, resulting in water washing into the trench through open sheeting joints, carrying sand with it and leaving cavities behind the sheeting. When the sheeting was pulled, the stone embedment lost support and moved into the cavities, allowing high pipe deflections. Migration of fines from the native sands into the voids in the open graded stone is also believed to have contributed to the loss of pipe support gradually after construction.

A sewer collection system designed for a Middle Eastern city was installed between 1979 and 1981. Some 11 km of fiberglass reinforced plastic mortar (RPM) sewer pipe, between 500 and 1100 mm in diameter, was incorporated into the system. Just before the lines were put into service, several leaks were discovered in the network. Investigations showed that a large portion of the RPM pipe system was deflected well over the 5 percent limit set by the contract documents, with some portions deflected up to about 20 percent of their original diameter, and that numerous pipes had cracked at the crown. Subsequently some pipes collapsed, causing failure of the roadway above the pipe. The high deflections were surprising because the pipe trenches were backfilled with crushed stone, which normally provides excellent pipe support with minimal compactive effort. Information related to geotechnical aspects of the installation that resulted in the high deflections is presented in this paper. Performance of the pipe and a detailed discussion of the failure mechanism has been presented previously (*1*).

BACKGROUND

The sewer collection system was designed as a gravity flow system. Because the city was on the coast, there was a natural upward grade of the land surface away from the coast. The system design took advantage of the natural grade by conducting flow downhill to pumping plants near the coast, where the effluent was pumped via pressure lines to a treatment plant. This resulted in a relatively constant depth of burial for the entire system of about 3 to 4 m.

The native soils were predominantly sands that allow relatively free flow of groundwater. Sieve analysis during the investigation showed the material to be nearly 100 percent between 2 mm (No. 10 sieve) and 0.075 mm (No. 200 sieve), making it a medium to fine sand. The water table was within 0.2 m of the ground surface at the coast and gradually became deeper with increasing distance from the coast, where the elevation was higher. It was below the pipe invert at the highest parts of the system. In some of the higher regions the sand was underlain by limestone, which formed the walls and bottom of the pipe trench.

RPM pipe was selected for the large-diameter portions of the system because of its good performance in corrosive environments. The ground conditions were very severe, and traditional types of pipe materials had not performed well in the past. Eleven km of pipe, between 500 and 1100 mm in diameter, was installed. The RPM had a pipe stiffness (load per unit deflection or $EI/0.149R^3$ per ASTM D2412) of about 100 kN/m/m. The contractor was to install the pipe with deflections less than 3 percent of the original diameter at the time of installation, and 5 percent long term.

The system was originally installed with no indication of problems; however, when manholes were being cleaned just before the lines were put into service, it was noted that there was water in the system, which should have been dry. An investigation made as a result of that finding showed that about one-half of the RPM pipe sections were deflected more than 5 percent and some sections more than 15 percent, and that 17 pipes were cracked in the crown. Later, pipe collapses occurred in which the top half of the pipe caved in. Since the water table was high, the groundwater would flow into the pipe and carry off the soil, in turn allowing more soil to flow into the pipe and be carried off. The final result was similar to a large sinkhole. The deflections tended to be highest nearest the coast, where the water table was highest, and lowest at the higher elevations, where the water table was deeper. The pipe failures occurred in the regions where the highest deflections were measured.

The pipe cracks and subsequent collapses were found to be the result of strain corrosion that occurred because of the excessive deflection levels. The investigation focused on the causes of the high deflection.

CONSTRUCTION METHODS

Project specifications called for the pipe to be installed in open trenches. The required trench width was 4/3 times the diameter

E. T. Selig, Department of Civil and Environmental Engineering, Marston Hall, Box 35205, University of Massachusetts, Amherst, Mass. 01003-5205. T. J. McGrath, Simpson Gumpertz & Heger, Inc., 297 Broadway, Arlington, Mass. 02174.

plus 45 cm. This provides a backfill width of 560 mm at each side of a 500-mm pipe and a width of 960 mm at each side of an 1100-mm pipe. Pipe backfill was to be crushed stone from a minimum of 1/6 times the diameter or 15 cm below the pipe as bedding up to a height above the invert of 0.7 times the pipe diameter. The requirement for shoring was anticipated by the designer, but all shoring used below 30 cm above the top of the pipe was required to be left in place. However, because of the expense that this involved, during the construction phase the contractor requested and was granted permission to remove the sheeting from the trench during backfilling.

Method of Excavation

During investigation of the high deflections and pipe failures an opportunity was available to observe the construction procedures because repairs of failures were in progress. Methods observed were reportedly the same as those used during the original construction. The excavation steps were as follows:

1. Remove the pavement.
2. Drive the sheeting at both sides of the proposed trench location with a vibratory driver. The sheeting came in 600-mm-wide sections that simply overlap at the edges. The sheeting did not have interlocking joints.
3. Install well points for dewatering. These are placed at about 1-m intervals along the outside of the trench sheeting. The well point pipes were about 6 m long with a plastic filter over the bottom meter to permit the entry of water but not sand. The pipes were long enough so that the filter portion was well below the bottom of the trench. A ball-check valve was located on the end of each pipe to permit installation by jetting but to prevent inflow of sand during dewatering.
4. The dewatering pumps were then set up and allowed to run for several days. It was obvious during the investigation that the free flow of water through the native sands made dewatering a difficult task.
5. Excavation was with a backhoe. Cross bracing was installed at an appropriate depth.
6. If water was seeping into the trench, the contractor would dig a small sump hole and insert a hose connected to the vacuum dewatering system. Whereas this helped control the water in the trench, it undoubtedly reduced the efficiency of the dewatering system by breaking the vacuum and probably increased the overall flow of water into the trench.

The typical trench installation configuration using the preceding construction methods is shown in Figure 1. Although it was not directly observed during the investigation, a second sheeting system was reportedly used at some parts of the project. This method consisted of H-piles and timber lagging. As noted later, remnants of timber lagging were found at several locations during the investigation. No specific information is available on how this system was installed; however, typically the H-piles are driven before excavation and the timber lagging is installed as excavation proceeds.

Method of Backfill

Crushed stone backfill was placed on the bottom of the trench and compacted, followed by pipe installation. Later sieve analyses

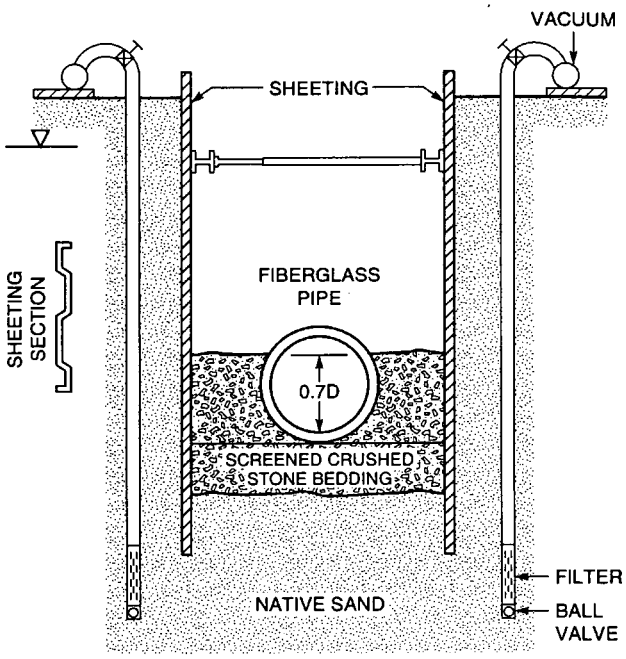

FIGURE 1 Typical braced sheeting installation.

showed the gravel to be 100 percent between 19 and 4.8 mm, giving it a classification of fine gravel. The stone backfill was then placed in layers and compacted to a height above the invert of 0.7 times the diameter of the pipe. The layer thicknesses are not known; however, the open-graded stone backfill requires only minimal compaction to provide proper support to buried pipe. Above the stone a sand backfill material was used. This material was very similar to the native sand. During backfilling the sheeting was pulled with the aid of vibration. There is no evidence that the pipe deflections were monitored during any part of the pipe installation process.

INVESTIGATION OF CAUSES OF DEFLECTION

The investigation into the causes of the failures consisted of review of available documents, interviews with personnel involved in the project, and inspection and testing of failed sections of pipe. Several failure sites were investigated during repairs. The following is a presentation of the significant findings.

Dewatering System

The dewatering system used during the replacement of failed pipe was reportedly the same as used for the original construction. It became evident as the repair excavations progressed that the system was inadequate and the water level just outside of the sheeting was well above the invert of the trench. This was confirmed by using some of the dewatering pipes as observation wells. As a result, large quantities of water flowed into the trench through the sheeting and the trench bottom. Aspects of this condition include the following:

- As noted earlier, if water collected in the trench the contractor would use a line from the dewatering system to remove the free

water. This results in breaking the dewatering vacuum, reducing the effectiveness of the system substantially, and increasing the water level outside of the sheeting.

- Because the sheeting did not have interlocking joints, the sheets separated as they were driven. The gaps between sheets were observed to be up to 12 in. during the investigation. Groundwater flowing into the trench through these gaps carried native sand with it and created voids behind the sheeting. These voids were also observed before the investigation conducted by the authors. At that time some were observed to be as large as 1 m^3. Where the sand was above the phreatic surface, where pore pressures are negative, it was stable, even if the sheeting joints were open.
- Sheeting could not be driven where the lines were crossed by utilities. At these locations the contractor used lumber to support the trench walls; however, this was only partly successful, and gaps occurred at these locations as well.
- At the ends of the excavations, the gravel backfill around the adjacent existing pipe allowed water to flow even more freely than did the native sand. This provides a great deal of water to further overload the dewatering system.

During the investigation by the authors, the contractor was aware of the voids and made attempts to fill them with stone before backfilling. If this was not done, the removal of the sheeting allowed the movement of the stone backfill out into the voids and the subsequent loss of support to the pipe. This process of stone movement is accelerated when the sheeting is removed with the aid of vibration, as was the case on this project.

Migration of Fines

It is well known that when a coarse, open-graded material is placed next to a finer-grained material, a flow of water can carry the fine material into the voids of the coarse material. This mixing of the materials causes a net loss of total volume and, when it occurs next to a pipe, can cause a loss of support to the pipe. This mechanism is called migration. The major factors in migration are the gradations of the two adjacent materials and the presence of flowing groundwater to carry the particles.

Current installation specifications, such as ASTM D2321 *Standard Practice for Underground Installation of Thermoplastic Pipe for Sewers and Other Gravity-Flow Applications,* provide the following guidelines for the gradation of adjacent materials to prevent this migration:

$$D_{15} < 5d_{85} \quad (1)$$

$$D_{50} < 25d_{50} \quad (2)$$

where D_n is the sieve opening size passing n percent by weight of the coarser material and d_n is the sieve opening size passing n percent by weight of the finer material.

Figure 2 shows the gradation of the trench backfill sand, the adjacent natural sand, and the pipe embedment crushed stone. Also shown in the shaded area is the required gradation of pipe embedment material that is compatible with the sand gradation based on the preceding criteria. The figure clearly shows that the crushed stone backfill is too coarse to prevent migration of fines.

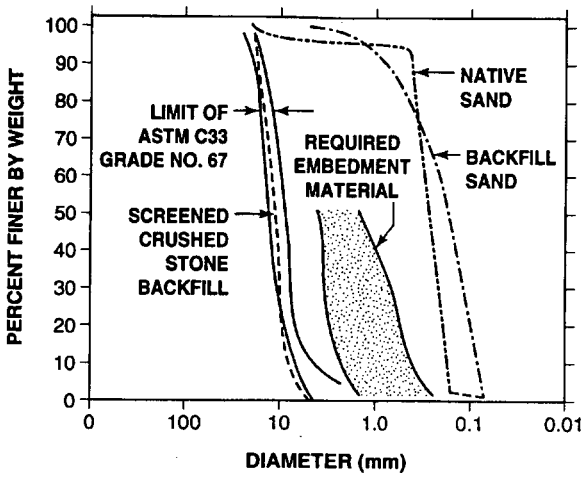

FIGURE 2 Gradations of sands and crushed stone materials.

The investigation showed that flow of water was likely to exist at the site. The groundwater level was well above the pipe crown in most areas, and there were at least three possible sources of a pressure head to cause a flow of that water:

1. Dewatering operations—During the original construction the dewatering of one section could cause substantial flow of water in the previously installed sections. Even though only a small section of trench would be open at any one time, the crushed stone around the previously installed sections can act as a French drain by conducting water toward the excavation and, as a result, cause flow from the sand into the stone for a considerable distance from the excavation. This could also occur during any subsequent excavations near the pipe, and especially during repairs of failures.
2. Termination of dewatering—Groundwater will move after termination of dewatering as the water returns to its normal elevation.
3. Natural changes in groundwater—Seasonal changes can cause the groundwater to fluctuate and in this case, because the town is on the coast, there can be daily fluctuations due to tidal changes. The variation of the natural groundwater level was not investigated in this project, but it is not believed to be as likely a source of groundwater flow as the dewatering operations.

All of these mechanisms are greatly enhanced by the lack of fines in the in situ sand, which allows free flow of water. In many cases where the preceding rules for relative gradation of adjacent materials are not met, migration would not occur because the ground conditions do not permit water velocities sufficient to move substantial amounts of material.

During investigation of the failures, cross sections of the backfill were carefully excavated, and the migration of fines could be clearly seen. This was quantified by taking successive samples across the width and depth of the stone backfill. Since the largest particles of the sand were typically smaller than the smallest particles of the crushed stone, it was a simple matter to distinguish the amount of penetration of fines by evaluating the particle gradation on the basis that any material finer than 2 mm (No. 10 sieve) was from the sand. Figures 3 and 4 show the results of such measurements taken in the stone near the sites of two sep-

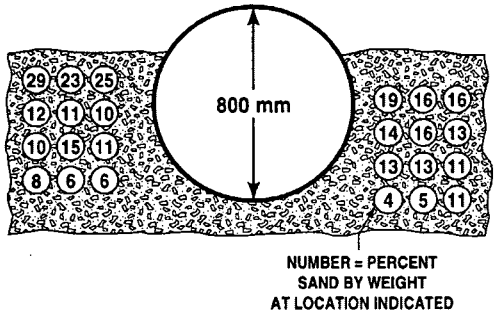

FIGURE 3 Percentage of sand in crushed stone backfill at failure site of 800-mm-diameter pipe.

arate failures. Both show the results of gradation tests taken at approximately 150-mm spacing across the stone backfill. The figures suggest that migration was occurring, although much more dramatically in the 800-mm-diameter pipe than in the 600-mm pipe. Some mixing of the sand and stone will occur during installation but would not contribute to deflection of the pipe; however, the broad distribution of the finer than 2 mm fraction and the significant percentages present suggest that migration could have been a significant contributor to the overall deflections being recorded.

The significance of migration can be calculated. On the basis of measurements of samples, the stone backfill had a bulk specific gravity of 2.47 and a rodded density of 14.9 kN/m^3. This indicates a porosity (ratio of volume of voids to total volume) of 38 percent. Because of the large particle size and the nearly complete lack of fines in the stone backfill, nearly all of the voids in the stone could be filled by the sand. Assuming that migration only takes place in the outer 150-mm portion of the stone and that only 50 percent of the voids are filled with sand at its in situ density, 29 mm of thickness is lost. If this all translates into deflection, then for 500- and 1000-mm pipes 5.8 and 2.9 percent deflections will occur. Assuming again that the in situ density of the sand is 15 kN/m^3, the foregoing migration would produce 16 percent sand content in the stone.

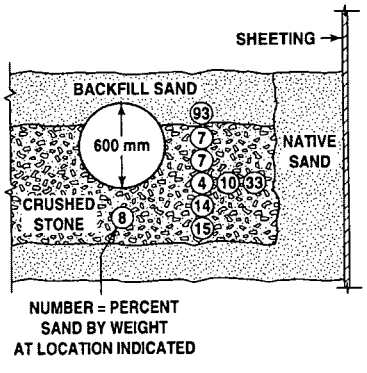

FIGURE 4 Percentage of sand in crushed stone backfill at failure site of 600-mm-diameter pipe.

DISCUSSION OF PROBLEMS

As noted, the principal causes of the deflection problems were the improper control of the groundwater during construction and the failure to address the possibility of migration of fines in the design phase of the project. These issues and their proper treatment during construction are discussed in this section.

Control of Groundwater During Construction

After installation, the embedment zone material should provide firm support for the buried pipe. This requires proper placement and compaction of the material, a process that can be completed most successfully in dry trenches and at proper backfill moisture contents. On this project the groundwater was not controlled properly, with disastrous results. Elements of the dewatering system and trench bracing contributed to the problems encountered.

Dewatering System

To be effective, a dewatering system must maintain the groundwater level below the bottom of the trench during excavation. In this project this was a demanding task because of the high water table and high permeability of the native sand material. The performance of the dewatering system was apparently never actually assessed for its effectiveness in practice. The dewatering pipes were always spaced at 1-m intervals and the same pumping equipment was always used, regardless of the performance. When water was encountered inside the trenches during excavation, the approach taken was to cope with the water by bringing a suction line into the trench rather than to consider why the water was there in the first place. The use of the suction line probably exacerbated the situation by further reducing the effectiveness of the overall dewatering system. This is a classic case of trying to cope with the symptoms of a problem rather than eliminate the cause.

In such difficult conditions, correcting the dewatering system would probably be expensive. More pumping capacity and possibly a closer spacing of the dewatering pipes would be required. Installation of two lines of sheeting, with dewatering in between, could create a barrier sufficient to reduce groundwater flow to a level that could be handled with the existing system. Drainage through the ends of the excavation also needs to be considered, especially because of the French drain effect in the backfill stone. This could be handled with waterstops installed periodically to reduce the flow.

On this project the use of sheeting with noninterlocking joints also contributed to the problem. Since the noninterlocking joints open up as the sheeting is driven, paths are created for sand to flow through the joints. Sheeting with interlocking joints may well have reduced the problem on this project. However, as observed at many locations, when the phreatic surface is maintained below the bottom of the trench, the sand is stable even when the joints are open.

The decision to remove the sheeting below the crown of the pipe was also a significant contributor to the overall problem. Not only did pulling the sheeting remove a barrier between the stone backfill and the voids, but also the vibration used caused the stone to settle into the void at a faster rate. These factors are in addition

to displacement of the backfill to fill the space occupied by the sheeting.

Any one of the preceding problems may not have created the major problems encountered on the project. For example, the ineffective dewatering system may have been tolerable if the sheeting had had interlocking joints. If the sheeting were left in place, the sand may have settled and filled the voids from above and not disrupted the support to the stone backfill (although problems with street settlement could have been significant). Given all of the problems occurring simultaneously, the high deflections were likely. If there were no voids at the sides of the pipe the loss of support created by the voids might not have occurred; however, this is a procedure that has long been recognized as a potential problem because pulling the sheeting can cause serious disruption by dragging compacted fill with it. Most standard installation specifications recommend that sheeting be left in place below the crown of the pipe.

Migration of Fines

Two solutions are available to prevent the problem of migration of fines. One is to place only compatible materials, based on the foregoing gradation criteria, next to each other. The other is to use a geotextile (filter fabric) between the incompatible materials. The mixing of dissimilar materials has long been known to be a problem for many construction situations (*2*); however, its impact on pipeline behavior is often ignored by specifiers. Even though ASTM D2321 has carried a warning against migration of fines since 1974, it was not until 1990 that specific guidance in the form of Equations 1 and 2 was incorporated into the standard. One reason why the issue of migration is often ignored is that many installations do not meet the gradation criteria but perform well. The authors believe that this is often because there is insufficient flow of groundwater to mix the adjacent materials. Unfortunately, no standard criteria are available to address this aspect of migration.

SUMMARY

The investigation into the high deflections observed in a project with 11 km of RPM sewer pipe showed the problems to be the result of inadequate control of the dewatering system during the original installation and migration of fines from the in situ sand materials into the voids of the open-graded stone used for pipe embedment. The dewatering problem had many aspects, including insufficient overall pumping capacity, noninterlocking sheeting, and end drainage due to open-graded stone in previously installed pipe sections. The migration of fines resulted from the use of a coarse backfill material with no fines next to a uniform sand. The high groundwater table and high permeability of the sand created a situation in which high flows could occur to cause mixing of the adjacent materials.

These problems may not have been anticipated by the engineer or the contractor; however, if observation of the pipe deflections had been made at the end of installation, the problems should have been identified and corrected before putting the lines into service. Furthermore, the inadequacies of the dewatering should have been apparent to knowledgeable inspectors during construction.

REFERENCES

1. Rund, R. E., R. E. Chambers, and T. J. McGrath. Strain Corrosion Performance of Fiberglass Reinforced Plastic Sewer Pipe. Presented at 42nd Annual Technical Conference, Reinforced Plastic/Composites Institute, Society of the Plastics Industry, 1987.
2. Cedergren, H. R. *Seepage, Drainage and Flow Nets* (2nd edition). John Wiley and Sons, New York, 1977.

Publication of this paper sponsored by Committee on Subsurface Soil-Structure Interaction.

Backfill Placement Methods Lead to Flexible Pipe Distortion

TIMOTHY J. MCGRATH AND ERNEST T. SELIG

Achieving good results in compacting fill around flexible culverts requires a proper matching of pipe, backfill type, and backfill placement and compaction methods. In the construction of a nuclear power plant, the circulating water lines were designed as 3600-mm-diameter, filament-wound glass-fiber reinforced plastic pipe of low stiffness. Because of a high groundwater table and concern that liquefaction might occur during a seismic event, the specifications called for compaction of all site backfill, including backfill for the circulating water pipe, to 85 percent relative density. After construction, the pipe was found to be deflected upward beyond project limits. The pipe shape was distorted, and the joints were delaminated. Investigation showed that the backfill was compacted with large self-propelled vibratory rollers operated to achieve the required density with insufficient monitoring of the pipe condition. The emphasis on meeting the compaction requirement was demonstrated by the fact that 171 density tests were conducted at the sides of the pipe and within one diameter width of the pipe, yet observations of the condition of the pipe, which indicated the presence of a problem early in the project, were not given sufficient weight. Observations during construction indicated that the compaction equipment was operated too close to the pipe, and analysis confirmed that this could result in the observed deformations. The investigative team concluded that the pipe could have been properly installed with proper selection of compaction equipment and procedures.

A nuclear power plant was to be built on a site with a high groundwater table, and there was concern that a seismic event could cause liquefaction. Compaction requirements for all site backfill were set at 85 percent relative density to minimize this risk. To ensure that this requirement was achieved, and because of the large nature of the overall project, the contractor used large compaction equipment, and the engineer required extensive compaction testing. This approach resulted in serious problems during installation of the circulating water pipe 3600 mm (12 ft) in diameter. Unfortunately, the site personnel failed to observe what was happening to the pipe even though there was ample evidence early in the project that the pipe was in distress.

This paper describes the project specifications, features of the pipe design, construction methods, and resulting problems. The paper concludes with a discussion of lessons learned from the project. All of the problems discussed in this paper were discovered before the end of construction and before the lines were put into service. Thus operating conditions such as internal pressure and temperature are not factors in assessing the causes of the problems.

PROJECT DESCRIPTION

The plant was designed with cooling towers to chill the circulating water for the two power generating units at the plant. There were four principal runs of pipe, a supply and return line for each unit, each between 170 and 250 m (550 and 750 ft) long. The supply lines brought water from the cooling towers to the turbines, and the return lines brought heated water back to the cooling towers.

The upper 7.5 m (25 ft) of the natural soil deposit excavated for pipe installation consisted of lacustrine sediments of stratified silty and clayey fine sands (SM, SC), silts (ML), and silty clay (CL). Underlying these sediments was fine, sandy, silty, clay till (CL). The natural groundwater level was near the surface at times.

Specifications called for the circulating water pipe to be 3600 mm (12 ft) in diameter. It was to be filament-wound, glass-fiber reinforced thermoset plastic (fiberglass). Pipe burial depths ranged from 1.5 to 6.1 m (5 to 20 ft). All pipe was to be designed for an H-20 surface loading [a 71-kN (16,000-lb) wheel load] and, under a haul road where the fill height was 3.4 m (11 ft), the pipe was to be designed for a 515-kPa (75-psi) surface load applied over an area of 3 by 12 m (10 by 40 ft). The supply and return lines were to be designed for internal pressures of 700 and 350 kPa (100 and 50 psi), respectively, although the actual operating pressures were expected to be 350 and 180 kPa (50 and 26 psi). At numerous locations the lines were crossed by other piping systems.

The pipe wall was designed by the manufacturer to be approximately 28 mm (1.1 in.) thick, resulting in a pipe stiffness ($EI/0.149R^3$) of about 35 kN/m/m (5 lb/in./in.). The pipe was manufactured in typical 15.2-m (50-ft) lengths with double-gasketed bell and spigot joints. Joints at bends were constructed in the field as overlay joints. The four pipe lengths designed for service under the haul road were designed with stiffening ribs, producing a pipe stiffness of about 170 kN/m/m (25 lb/in./in.). The bells of the pipe were up to 125 mm (5 in.) thick, resulting in a pipe stiffness of about 2750 kN/m/m (400 lb/in./in.).

PROJECT SPECIFICATIONS

For this project the owner elected to purchase the circulating water pipe directly from the manufacturer and contract separately for it to be installed. This was done to allow the pipe to be purchased and ready for installation when the installation contract was signed. In the following paragraphs the two contracts are only distinguished where relevant to the problems encountered.

Specifications called for the pipe to be installed in open trenches. Backfill was to be a granular material compacted to a minimum of 85 percent relative density per ASTM D2049 (this standard has since been replaced with ASTM D4253 and D4254). Lift thicknesses were restricted to 225 mm (9 in.) before compaction. Trench backfill was to be compacted out to the trench walls or for two pipe diameters on each side of the pipe, whichever was less.

T. J. McGrath, Simpson Gumpertz and Heger, Inc., 297 Broadway, Arlington, Mass. 02174. E. T. Selig, Department of Civil Engineering, University of Massachusetts, 28 Marston Hall, Amherst, Mass. 01003.

Although impact compaction tests (often referred to as the Proctor test) were not performed on the backfill samples, experience from other projects suggests that the 85 percent relative density requirement may be equivalent to 95 to 100 percent maximum dry density per ASTM D698 and could be higher than 100 percent maximum dry density. The use of a relative density type specification rather than a percent maximum dry density specification probably came from the concern for liquefaction during a seismic event. It is a reasonable specification for the type of backfill used.

The controls on the use of compaction equipment near the pipe included the following:

- "The compaction within 150 mm to 450 mm (6 in. to 18 in.) of the pipe shall be done with hand tampers . . ."
- "Wheel type earth moving equipment or track mounted equipment of less than 34.5 kPa (5 psi) earth pressure is permitted 600 mm (24 in.) away from the pipe and not across the pipe until 1.2 m (4 ft) of overburden is compacted."
- "Care shall be taken when compacting sidefill to avoid shifting the pipe."

The specifications restricted upward deflection of the pipe during compaction operations to 3 percent of the pipe diameter and downward deflection, after placement of all backfill, to 5 percent of the pipe diameter. If the 3 percent upward deflection limit was exceeded, the compaction density was to be decreased to 75 percent relative density. The pipe manufacturer's installation guidelines further expanded on this by stating that deflection measurements should only be taken at the center of the pipe. This is where the largest deflections are expected because the thick joints make the pipe ends much stiffer.

Requirements for the presence of the pipe manufacturer's personnel during pipe assembly and backfilling operations were inconsistent. The pipe manufacturer's contract stated that the pipe manufacturer shall provide a "field service technician for 5 days to advise and instruct the contractor's personnel." However, the pipe installation contract stated that "the pipe manufacturer will provide technical assistance for all field fabrication, installation and backfilling operations" and further stated that "a field service technician will be present during the entire period of actual pipe installation to ensure that the pipe work is installed and jointed correctly and in accordance with the manufacturer's recommendations." This conflict sets up the situation that the pipe manufacturer is only required to be on site for 5 days, whereas the contractor could fairly expect full-time assistance.

INSTALLATION

Records show that the pipe installation started and stopped a number of times, and the entire process took approximately 18 months. The principal reason for the delays was other construction activities at the site. Tests on samples taken during construction showed that the backfill was poorly graded sand (SP). Most of the backfill was compacted with large self-propelled vibratory rollers, which applied dynamic compaction forces of up to 93 kN (21,000 lb). Many roller passes (8 to 12) were made. Observers reported the use of this method within 600 mm (24 in.) of the pipe.

During backfilling there were a number of reports from the contractor that the compactive effort was causing excessive upward deflection in the pipe. In one instance the construction monitors noted that the backfill compaction tests were 70.1 and 80.9 percent relative density, even though the requirement was for 85 percent. The contractor responded that this was in accordance with the specifications, which allowed the reduction in compaction if the pipe is being deflected upward more than 3 percent. The site personnel in turn noted that the final deflection limit was 5 percent and that the 85 percent relative density requirement should be complied with. In this exchange the site personnel did not appreciate that the 3 percent upward deflection limit was the controlling factor and that the 5 percent limit only applied to downward deflection, nor did they institute a review of the compaction procedures. The pipe manufacturer was not contacted for guidance during the backfilling.

Overall, records of 910 laboratory determinations of maximum and minimum relative density and 624 determinations of in situ density were available. Of these tests, 171 were conducted within one diameter of the pipe springline, at elevations between the crown and invert. The mean relative density from these tests near the pipe was 86.7 percent, and the standard deviation was 13.2 percent. Of the 171 tests, 26 test results were greater than 100 percent relative density, and 47 test results were between 90 and 100 percent. Figure 1 shows the maximum, minimum, and in situ density for the entire data base of test results. Figure 2 shows the results of tests conducted close to the pipe in terms of percent relative density as reported by the testing agency. In analyzing the data it was not possible to reliably separate the tests that were considered failed by the testing agency from those that were considered acceptable. Thus the in situ test results in Figures 1 and

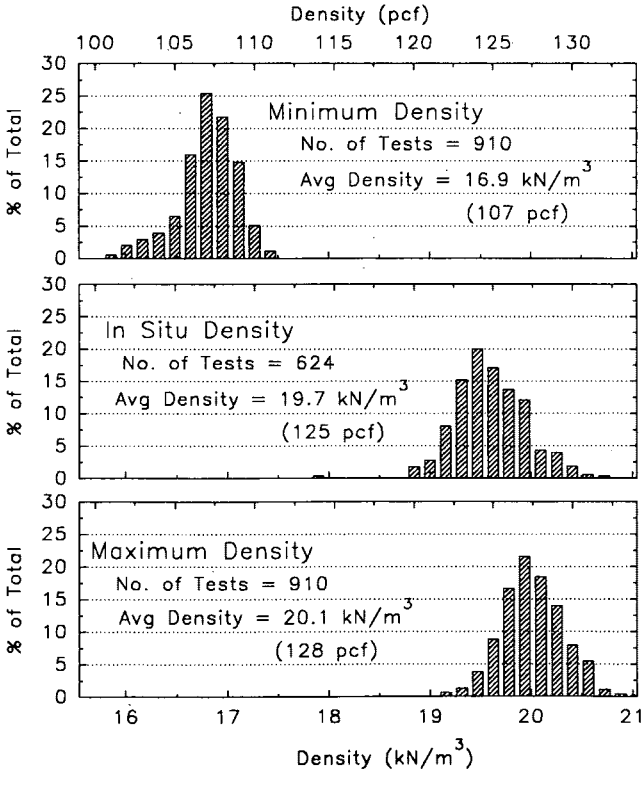

FIGURE 1 Results of all available reference and in situ density test results.

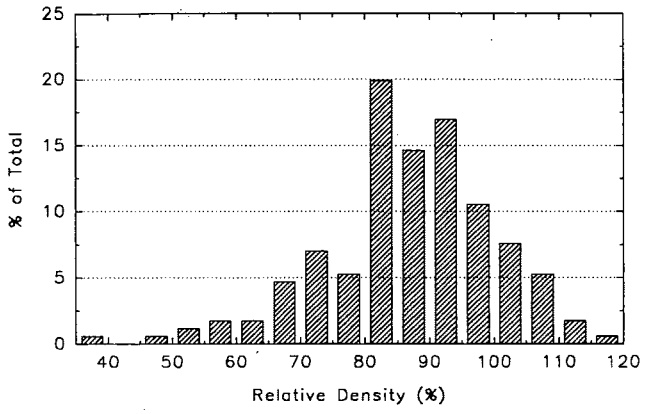

FIGURE 2 Results of relative density determinations near pipe.

2 include both. Because of this, the final, mean, in situ density is most likely higher than suggested by the figures.

The pipelines were crossed numerous times by heavy equipment involved in other aspects of the plant construction. Some of these crossings were planned and attempts were made to protect the pipe, whereas others were made without authorization. Equipment crossing the lines included a special Lampson crane brought on site to place the reactor domes and weighing 8.9 GN (2,000,000 lb) and a Manitowoc 4600 weighing 1.7 GN (390,000 lb).

PROBLEMS ENCOUNTERED

Problems with the condition of the circulating water pipe were not discovered until construction of the lines was nearly completed, even though the construction took 18 months and there was ample evidence that problems existed. Conditions that were found included the following:

- Almost all of the circulating water pipe was deflected upward at the time of the investigation, which was well after the completion of construction. Of 39 straight pipe lengths, 31 were deflected upward more than the 3 percent limit allowed by the specifications. The maximum upward deflection at the time of the investigation (backfilling complete) was 5.3 percent. The very first pipe installed on the project was deflected upward 4.6 percent. The peak upward deflections should have occurred during construction, when the backfill was near the level of the crown of the pipe. The fill above the crown should have decreased the upward deflection caused by the backfilling operations up to that level. Thus the deflections measured during the investigation were not the peak values.
- The deflected pipe shapes were distorted from the ideal elliptical shape, and the major axis of the deflected shape was frequently off-line from vertical. The pipe barrels were distorted more than anticipated by design standards for fiberglass pipe. Strains in the pipe, estimated from sagitta measurements, were commonly 0.4 to 0.6 percent at deflection levels between 3 and 5 percent. The design flexural strains at 5 percent deflection, based on American Water Works Association Standard C950, were 0.23 percent (on the basis of a shape factor, $D_f = 6$).
- The bells of the pipe deflected significantly less than the barrels because of the higher stiffness. However, of the above 39 pipe lengths, 12 joints were deflected upward more than 3 percent and 14 were deflected upward between 2 and 3 percent.
- Many of the pipe joints were delaminated and cracked.
- At two locations of known crane crossings, the pipe barrels developed helical cracks in the fiberglass laminate.

FACTORS RELATED TO DISTRESS PROBLEMS

The principal distress problems of the pipelines in this project were the upward deflection, distorted shapes of the pipe barrels, and the delaminated pipe joints.

Upward Deflection

The contractor complained repeatedly that it was difficult to compact at the sides of the pipe without distorting the pipe upward beyond the 3 percent limit. The very first full length of pipe installed was deflected upward 4.6 percent even after 7 ft of fill was placed over the top of the pipe. In spite of this condition there is no record that anyone considered changing compaction procedures or using lighter compaction equipment. Unfortunately, construction continued, and the excessive upward deflection continued for the remainder of the project. It should be a fundamental rule of installation to carefully monitor construction methods early in a project so that any problems can be corrected before their effects multiply over an entire pipeline. In this case the problem was acknowledged by the contractor but not the site monitors, and, surprisingly, the manufacturer was not consulted on the matter. The cause of the excessive upward deflection, as discussed in subsequent paragraphs, was the combination of the heavy equipment used to achieve the required density and the low pipe stiffness. The records do not show that any attempt was made to evaluate or modify the compaction procedures around the pipe to control the upward deflection.

Relative Density Compaction Requirement

The use of a relative density specification requires three measurements: a maximum reference density, a minimum reference density, and an in situ density. Each of these has considerable variability [see Figure 1 and Selig and Ladd (*1*)]. The percent variability in relative density is much greater than the percent variability in percent compaction (based on the Proctor test) because a 1 percent change in percent compaction represents a 6 to 7 percent change in relative density. As is usually the case, compaction specifications for this project did not consider this variability. They only required compaction to exceed the specified value, making no allowance for the fact that a certain percent of the backfill must fall below the specification because of normal variability. Thus, the more rigorously the specification is enforced, the higher will be the average compaction, because when test values fall below the specification more compaction is usually required, assuming that the tests are considered good (*2*).

The maximum, minimum, and in situ densities for all backfill tests during overall project construction were presented in Figure 1. The resulting variability for relative density for tests taken

around the pipe was presented in Figure 2. Figure 2 shows an average density of 87 percent, with 58 percent of the tests greater than the required 85 percent relative density specified, even when failed and acceptable test results are considered. The final in situ density would likely be higher than 90 percent relative density if the failed tests could be discounted.

The figures show that the 85 percent relative compaction requirement was clearly achievable, although it was perceived by many to be the source of the upward deflection problem. The problem was actually the result of the large compaction equipment operating too close to the pipe. It is frequently thought that to obtain a high amount of compaction large equipment must be used; however, analysis shows that this is not the case (*3*). Size and weight of compaction equipment relate to the productivity of the compaction process far more than to level of compaction achieved. In this case the required density could have been achieved by the use of small equipment near the pipe to reduce the forces applied to the pipe during compaction. This issue is discussed further in the following section.

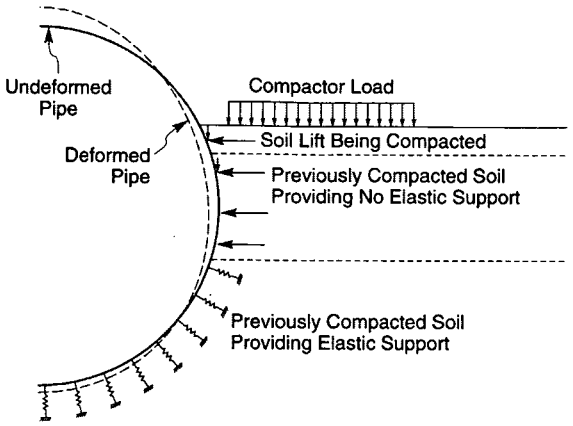

FIGURE 3 Computer model used to analyze compaction effects.

Compaction-Induced Deformation

The upward deflection was clearly the result of the compaction of backfill at the sides of the pipe. The fact that the major axis of the deflected pipe was not vertical further suggests that the backfill was not brought up evenly on both sides of the pipe. The upward deflection during construction was limited to 3 percent because compaction forces tend to be relatively concentrated and can result in local distortions. Downward deflections are caused by earth pressures, which tend to be more evenly distributed, allowing a higher limit.

The compaction was achieved by the use of large, self-propelled vibratory rollers, providing dynamic compaction force of up to 93 kN (21,000 lb) and dynamic soil pressures under the roller of 255 kPa (37 psi). This is far more than the specifications intended if the equipment is allowed closer than 450 mm (18 in.) to the pipe.

Flexible pipe can be deformed by compaction forces; however, the high stresses caused by compaction equipment dissipate very rapidly with increasing space between the pipe and the equipment. On this project there were reports that the compaction equipment was being operated very close to the pipe. To investigate the effect of this, the authors developed a simple computer model to represent compaction effects. The model used a ring to represent the pipe and springs to represent the surrounding soil, as shown in Figure 3. The pressures applied to the pipe were based on the Boussinesq distribution shown in Figure 4. Figure 4 shows two curves representing the pipe at 150 and 600 mm (6 and 24 in.) from the compaction equipment. The figure shows that the vertical soil stresses at the pipe-soil interface, when the compaction equipment is 150 mm (6 in.) from the pipe, are 5 to 10 times the pressures resulting when the equipment is held 600 mm (24 in.) from the pipe. Horizontal pressures were computed by applying a factor of 0.4 to the vertical pressures. The principal assumptions of the model were that the backfill layer currently being compacted would undergo significant lateral strains that could deform the pipe, whereas prior lifts, having already been compacted, provide a reduced lateral force on the pipe.

On the basis of a paper by Duncan and Seed (*4*), 55 percent of the lateral pressures produced under peak compaction loads were assumed to remain in the layer being compacted. In previous layers the residual lateral pressures are assumed to vary gradually from 27 to 0 percent of peak over the several previous lifts. This model had to be run iteratively for each backfill layer to be certain that springs resisting outward motion were only acting in compression. The resulting deformations were then accumulated for each layer. The deformed shape of the pipe resulting from the two conditions, 150 and 600 mm (6 and 24 in.) between pipe and compactor, are shown in Figure 5. The upward deformation when the compactor was 150 mm (6 in.) from the pipe was 6.9 percent of the pipe diameter, or almost three times the 2.5 percent deflection resulting from a 600-mm (24-in.) separation. Although it is not a rigorous treatment of the complex pipe-soil interactions taking place during backfill compaction around buried pipe, this computer model clearly demonstrates the sensitivity to deformations when large equipment is operated too close to the pipe.

The preceding analysis can be further evaluated by analyzing the behavior of the pipe due strictly to the weight of the soil, as

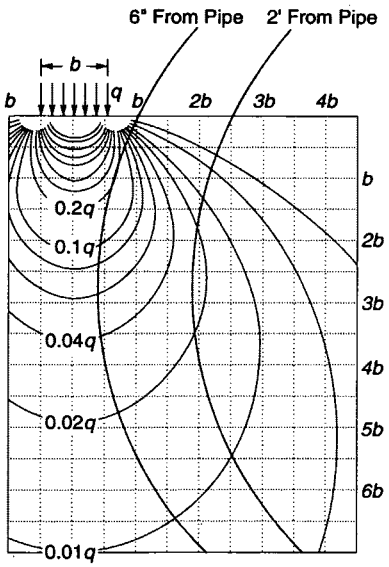

FIGURE 4 Soil stresses due to compaction near pipe.

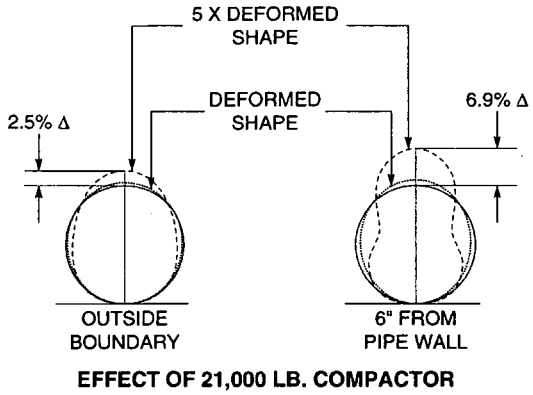

FIGURE 5 Computer model results for deformed pipe shape due to compaction effects.

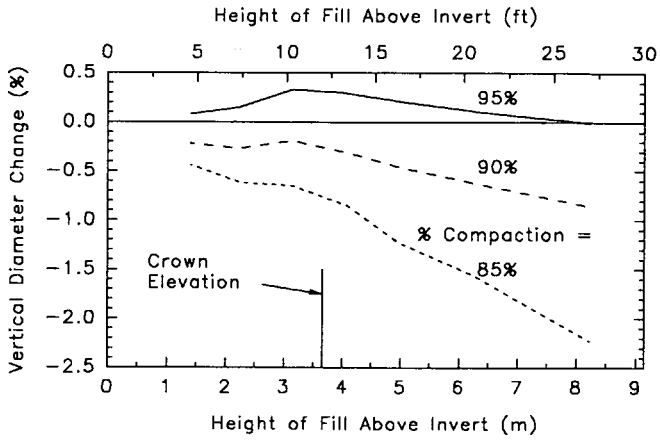

FIGURE 7 Predicted vertical diameter change with fill height for compacted sand backfill.

is the analysis made with most currently available finite element soil structure interaction computer models. Using the program SOILCON (*5*), the pipe installation was modeled as shown in Figure 6. This models a 3600-mm pipe with 4.6 m of cover over the crown. Using this model and considering three types of backfill (SW at 85, 90, or 95 percent maximum dry density, ASTM D698) the pipe deflections were monitored as fill was placed beside and over the pipe. The results are shown in Figure 7. When only the weight of soil is considered, upward deflection occurs only for the densest soil (95 percent maximum dry density), and even in that case the upward displacement is less than 0.5 percent.

Differential Stiffness of Pipe Joint and Pipe Barrel

When a pipe barrel and pipe joint have significantly different ring stiffness, the deflection levels will vary. This is in part because of typical soil-structure interaction, as predicted by the Iowa formula (*6*), and partly because flexible sections tend to deform more than stiffer sections as a consequence of installation procedures and compaction effects, called installation deflection (*7*). The principal problem with differential stiffness between the pipe joint and the barrel is that the stiff element tends to resist a greater portion of the load and restrains the deflection of the flexible element. Thus the stiffer element will deflect more than it would if the entire pipe were stiff, and it will be subject to longitudinal stresses that can be high enough to cause failure. The differential stiffness in this project was significant, the joint being about 100 times stiffer than the barrel. Because of the excessive deflections, the pipe joints delaminated and circumferential cracks occurred. However, stress analysis of the joints using the NASTRAN finite element program showed that the pipe would have performed satisfactorily if the deflection limits had been adhered to. The results of this analysis are consistent with experiences on other projects, where the only time such failures are observed is when deflection limits are exceeded. This is logical since the effects of differential stiffness will be more pronounced as deflection levels increase. In current practice, pipe manufacturers generally avoid differential stiffness in pipe and barrels, thus avoiding the problem altogether.

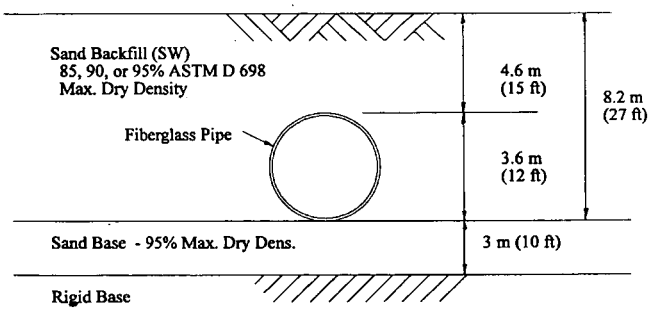

FIGURE 6 Configuration of pipe installation for SOILCON analysis.

Use of Spiders To Prevent Pipe Deformation

An alternative method of controlling pipe deformation from compaction would have been the use of spiders to temporarily increase the effective pipe stiffness during compaction. Whereas this is certainly feasible, it is an added complexity in the construction procedure and is not required if compaction equipment is properly selected and controlled. The use of spiders can also introduce a new source of differential stiffness that results in longitudinal stresses due to nonuniform deflection. This is especially true if the spiders give the installer the false idea that spiders provide complete protection from damage.

Manufacturer's Field Assistance During Backfilling

As noted earlier, the specifications are inconsistent on the requirements of the manufacturer to assist in monitoring the pipe-laying operations. On the basis of a review of project records, the actual interpretation of the specifications at the time of construction appeared to be that the manufacturer was required on site to train the contractor's personnel in making the layup joints required at the bends in the lines, but not during backfilling operations.

CONCLUSIONS

A circulating water pipe 3600 mm (12 ft) in diameter was deflected upward beyond specification limits and distorted beyond

its strength limits. The main axis of the deflected shape was not vertical. Pipe joints were delaminated. The principal reason for these problems was a failure to control compaction methods exacerbated by extensive compaction testing. Large compaction equipment was used too close to the pipe, and the resulting deflections were up to about 5 percent.

Perhaps the most important lesson from this project is to pay careful attention to the results of construction methods at the very beginning of a project and prevent any problems that are present from repeating. A careful review of construction methods after the first few pipe lengths were installed may have prevented the major financial disaster that resulted on this project.

REFERENCES

1. Selig, E. T., and R. S. Ladd. Evaluation of Relative Density and Its Role in Geotechnical Engineering. *Special Technical Publication 523*, ASTM, July 1973.
2. Selig, E. T. Compaction Procedures, Specifications and Control Considerations. In *Transportation Research Record 897*, TRB, National Research Council, Washington, D.C., 1982, pp. 1–8.
3. Selig, E. T. Unified System for Compactor Performance Specification. *Transactions*, Society of Automotive Engineers, 1972, pp. 2454–2464.
4. Duncan, J. M., and R. B. Seed. Compaction-Induced Earth Pressure Under K_o-Conditions. *Journal of Geotechnical Engineering*, American Society of Civil Engineers, Vol. 112, No. 1, Jan. 1986.
5. Haggag, A. T. *Structural Backfill Design for Corrugated-Metal Buried Conduits*. Ph.D. dissertation. University of Massachusetts, Amherst, May 1989.
6. Spangler, M. G. *Structural Design of Flexible Pipe Culverts*. Bulletin 153, Iowa Engineering Experiment Station, 1941.
7. McGrath, T. J., and R. E. Chambers. Field Performance of Buried Plastic Pipe. *Proc., International Conference on Underground Plastic Pipe*, American Society of Civil Engineers, 1981.

Publication of this paper sponsored by Committee on Subsurface Soil-Structure Interaction.

Centrifuge Modeling of Laterally Loaded Pipelines

F. POOROOSHASB, M. J. PAULIN, M. RIZKALLA, AND J. I. CLARK

The state of practice (SOP) for pipeline design in areas where pipelines may move relative to the soil involves considering the pipeline to be made up of discrete segments and the segments to be coupled to the soil via a set of spring/sliders. Much of the theory behind this SOP is derived from other geotechnical applications such as pile/soil interaction. There is little or no physical verification of the mechanisms or the magnitude of forces assumed during pipeline displacement. An experimental model examination of displaced pipelines using the centrifuge modeling technique to create similitude between model and prototype or the actual situation is presented. The SOP, the experimental program, and the results of eight pipeline model tests are presented. The results are discussed, with particular reference to the magnitude of loads transmitted to the pipes and the development of the pipeline/soil interaction. The test results are compared with the loads that would be predicted by the SOP design calculations. The main conclusion is that the SOP formulation appears to be unconservative, predicting loads acting on the pipeline about 50 percent lower than those measured experimentally.

When a buried pipeline is subjected to ground movement such as a landslide or downslope creep of soil, the pipe's integrity and operating safety are both of concern. Computer-based analyses are the primary engineering tools available to evaluate the state of the pipeline to determine the need for remedial or mitigative action. In finite element modeling techniques used in pipeline analyses, the interaction between the pipe and soil is commonly described by spring elements. The parameters describing these spring elements have generally been assumed from other soil/structure interaction studies (e.g., anchors and piles), and much of the experimental and analytical work cited in pipeline analysis has been undertaken from a foundation design perspective.

Review of the literature has indicated that there is little realistic pipeline-specific experimental information available. Studies carried out by the NOVA Corporation of Alberta have shown that typical rates of ground movement for creeping type landslides experienced by the industry range from less than 1 to 6 cm/year. Lateral pipeline/soil experiments reported are generally small in scale, ignore construction considerations such as the presence of a distinct backfill material, and generally use idealized soils. Experimental work in this field needs to be extended.

A simple engineering analysis of the pipeline/soil interaction problem can be expressed as (*1*)

$$P_{ult} = DC_uN \quad (1)$$

where

P_{ult} = ultimate load transferred to the pipe,
D = pipeline diameter,
C_u = undrained shear strength of the soil, and
N = interaction factor.

The objectives of this experimental program were to examine the phenomenon of pipeline/soil interaction, and, specifically, to determine the value of N, the shape of the load-displacement curve, and the effect of ditch width and depth on the interaction.

LATERAL PIPELINE/SOIL INTERACTION

Modeling Considerations

Several considerations arise in undertaking either physical or numerical modeling studies of lateral pipeline/soil interaction. Figure 1 shows a laterally displaced pipeline and indicates the various aspects of the problem that present modeling complexities. Modeling of the soil separation behind the pipe and both the contact surface and the soil strain hardening or softening in front of the pipe pose numerical modeling difficulties. Choosing an appropriate rate of pipeline displacement against the soil is another significant modeling consideration (depending on whether the pipeline is loaded by a creeping soil or a landslide condition).

Development of SOP Formulations

Rowe and Davis (*2*) simulated the behavior of vertically oriented smooth anchors in saturated clay using elastoplastic finite element analyses. For such anchors, the limiting loading cases are those in which the back of the anchor either remains in contact with the surrounding soil (no breakaway condition) or breaks away immediately (immediate breakaway condition).

A monograph by the Committee on Gas and Liquid Fuel Lifelines (CGL) (*3*) concluded that pertinent data on laterally displaced pipelines in clay indicate a trend toward increased levels of ultimate load until H/D (depth to pipe's springline divided by diameter) reaches a value of 6. Furthermore, the CGL suggests that the Hansen bearing capacity model (*4*) can be used to estimate the maximum horizontal pipeline force per unit length in clay.

The SOP formulations routinely used in design are based on the work of Rowe and Davis (*2*) and the CGL (*3*) guidelines. In a later section, the results of the centrifuge program will be compared with these formulations.

F. Poorooshasb, Centre for Cold Ocean Resources Engineering, Memorial University of Newfoundland, St. John's, Newfoundland, Canada A1B 3X5. Current address: 365 Pennsylvania Avenue, Los Gatos, Calif. 95030. M. J. Paulin and J. I. Clark, Centre for Cold Ocean Resources Engineering, Memorial University of Newfoundland, St. John's, Newfoundland, Canada A1B 3X5. M. Rizkalla, NOVA Corporation of Alberta, Alberta Gas Transmission Division, P.O. Box 2535, Station M, Calgary, Alberta, Canada T2P 2N6.

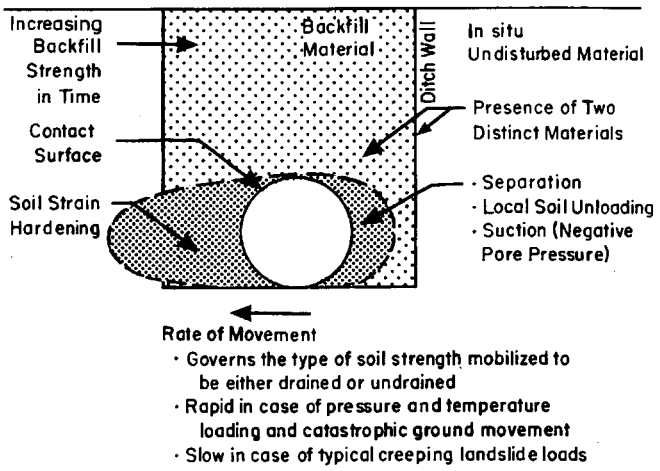

FIGURE 1 Aspects of lateral pipeline/soil interaction that present modeling complexities.

CENTRIFUGE MODELING

Centrifuge modeling has been used for several decades for geotechnical investigations. Its current stage of development is considered by many in the geotechnical engineering community to be comparable with the developmental stage of numerical modeling two decades ago (*5*). As an experimental method, it has been widely accepted in Europe and Japan and is being increasingly used in North America.

The centrifuge modeling technique allows gravitational effects to be replicated by substituting the centripetal acceleration experienced by an object in circular flight at the end of a rotating beam for true gravitational acceleration. The rationale behind this modeling technique is as follows. If an actual earth structure is represented by a model manufactured of the same material to a scale of N (every linear dimension in the prototype being N times greater than in the model), the stress levels due to self-weight will be N times greater at any position in the actual structure than at the corresponding point in the model. However, if the model is subjected to an acceleration N times greater than gravitational acceleration, the stress distribution in the actual structure and in the model will be identical. The strain fields will also be identical, since the constitutive laws governing the soils are the same. Furthermore, if any external loadings are applied, they must be scaled to maintain correspondence of stress fields. If these conditions are met, the reaction of the model to the external loading will be identical to the actual structure's behavior and will provide a valuable understanding of the deformations and failures involved in actual events (*6*).

A theoretical treatment of the basis of centrifuge modeling is beyond the scope of this paper and is presented elsewhere (*5,7,8*). The scaling relationships for a modeling program are presented in Table 1.

EXPERIMENTAL PROGRAM AND RESULTS

Model Development

In small-scale modeling, three situations need to be considered. The first is the actual situation of interest to the modeler. The second is the model itself. Both of these items are tangible situations. The third item is the prototype, which refers to the actual situation that the small-scale model represents. The prototype is a theoretical situation and is determined by applying the correct scale factors to all aspects of the model. The similitude of the prototype to the actual situation determines the relevance of the small-scale modeling to reality. Figure 2 shows the actual situation of interest, the prototype, and the centrifuge model tested at 50 g (1:50 scale). The centrifuge model (described later) behaves at prototype scale like an extremely rigid pipeline section in soft kaolin clay. The degree of similarity of this prototype to a particular case of industrial interest determines the relevance of the experiments to the state of practice.

Experimental Description

The experimental program was conducted at the Laboratoire Central des Ponts et Chaussées (LCPC), Centre de Nantes. The facility houses an Acutronic 680-1 centrifuge, which has an effective radius of 5.5 m and a payload capability of more than 2 tonnes at 100 g.

The experimental program consisted of two centrifuge tests: Test Set A and Test Set B. A scale factor of 1:50 was chosen for

TABLE 1 Centrifuge Modeling Scaling Relationships

Quantity	Full Scale (Prototype)	Centrifugal model at N g's
Linear Dimension	1	1/N
Acceleration	1	1
Velocity	1	N
Stress (Force/Area)	1	1
Strain (Displacement/Unit Length)	1	1
Density	1	1
Frequency	1	N
Mass	1	$1/N^3$
Force	1	$1/N^2$
Displacement (Distance)	1	1/N
Time (Drainage)	1	$1/N^2$
Time (Dynamic)	1	1/N
Time (Viscous)	1	1

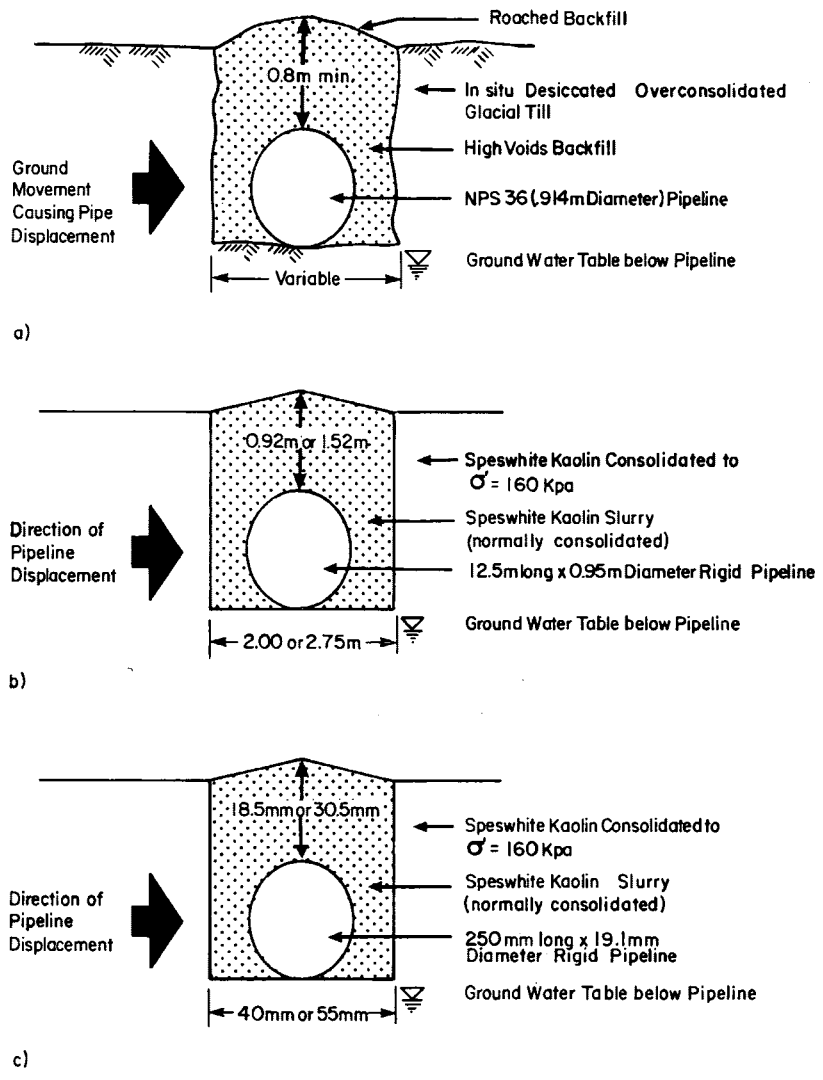

FIGURE 2 (*a*) **Actual event, (*b*) prototype event, and (*c*) model event.**

the current experimental program. This scale allows four pipelines to be tested during each test set. During the experiments, conducted at an acceleration level of 50 *g*, the rigid model pipelines (1:50 scale) were moved laterally through overconsolidated kaolin clay. The pipelines had been placed in model trenches at 1 *g*; these trenches were then backfilled to simulate construction procedures. As the pipelines were displaced, force displacement curves were obtained.

Experimental Apparatus and Setup

The model used to obtain the present results is shown in Figure 3. The equipment was contained in a standard LCPC strongbox, 800 by 1200 mm in internal plan and 360 mm deep. The central section of the box contained kaolin clay, which was retained by two bulkheads. Trenches were carved in the clay to the required width and depth to contain the model pipelines. Clay slurry was used to backfill the trenches after the pipelines had been positioned. Each of four pipelines was pulled through the clay by a pair of tension cables, which were connected to a prime mover, a DC variable speed gear drive, by means of pulleys mounted on a shaft. The pipelines were displaced at a nominal speed of 1 mm/sec. Data were collected before, during, and after the displacement of each pipeline.

During the test, the water level was kept constant by using a weir. The soil sample was probed with a miniature cone penetrometer to obtain the shear strength value required in Equation 1. After the tests, the sample was extruded from the strongbox and sectioned on the laboratory floor. Water content samples were obtained, and internal inspection was undertaken to determine displacement patterns within the soil.

Prototype

The prototype of the model described earlier is a system of four pipeline segments buried in overconsolidated kaolin clay. Before

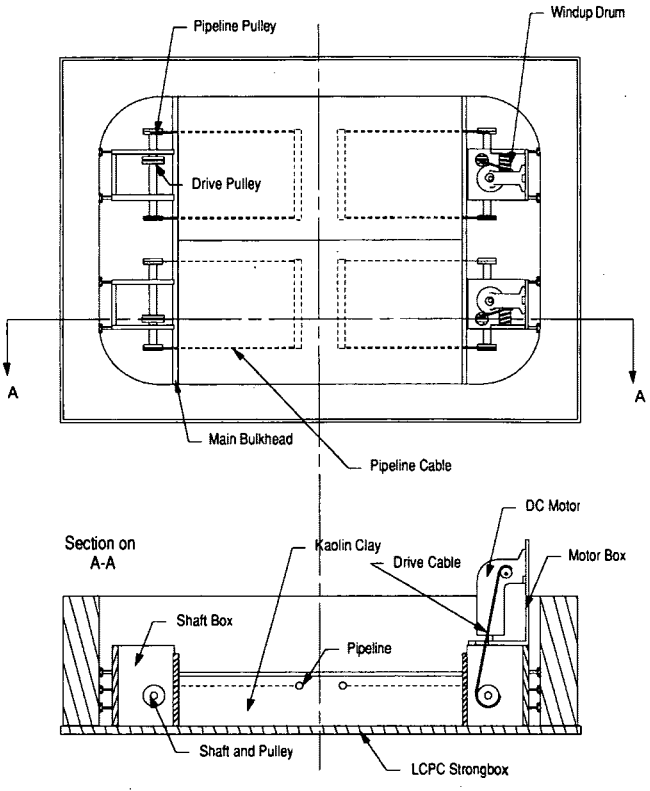

FIGURE 3 Package used in test series. DC motors are omitted from left-hand side of the package.

consolidation in the centrifuge, the clay was one-dimensionally preconsolidated to a vertical effective stress of 160 kPa. The backfill material was also kaolin clay, which was normally consolidated in the centrifuge.

The stainless steel pipelines were 0.95 m in diameter and 12.5 m long. They were pulled by a pair of stainless steel cables 0.158 m in diameter. At one end of each pipeline, an electrical cable approximately 0.25 m in diameter was pulled through a lubricated plastic channel.

The pipelines were pulled at a slow rate, so that the event was practically undrained and inertial events were insignificant. Two extremes of velocity were recorded during the same pipeline movement (Test Set A, Pipeline 4), and no significant effect on the soil response could be seen in the recorded data. The pipelines were pulled horizontally but were free to move vertically. The movements at either end of each pipeline were constrained so that they were equivalent.

The base of the pipeline trenches was approximately 5 m above a hard impermeable surface. There was 0.92 m of clay cover above each shallow pipeline and 1.52 m of cover above each deep pipeline. The distance between the pipelines was 5.48 m, and the distance from the end of the pipelines to the lateral vertical wall was 4.77 m. The water table was 3.1 m above the hard impermeable surface, about 1.9 m below the base of the pipeline trenches. Below the water table, the soil was saturated. Above the water table, various degrees of desiccation had occurred; this resulted in a lack of certainty about the effective stresses within the region above the water table. The trench geometry for each test is presented in Table 2.

TABLE 2 Trench Geometry and Undrained Shear Strength Measurements

Test Set	Test	Trench Width	Trench Cover Depth	C_u In Situ (kPa)	C_u Backfill (kPa)	Evidence of Desiccation
A	Pipeline 1	2.00m	0.92m	22.0	17.34	Strong
A	Pipeline 2	2.00m	1.52m	13.80	12.54	Strong
A	Pipeline 3	2.75m	0.92m	17.61	14.64	Strong
A	Pipeline 4	2.75m	1.52m	10.24	9.73	Weak
B	Pipeline 1	2.00m	0.92m	8.50	7.29	Weak
B	Pipeline 2	2.00m	1.52m	8.50	7.29	None
B	Pipeline 3	2.75m	0.92m	8.29	7.29	None
B	Pipeline 4	2.75m	1.52m	8.29	7.29	None

Review of Experimental Procedures

The measured shear strength of the in situ material was lower than expected from empirical correlations for 100 percent saturated kaolin clay. As a result, a distinct difference in strength between the in situ and backfill materials was not achieved. This obscured the effects of the ditch width. The shear strengths of the soil interpreted at the base of the pipelines are presented in Table 2. The cone penetrometer test locations from Test Set A are presented in Figure 4.

Below the water table, the soil was saturated. Above the water table some desiccation had occurred, so the magnitudes of the effective stresses within this region could not be determined exactly. To reduce desiccation during the second test, a layer of thin plastic film was used to cover the surface of the soil. Weights were placed on the perimeter of the film, and a slit was made in the film at the points where the boreholes were to be placed. The film reduced desiccation but did not eliminate it.

Pipeline Force Displacement Records

During Test Set A, of the four pipelines, Pipelines 1, 2, and 3 were displaced at nominally constant rates. Pipeline 3 was accelerated at the end of its displacement, but this appeared to have very little effect on the results. Pipeline 4 was displaced initially at a very low rate of 3.7×10^{-7} m/sec (prototype scale) and then stopped (some stress relief occurred). After a period of 30 min (52 days, prototype scale), excitation was reapplied and the pipeline began moving at a rate that varied between 1.08×10^{-8} and 7.3×10^{-6} m/sec. Figure 5 indicates that the effect of the loading being stopped and then reapplied was negligible.

The general features of each curve are as follows. The initial response is one of increasing force with displacement. In Pipelines 3 and 4, the peak load is followed by a decrease in load and then a slow increase. The peak is observed between a pipeline movement of 0.25 to 0.5 diameters, and the subsequent decrease in response is at the minimum at approximately the point where the pipeline first touches the native material. The subsequent rise is observed as the pipeline begins to penetrate the native material. This peaked behavior is more marked than it was in the other two tests. Table 3 summarizes the results from these tests.

Examination of Table 3 indicates that there is some scatter in the displacement required to peak resistance, with extremes of 0.26 and 0.63 m. This is a function of different shapes of the peak. Pipelines 3 and 4 display much sharper peak behavior than

Pipelines 1 and 2. This may have been because the effect of the softer backfill was more pronounced in the wider trenches. A more consistent measurement of displacement to peak loads may be obtained by assessing the displacement required to achieve 90 percent of the peak load. This quantity may be expressed as

Displacement to 90 percent peak load

$$= 0.21 \text{ m} \pm 18 \text{ percent} \qquad (2)$$

The peak load is achieved when the pipeline is still totally within the trench, so the native material may not be a factor in calculating pipe loading. The 18 percent spread in this displacement value is also associated with the degree of desiccation (i.e., the greatest distance to 90 percent peak load is displayed by the most desiccated samples, Pipelines 1 and 3). The ratio of peak resistance to shear strength at the springline falls within a fairly narrow band. In all cases, the peak resistance is attained before the pipeline begins to enter the native material; therefore, the backfill shear strength is a suitable normalizing factor. The ratio, as measured in Test Set A, is given by

$$\frac{\text{Peak resistance per unit length}}{\text{backfill shear strength}} = 11.70 \pm 11 \text{ percent} \qquad (3)$$

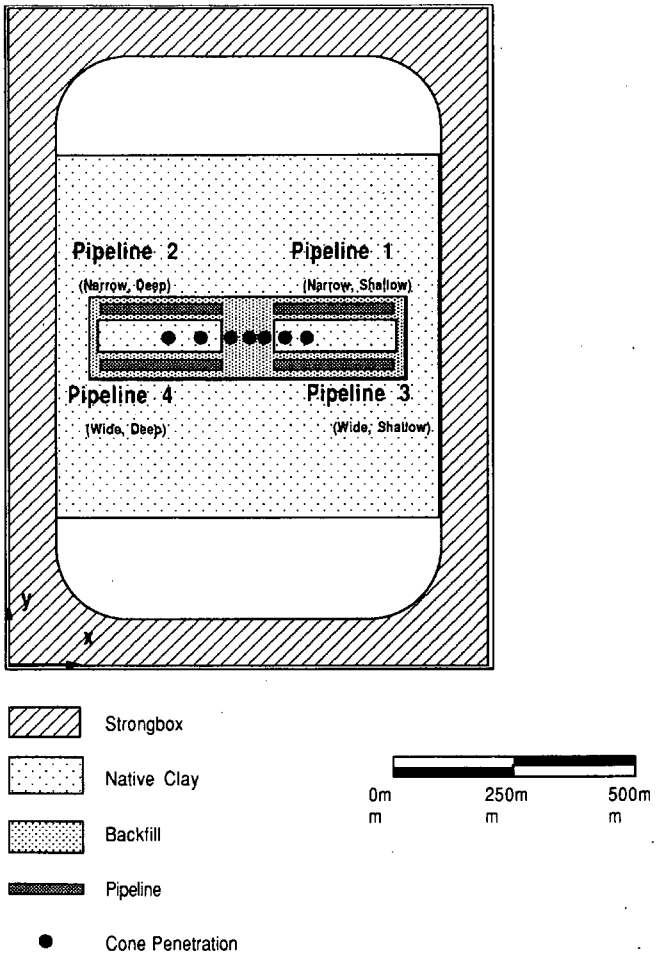

FIGURE 4 Test Set A geometry showing CPT locations.

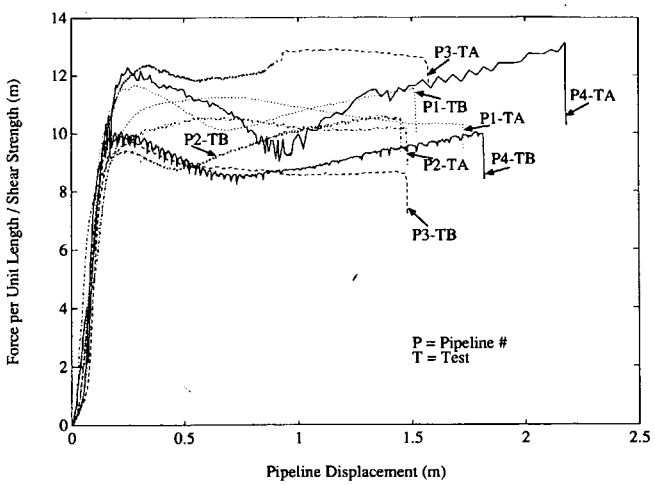

FIGURE 5 Normalized prototype force/displacement data, all tests.

The lower values in this range are those associated with the narrow trenches. This is contrary to intuition. It might be explained by a lower degree of consolidation of the backfill material in the narrow trenches (because of friction against the rigid pipeline). The effect, however, is not marked enough to draw a firm conclusion.

Also contrary to intuition, it is not obvious from this test alone that trench cover depth has any significant effect. Deeper pipelines would be expected to display a greater resistance to displacement, but this is not apparent.

The results obtained in Test Set B were similar to those obtained in Test Set A. The results are presented in Table 4 and Figure 5. The peak in resistive load was noticed in all pipelines; a postpeak minimum and subsequent rise occurred in all pipelines except Pipeline 3. In Test Set B, pipelines were displaced at a much more uniform speed. The maximum speed was 6.5×10^{-6} m/sec (prototype scale), and the minimum was 1.25×10^{-6} m/sec. A variation of less than 5 percent was maintained for all tests.

The peak loads normalized against shear strength (of the backfill) can be represented by

$$\frac{\text{Peak resistance per unit length}}{\text{backfill shear strength}} = 10.01 \pm 11 \text{ percent} \qquad (4)$$

and the distance to 90 percent of the peak resistance is given by

Displacement to 90 percent peak load

$$= 0.15 \text{ m} \pm 12 \text{ percent} \qquad (5)$$

Overall, for all data sets, the normalized peak resistance is given by

$$\frac{\text{Peak resistance per unit length}}{\text{backfill shear strength}} = 10.86 \pm 20 \text{ percent} \qquad (6)$$

and the distance to 90 percent of the peak resistance can be expressed by

Displacement to 90 percent peak load

$$= 0.18 \text{ m} \pm 39 \text{ percent} \qquad (7)$$

TABLE 3 Summary of Test Set A Pipeline Results

	Pipeline 1	Pipeline 2	Pipeline 3	Pipeline 4
Peak Resistance per Unit Length (kN/m)	196	131	182	118
Normalised Peak Resistance (m)	11.30 (8.91)	10.45 (9.49)	12.43 (10.34)	12.13 (11.52)
Post Peak Minimum Resistance (kN/m)	179	127	174	88
Normalised Minimum Resistance (m)	10.32 (8.14)	10.13 (9.20)	11.89 (9.88)	9.04 (8.59)
Distance to Peak Resistance (m)	0.61	0.63	0.34	0.26
Distance to 90% of Peak Resistance (m)	0.25	0.20	0.21	0.19
Distance to Minimum Resistance (m)	1.73	1.21	0.57	0.91
Evidence of Desiccation	Strong	Strong	Strong	Weak
D_d, Distance to Peak Resistance per Unit Length = 8.263 C_u*D	0.151D	0.071D	0.119D	0.131D

(The figures in brackets refer to the native material)

DISCUSSION OF RESULTS

Force-Displacement Curves

The equations presented in an earlier section of the paper show the normalized peak loads and the distance to 90 percent peak load. It can be seen that the uncertainty bands are fairly low; however, the mean values for the two different tests (for both displacement and load) vary widely. This indicates that the results of these tests must have been influenced by desiccation, the only factor that varied considerably between tests.

The initial portions of the traces all coincide (see Figure 5). At a normalized resistance of about 9 C_u, the displacement curves begin to diverge, but before this point they are essentially the same curve. This might be the zone of elastic deformation, but the displacements at this stage are rather large (0.15 m, prototype scale) for this to be the case.

A theoretical means of predicting the stresses on a pipeline due to relative motion is thus given by this linear portion. If a benchmark nondimensionalized, normalized resistance [peak resistance per unit length/(C_u * pipeline diameter)] of approximately 8.3 is considered, this normalized resistance will be reached when the displaced distance, D_d, is approximately 0.125 pipeline diameters (0.12 m). This would give an indication of the correct point for remedial action. D_d values for each of the tests are presented in Tables 3 and 4.

Comparison of Centrifuge Modeling and SOP

Table 5 compares the backcalculated interaction factor N of Equation 1 from the centrifuge tests with the recommended factors of Hansen (*4*) and Rowe and Davis (*2*). For the conditions modeled, the Hansen interaction factors tend to underestimate the magnitude

TABLE 4 Summary of Test Set B Pipeline Results

	Pipeline 1	Pipeline 2	Pipeline 3	Pipeline 4
Peak Resistance per Unit Length (kN/m)	85	69	73	74
Normalised Peak Resistance (m)	11.66 (10.00)	9.47 (8.12)	10.01 (8.81)	10.15 (8.93)
Post Peak Minimum Resistance (kN/m)	74	64	62	72
Normalised Minimum Resistance (m)	10.15 (8.71)	8.78 (7.53)	8.50 (7.48)	9.89 (8.68)
Distance to Peak Resistance (m)	0.27	0.23	0.21	0.22
Distance to 90% of Peak Resistance (m)	0.16	0.15	0.15	0.13
Distance to Minimum Resistance	0.69	0.46	1.06	0.74
Evidence of Desiccation	Weak	None	None	None
D_d, Distance to Peak Resistance Per Unit Length = 8.263 C_u*D	0.119D	0.156D	0.140D	0.115D

(The figures in brackets refer to shear strengths in the native material)

TABLE 5 Comparison of Experimentally Derived Interaction Factors and SOP Factors

Test Set	Pipeline	Evidence of Desiccation	Experimental Interaction Factor (N) Normalized to Backfill Strength	Experimental Interaction Factor (N) Normalized to In Situ Strength	Experimental Interaction Factor (N) Normalized to Average Strength	CGL Recommended Interaction Factor (N) Based on Hansen (1961)	Rowe and Davis (1982) Interaction Factors (N) Assuming Immediate Breakaway	Rowe and Davis (1982) Interaction Factors (N) Assuming No Breakaway
A	1	Strong	11.9	9.4	10.5	5.5	4.3	9.5
A	2	Strong	11.0	10.0	10.5	6.0	4.7	11.1
A	3	Strong	13.1	10.9	11.9	5.5	4.3	9.5
A	4	Weak*	12.8	12.1	12.4	6.0	4.7	11.1*
B	1	Weak*	12.3	10.5	11.3	5.5	4.3	9.5*
B	2	None*	10.0	8.5	9.2	6.0	4.7	11.1*
B	3	None*	10.5	9.3	9.9	5.5	4.3	9.5*
B	4	None*	10.7	9.4	10.0	6.0	4.7	11.1*

of loads transferred to the pipeline by nearly 50 percent. Similarly, the Rowe and Davis factors assuming "immediate breakaway" conditions significantly underestimate the loads transferred to the pipe.

There is agreement between the experimentally derived interaction factors and the Rowe and Davis factors for the "no breakaway" conditions for the five tests marked with an asterisk in Table 5. Reasonable agreement (within ± 20 percent) was achieved in these cases. The development of such a condition was unlikely for the following reasons:

1. Rowe and Davis note in their paper that tension cracking for shallow anchors and pipes (embedment ratio less than 3) as modeled in the present study would be expected to relieve suction and reduce the soil's bearing resistance. This would lead to a condition nearer to the "immediate breakaway" limit of their formulation.
2. The experimental setup precluded the development of suction behind the displaced pipeline by introducing air through the conduit around the pulling cables and in turn through the partially hollow pipe section.
3. The very large pipe displacements probably dissipated the suction that might have developed at the onset of the displacement. This would have been reflected as a postpeak drop in the measured load-displacement response. No significant postpeak drops in resistance were observed.
4. The values of interaction factors in the asterisked tests are very similar to those measured for the first three tests, in which strong physical evidence of breakaway was observed. It should follow that similar interaction factors would arise from similar breakaway conditions.

The practical implications of the SOP formulations underestimating the magnitude of ground movement induced loads being transferred to a buried pipeline are significant. Whereas further testing is certainly required to verify the results of this preliminary study, indications are that the lateral pipe/soil interaction inputs to pipeline stress analysis based on the presently accepted formulations may lead to errantly favorable assessments of the integrity and operating safety of pipelines in unstable ground conditions. Such errant assessments may contribute to decisions delaying necessary remedial strain-relieving operations.

SUMMARY AND CONCLUSIONS

Eight model pipelines were tested in a centrifuge at 50 g to investigate the soil response to laterally displaced buried pipelines. The experimental program is relevant to studies being carried out by pipeline engineers to determine the effects of slowly creeping slopes on buried pipelines. The two primary objectives of this experimental investigation were to obtain force-displacement curves for the buried pipelines and to ascertain the effects of trench width and cover depth.

As a result of the experimental program and comparison with SOP, the following conclusions were reached:

1. Centrifuge modeling is a suitable technique for determining the soil response to laterally loaded pipelines.
2. For model pipelines 0.95 m in diameter, average peak loads per unit length of 11.7 and 10.0 times the shear strength of the soil were recorded for desiccated and saturated soils, respectively. The lateral displacements required to develop 90 percent of the peak loads were 0.21 and 0.15 m.
3. The loads predicted by the SOP are approximately half of those measured in this test program. The current SOP may be unconservative.
4. For most samples, the distance required to develop a peak resistance per unit length of approximately $8.3C_u * D$ (a suitable benchmark) was approximately 0.125 pipeline diameters.
5. The effects of trench geometry were negligible compared with effects due to variations in soil properties.
6. A further test program is required to elucidate the effects of trench geometry when there is a significant difference between backfill and native material properties and to investigate the effect that rate (and hence drainage) has on the lateral load transfer to a pipeline.
7. Future refinements to pipe/soil interaction modeling should use centrifuge modeling to complement numerical modeling work.

ACKNOWLEDGMENTS

The authors gratefully acknowledge the support of NOVA Gas Transmission Division management and the Natural Sciences and Engineering Research Council for their support of this study. Spe-

cial thanks are extended to Jacques Garnier and the capable staff at LCPC and to Ryan Phillips and Paul Lach of C-CORE, who conducted the technical review. The authors thank Gail Greenslade for the careful preparation of this manuscript and Eleanor Nesbitt for the editorial review.

REFERENCES

1. Rizkalla, M., F. Poorooshasb, and J. I. Clark. Centrifuge Modeling of Lateral Pipeline/Soil Interaction. *Proc., 11th Offshore Mechanics and Arctic Engineering Conference*, Calgary, Alberta, Canada, 1992.
2. Rowe, R. K., and E. H. Davis. The Behaviour of Anchor Plates in Clay. *Geotechnique*, Vol. 32, No. 1, 1982, pp. 1–24.
3. Committee on Gas and Liquid Fuel Lifelines. *Guidelines for the Seismic Design of Oil and Gas Pipeline Systems.* American Society of Civil Engineers, 1984.
4. Hansen, J. B. *The Ultimate Resistance of Rigid Piles Against Transversal Forces.* Bulletin 12. Danish Geotechnical Institute, Copenhagen, Denmark, 1961.
5. Mitchell, R. J. Centrifuge Modeling as a Consulting Tool. *Canadian Geotechnical Journal,* Vol. 28, 1991, pp. 162–167.
6. Poorooshasb, F. On Centrifuge Use for Ocean Research. *Marine Geotechnology,* Vol. 9, 1990, pp. 141–158.
7. Corté, J. F. Preface to Centrifuge '88. In *Centrifuge '88: Proceedings of the International Conference on Geotechnical Centrifuge Modeling* (J. F. Corté, ed.), A. A. Balkema, Rotterdam, Netherlands, 1988.
8. Schofield, A. N. Twentieth Rankine Lecture: Cambridge Geotechnical Centrifuge Operations. *Geotechnique,* Vol. 30, No. 3, 1980, pp. 227–268.

Publication of this paper sponsored by Committee on Subsurface Soil-Structure Interaction.

Overstressed Precast Concrete Pipe Arch and Its Redesign

JAMES J. HILL AND FLOYD J. LAUMANN

In 1967, a large precast concrete pipe arch was installed on Trunk Highway 90 in Worthington, Minnesota, under a high fill. Some cracking in the haunches of the pipe arch was observed after a heavy rainfall in 1969. Analyses of the original D-load design and a direct field load design that was completed after the failure are presented. The direct design indicated a need for additional shear steel in the haunch locations. A rehabilitation method that proved successful in keeping the arch pipe functional for the last 23 years is included.

In October 1967 a 3100- × 1980-mm (122- × 78-in.) precast concrete arch pipe was installed under I-90 in Worthington, Minnesota, with an overfill of 7.2 m (24 ft). A Class IV, D-load design pipe was used at this installation (see Figure 1 for details of structural design). After a heavy rain in June 1969, some sections of the pipe were observed to have severe structural distress. Longitudinal cracks were located roughly at the junction of the long-radius base slab and the short-radius lower haunches of the pipe as shown in Figure 2. In general there was only one crack in each cracked pipe section, but they were not all on the same side. Several of the cracks had opened up about 50 mm (2 in.) and were observed to extend diagonally downward and inward toward the centerline of the culvert in an orientation typical of a diagonal tension failure (see Figure 2). However, in most of the 8-ft pipe section, the cracks had not opened up sufficiently to observe crack orientation and depth. A routine inspection conducted several months earlier did not show any signs of distress. Thus, it was concluded that the heavy runoff caused the structural distress. There was no indication of piping or water running alongside or under the culvert. However, saturation of the surrounding soil may have occurred from water flowing through the joints. This may have resulted in loss of lateral soil support and subsequently increased stresses in the pipe.

According to the construction inspector, all pipe sections were placed on a high-quality bedding consisting of about 150 mm (6 in.) of sand/gravel material that overlaid the in situ silty clay soil. To obtain good bearing, the bedding was template shaped for almost the full width of the pipe. Several feet of compacted backfill was placed adjacent to the pipe to an elevation above the springline (see Figure 3). By using the rated three-edge bearing (TEB) strength of a Class IV pipe with 7.2-m (24-ft) overfill and a Class B bedding, the safety factors for loading are 1.0 for a 0.25-mm (0.01-in.) crack and 1.5 for ultimate load. [$D_{0.25\ mm\ (0.01\ in.)} \leq 100$ N/lin. m (2,000 lb/lin. ft); $D_{ult.} \leq 150$ N/lin. m (3,000 lb/lin. ft) for Class IV pipe.]

J. J. Hill, Minnesota Department of Transportation Bridge Office, 1500 W. County Road B2, Roseville, Minn. 55113. F. J. Laumann, Hancock Concrete Production Co., Inc., 5275 Edina Industrial Blvd., Minneapolis, Minn. 55439-2919.

DESIGN PROCEDURES

The original design of precast concrete arch pipes was based on D-loading criteria. These arch pipes were introduced as culvert members in the early 1960s in Minnesota. Their design was based on the standard TEB test method specification in ASTM C497 and ASTM C506. See Figure 4 for original design results of shear steel location and magnitude.

The pipe was not TEB tested but was state inspected to ensure proper steel area was used and placed correctly. Concrete cylinders were taken and tested to meet the minimum requirement of 34.5 MPa (5,000 psi).

For installations under high fills, the indirect design method, based on TEB tests and bedding factors, is inappropriate. TEB tests create a maximum flexural and shear force near the center of the pipe invert. Pipe designers provide the necessary flexural and radial reinforcing steel at these locations so the pipe will pass the TEB test. When a pipe is properly installed, the bedding material provides uniform support to the pipe invert. Uniform support, differing from the TEB test condition, shifts the point of maximum shear out from the center of the pipe toward the edges of the pipe invert. Uniform support also increases the ability of the pipe to support vertical loads that are greater than the load applied during a TEB test. Therefore, installed pipes must resist shear loads at locations different from a similar pipe designed to pass a TEB test. For high overfill installations a direct design method based on actual installed conditions provides a better means of analysis than the traditional indirect design method. See Figure 4 for direct design results of shear steel locations and magnitudes.

DIRECT DESIGN ANALYSIS

A structural direct design analysis of the in-place pipe was made by Minnesota Department of Transportation and a consultant using the actual field loads and bedding conditions as shown in Figure 5. (This included eccentric loadings.) Results indicated shear (diagonal tension) failure where the actual cracking occurred. Lack of shear steel at these locations allowed cracking to occur, which resulted in wall shear failures (see Figures 2 and 4). As a result of these analyses, additional shear reinforcement was added in these locations.

In 1972 the Minnesota Department of Transportation produced a new structural design table for precast concrete pipe arches using the direct design analysis. Pipe sizes ranged in span from 560 to 4290 mm (22 to 169 in.). Standard AASHTO load factors of 1.5 for dead load and 2.5 for live load were used. The analysis assumed a bedding support of 80 percent of the bottom width and

1967 DESIGN DATA OF CLASS IV PIPE			
RISE			1980MM (78 IN.)
SPAN			3100MM (122 IN.)
THICKNESS			230MM (9 IN.)
① CONTINUOUS BASIC REINF.	INNER CAGE		16.3 (0.77)
	OUTER CAGE		11.9 (0.56)
① ADDITIONAL CAGE REINF.	U (INNER CAGE)	LGTH.	2.1M (6'-10")
			16.3 (0.77)
	V (OUTER CAGE)	LGTH.	4.9M (16'-0")
			11.9 (0.56)
f'c CL. IV			34470KPa (5KSI)
WEIGHT PER M (FT.)			4900Kg (3300 LB.)

① REINFORCEMENT AREA SHOWN IS MINIMUM CIRCUMFERENTIAL STEEL AREA IN SQUARE MM (INCHES) PER LINEAL CM (FT.) OF PIPE BARREL.

STIRRUP REQUIREMENTS
X=1.8M (6'), As=16.3 (.77)
Y=2.1M (7'), As=33.2 (1.57)
MINIMUM SPACING 300MM (12 IN.)

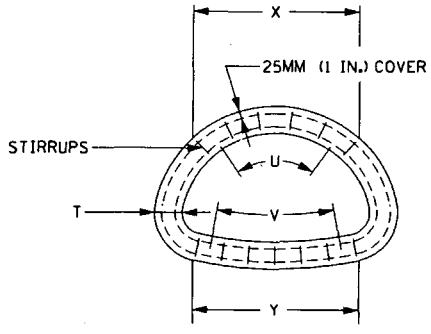

FIGURE 1 Details of structural design, Class IV pipe, 1967.

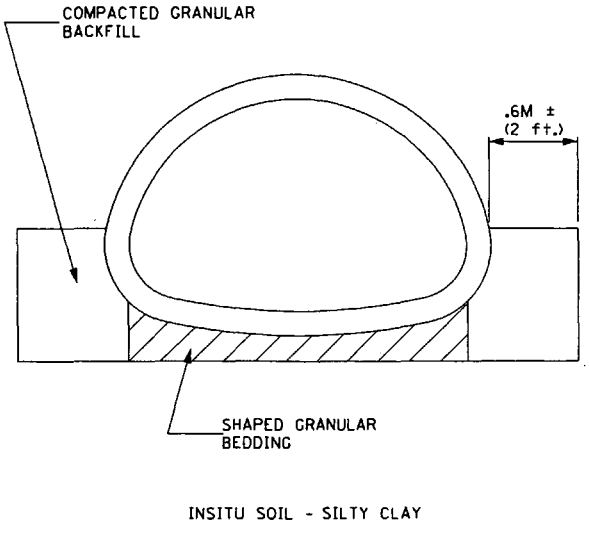

FIGURE 3 Typical installation.

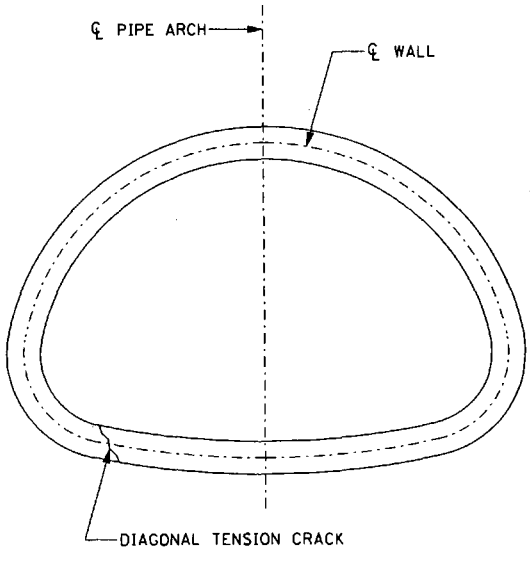

FIGURE 2 Diagonal tension failure.

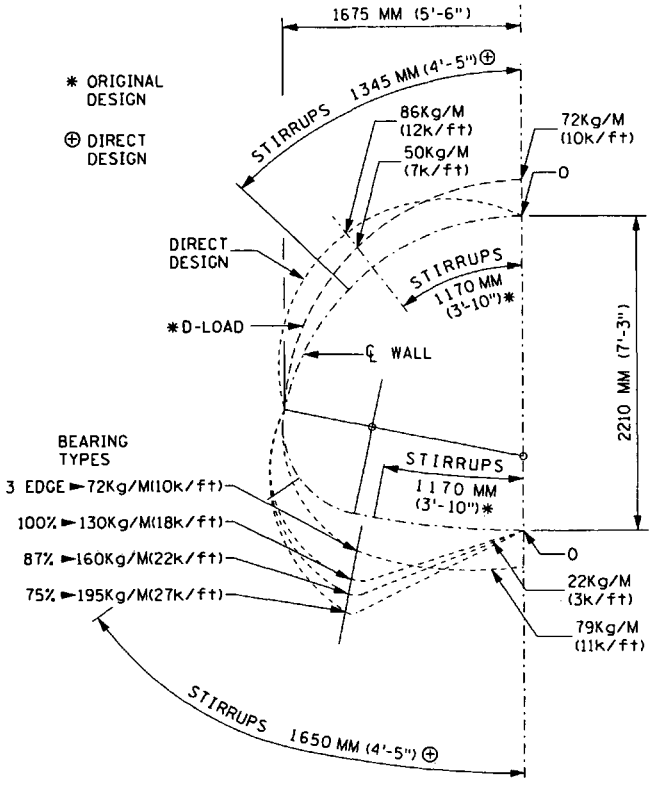

FIGURE 4 Original and direct design results.

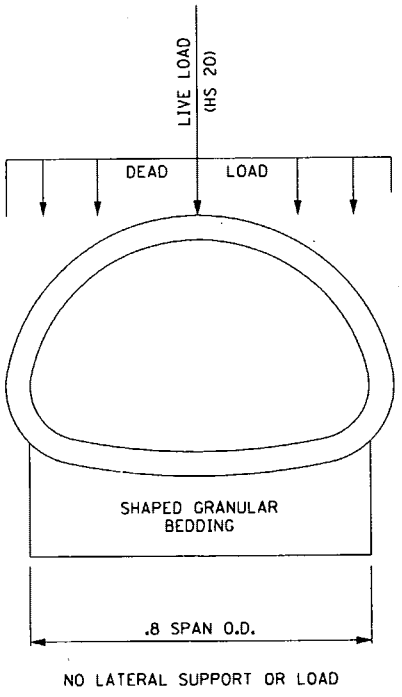

FIGURE 5 Direct design load assumption.

1972 DESIGN DATA OF CLASS IV PIPE			
RISE			1980MM (78 IN.)
SPAN			3100MM (122 IN.)
THICKNESS			230MM (9 IN.)
(1) CONTINUOUS BASIC REINF.	INNER CAGE		19.1 (0.90)
	OUTER CAGE		18.9 (0.89)
(1) ADDITIONAL CAGE REINF.	U (INNER CAGE)	LGTH.	1.2M (3'-10")
			4.7 (0.22) TOP
			19.1 (0.90) BOT
	V (OUTER CAGE)	LGTH.	2.6M (8-6")
			18.8 (0.89)
f'c CL. IV			34.5MPa (5KSI)
WEIGHT PER M (FT.)			4880Kg (3285 LB.)

STIRRUP REQUIREMENTS
X=1.35M (4'-5"), As1=.14 (.2), MAX. SPCG. 175M (7 IN.)
Y=1.00M (3'-3"), As1=.47 (.67), MAX. SPCG. 100M (4 IN.)
Z=0.66M (2'-2"), As1=.14 (.2), MAX. SPCG. 175M (7 IN.)

As1=MINIMUM STEEL AREA IN SQUARE MM (INCHES) PER SQ. CM. (FT.) OF WALL MEASURED AT ℄ OF WALL.

(1) As=CIRCUMFERENTIAL STEEL AREA IN SQUARE MM (IN.) PER LIN. CM (FT.) OF PIPE BARREL.

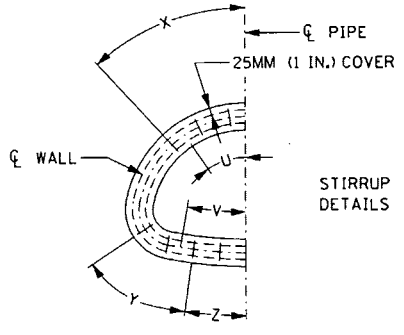

FIGURE 6 Details of structural design, Class IV pipe, 1972.

TABLE 1 Pipe Properties

Nominal Pipe Diameter(in)	124
Concrete Compressive Strength(psi)	5000
Concrete Elastic Modulus(psi)	4286826
Concrete Poisson Ratio	0.17
Density of Pipe(pcf)	0
Steel Yield Strength(psi)	60000
Steel Elastic Modulus(psi)	29000000
Steel Poisson Ratio	0.3
Concrete Cracking Strain	0
Concrete Yielding Strain	0.000566
Concrete Crushing Strain	0.002
Steel Yielding Strain	0.001883
Wall Thickness(in)	9

TABLE 2 Properties of In Situ Material (Duncan Soil Model Parameters)

Soil Classification	sc 100
Density	120
Cohesion Intercept	3.472
Friction Angle	0.576
Scaled Modulus Number	400
Modulus Exponent	0.6
Failure Ratio	0.7
Bulk Modulus Number	200
Bulk Modulus Exponent	0.5

TABLE 3 Properties of Bedding and Backfill Material (Duncan Soil Parameters)

Soil Classification	sm100
Density(pcf)	120
Cohesion Intercept	0
Friction Angle	0.628
Scaled Modulus Number	600
Modulus Exponent	0.25
Failure Ratio	0.7
Bulk Modulus Number	450
Bulk Modulus Exponent	0

TABLE 4 Stresses in Culvert Wall (psi)

Nodes	Inner Cage Steel	Outer Cage Steel	Concrete Compression	Shear Stress
1	12583	-6433.8	-1397.8	0
2	10141	-5535.1	-1184.3	28.92
3	3608	-3105.4	-609	47.59
4	-2382.9	2281.2	454.3	53.04
5	-5512.9	14098	-1286	46.88
6	-7744.4	22871	-1888.3	9.3
7	-6243.1	18134	-1514.2	-54.77
8	-425.6	-297.6	-62.4	-84.5
9	10530	-4565.9	-1034.6	-65.2
10	17240	-6849.4	-1590.5	-32.83
11	19529	-7616.3	-1778.1	0

TABLE 5 Strains in the Inner and Outer Fiber of the Culvert Wall

NODES	INNER STRAIN	OUTER STRAIN
1	0.00050959	-0.00031664
2	0.00041281	-0.00026828
3	0.00015373	-0.00013796
4	-0.00010292	0.00099729
5	-0.00029133	0.00056071
6	-0.00042776	0.00090242
7	-0.00034301	0.00071614
8	-0.00014129	-0.00000856
9	0.00042151	-0.00023437
10	0.00068635	-0.0003603
11	0.0007766	-0.0004028

no lateral support on the sides (see Figure 5). An 80 percent bearing width is more realistic because of the difficulty in obtaining compaction under the haunches. If good installation methods are used, lateral side support may be used in the analysis. Spans of 2590 mm (102 in.) or more required shear steel to be extended into the haunches where the diagonal cracks had occurred. Previous D-load designs had only required shear steel in the bottom and top of the arch. (See Figures 4 and 6 for new stirrup requirements.)

A recent analysis of 3100- × 1980-mm (122- × 78-in.) arch pipe was made using CANDE (culvert analysis and design software) version 1980. The Duncan soil model was used. The properties of the in situ silty clayey sand used in the model were as follows:

Location	*Type of Soil*	*Relative Compaction (%)*
In situ soil	Silty clayey sand	100
Bedding	Silty sand	100
Backfill	Silty sand	100

Density of in situ soil, bedding, and backfill was taken as 1.54 kg/m^3 (120 pcf).

The Duncan model is a nonlinear stress-strain model. The interface model, which takes into consideration the relative movement of the soil with respect to the pipe at the pipe-soil interface, was adopted for the analysis. Thus at each load step, tensile separation, frictional movement, and complete bond of the interface are possible. The pipe wall was divided into 10 elements that gave

TABLE 6 Safety Factors

Parameter	Ratio	Safety Factor	
		Desired	Compute
Concrete Crushing	Concrete Strength/ Max. Compressive Stress	>=2	2.648
Steel Yielding	Steel Yield Stress/ Max. Steel Stress	>=2	2.623
Diagonal Cracking	Wall Shear Capacity/ Max. Shear	>=2	1.32
Crack Width	0.01 inch/ Max Crack width	1	2.493
Bowstringing	Tensile Strength/ Stress From Bow String	1	4.897
Displacement	Allowable Displacement /Max. Disp	1	0.63

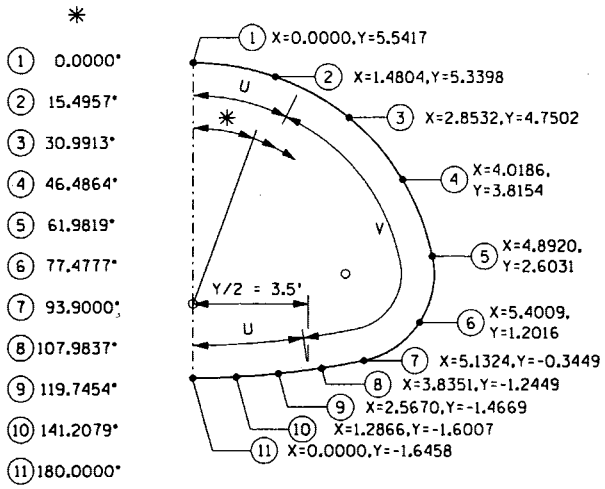

FIGURE 7 Computer analysis, 122-in. span.

output results corresponding to the 11 pipe nodes. (See Tables 1 through 6 and Figure 7 for input and output parameters.)

In the 1967 pipe design under consideration, a major crack was observed in the bottom of the pipe just outside the stirrup zone Y. From our CANDE analysis it was found that maximum shear stress was at Node 8, which is just outside the 1967 designed stirrup zone Y. The magnitude of this shear stress is 12.25 kPa (84.5 psi) > 0.95 $\sqrt{f'}$ c = 9.75 kPa (67.2 psi)—the allowable shear stress for concrete.

The safety factor for tensile stress was 1.32 (less than desirable value of 2), and the performance factor for bowstringing was 0.63 (less than desirable value of 1.0), suggesting that failure could have been due to a combination of diagonal tension and bowstringing action. See accompanying CANDE program input and output.

REHABILITATION OF ARCH PIPE

The distressed pipe and culvert sections were rehabilitated in 1970 with a vertical strut system using wide flange steel supports (see Figure 8). Galvanized sheets were placed over both sides of the vertical struts to reduce the potential for debris accumulation.

Holes were cored through the wall haunch areas to facilitate pressure grouting of haunch voids. About 5.5 m^3 (7 yd^3) of grout was used, indicating that considerable voids existed. As a result of these rehabilitation measures, the culvert is still functioning adequately.

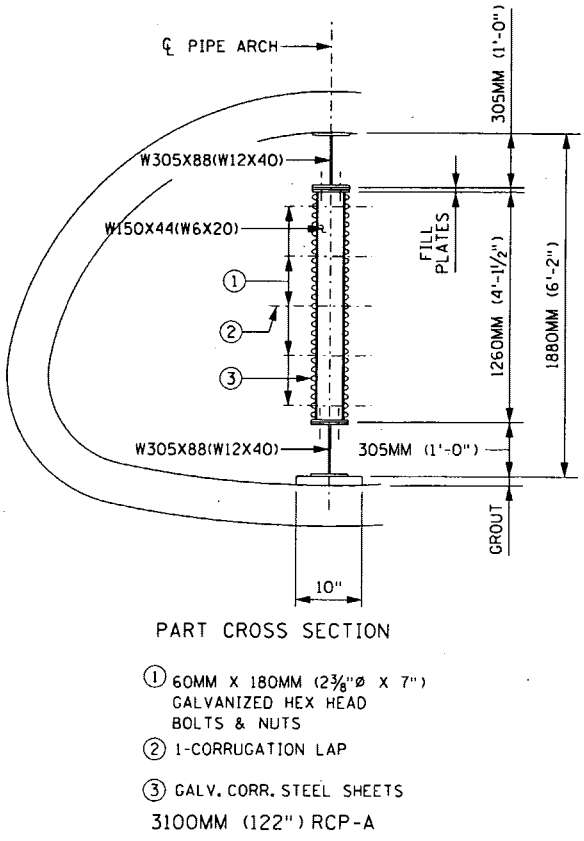

FIGURE 8 Rehabilitation of distressed arch pipe.

None of the arch pipe produced and installed since 1972 using the direct design analysis shows any signs of structural distress.

CONCLUSIONS

- Use an adequate amount of shear steel in top and bottom of arch pipe based on direct design loadings.
- Allow for loss of side support in questionable fill materials. To obtain lateral support, good fill materials and adequate compaction are required.
- Shaped granular beddings (0.8 span outside diameter) beneath arch pipes will provide uniform bearing pressures, which can be realistically achieved.
- Design of arch pipes with about 0.60 m (2 ft) of fill over them should include varying locations of concentrated live loads.

Publication of this paper sponsored by Committee on Subsurface Soil-Structure Interaction.

Rigid Pipe Distress in High Embankments over Soft Soil Strata

FRANK J. HEGER AND ERNEST T. SELIG

Two case histories of severe distress in actual rigid pipe installations are presented. They illustrate how soft soils in the region below the outer haunch or adjacent to the pipe within one diameter beyond the sides of the pipe resulted in significant increases in the load on the pipe and the shear and bending stress resultants, producing extensive flexural cracking and failures in diagonal and radial tension. For each installation, the pipe design and installation designs are presented along with a description of the failure. The results of soil-structure interaction analyses using the computer program SPIDA are presented on the basis of two models, one modeling the soft soils that existed at each side and the other modeling the same installation with the soft soils replaced by compact in situ or placed granular soils. The results show how the presence of soft soils under high fills increases the earth load and structural effects on the pipe compared with pipe in conventional installations. The results also show that the pipes in each of the two installations were not properly designed for the 18- to 20-m (60- to 65-ft) finished heights of fill over the pipe, even without the presence of the soft soils.

Pipe loads that exceed the earth load calculated using conventional Marston-Spangler theories for loads on positive and negative projecting embankments and sloping wall trenches (*1*) can occur in installations where the pipe itself is placed on a firm bedding and foundation, but the in situ soil in a subtrench wall, or embankment, adjacent to the bedding or to the pipe itself is soft. Two examples are described in this paper, showing how installations of this type resulted in excessive earth loads on the respective pipe culverts, causing large crack widths and shear and radial tension failures in the concrete pipe. The results of comparative soil-structure interaction analyses for determining the earth load and pressure distribution on the pipe in each installation, with and without the soft soil strata adjacent to the pipe, are presented.

PIPE AND SOIL INSTALLATION AT SITE 1

A precast concrete pipe culvert installed at Site 1 includes approximately 345 m (1,130 ft) of 2700-mm (108-in.) pipe, 98 m (320 ft) of 2850-mm (114-in.) pipe, and 173 m (566 ft) of 3000-mm (120-in.) pipe. The specified pipe strength is Class 5. The culvert pipes were placed in a subtrench cut into the earth using a shaped bedding with a sand cushion 150 mm (6 in.) thick between the lower part of the pipe and the in situ soil. The installation configuration is shown in Figure 1. At the site, the top of the original ground varies within a range between the top of the pipe and the lower quadrant of the pipe. The nature and thickness of the top layer of original ground vary. Most typically it is composed of 1 to 2 m (3 to 6 ft) of medium to soft soils, often with substantial amounts of clay, overlying a sandstone or shale rock substratum. The earth cover above the top of the pipe varies between about 15 and 18 m (50 and 65 ft) throughout most of the finished installation. However, the pipes failed and were repaired before that height of cover was reached.

The type and relative stiffness of the existing soils shown in Figure 1 were obtained from borings taken before construction of the culvert and embankment. The standard specifications used for construction of the embankment did not require removal of the soft soils that overlie the shale or sandstone substratum before placing the embankment.

Generally, the bottom of the pipe is located close to the top of the shale or sandstone. The remainder of the lower portion of the pipe is founded on the 150-mm (6-in.) sand cushion over the medium stiff to soft clay in situ soil that overlies the hard substratum as shown in Figure 1. Note from Figure 1 that the highly compacted select granular soil in the subtrench under and adjacent to the pipe haunches is founded on the medium to soft clay in situ soil below the bottom of the subtrench, whereas the sand layer 150 mm (6 in.) thick at the invert region of the pipe bottom is founded on the much stiffer shale or sandstone substratum.

The pipe manufacturer's design for the specified Class 5 pipe uses an arrangement of circumferential reinforcement consisting of full circular cages located near the inside and outside surfaces and additional mat reinforcement located near the inside surface in 90-degree quadrants centered on the crown and the invert. The pipe also has radial ties (i.e., stirrups) anchored to the inside cages and extending over the crown and invert quadrants. The design wall thicknesses, reinforcement areas, and welded wire fabric sizes used in the pipe are given in Table 1.

Stirrups were prefabricated in three-dimensional panels using cold drawn wire conforming to ASTM A82 [minimum yield strength 448 MPa (65,000 psi) after welding into fabric]. The stirrups are loops of two No. 10 wires resistance welded to No. 7 gauge wires extending longitudinally across the inside of the inside cage. The closed ends of the stirrup loops extend across the wall almost to the outside cage.

Three production pipes in each pipe size were subject to three edge bearing tests. The 0.01-in. crack strengths exceeded the specified 3000D strength by about 15 percent for the 2700- and 2850-mm (108- and 114-in.) pipe and by about 40 percent for the 3000-mm (120-in.) pipe. The ultimate strengths exceeded the specified 3750D strength within a range of about 0 to 20 percent. The test pipe typically failed in diagonal tension in the region containing stirrup reinforcing. The loads that produced diagonal tension (shear) failure exceeded the calculated strength for a pipe without stirrups and are estimated to have developed, or somewhat

F. J. Heger, Simpson Gumpertz and Heger, Inc., 297 Broadway, Arlington, Mass. 02174. E. T. Selig, Department of Civil Engineering, University of Massachusetts, 28 Marston Hall, Amherst, Mass. 01003.

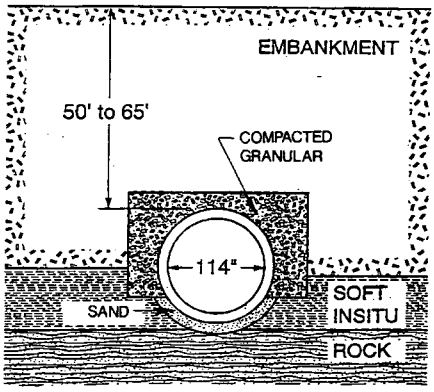

FIGURE 1 Idealization of typical installation at Site 1.

exceeded, the stirrup wire nominal yield strength of 448 MPa (65,000 psi), with failure at the anchorage of stirrups to inner reinforcing cage.

Compression tests on cores 150 mm (6 in.) in diameter taken from three cracked pipes indicated average strengths of 52.9 MPa (7,671 psi), 57.3 MPa (8,306 psi), and 38.1 MPa (5,531 psi), respectively.

When the level of backfill over the pipe culvert reached 12 to 14 m (40 to 46 ft), an inspection of the culvert interior revealed extensive longitudinal cracking with radial displacements and delamination of concrete cover over inner reinforcement in many pipes. Vertical and horizontal diameters were measured in 56 pipe sections. The largest decreases in vertical diameter were 94 mm (3.7 in.), 53 mm (2.1 in.), and 58 mm (2.3 in.) for pipe of diameter 2700, 2850, and 3000 mm (108, 114, and 120 in.), respectively. The largest increases in horizontal diameter were 76, 53, and 33 mm (3.0, 2.1, and 1.3 in.) for pipe of diameter 2700, 2850, and 3000 mm (108, 114, and 120 in.), respectively.

The difference between the measured horizontal and vertical diameters gives an indication of whether the pipe section probably has failed and also of the severity of the failure. The number of pipe sections (of the 56 sections that were measured) with various ranges of difference between measured horizontal and vertical diameter are given in Table 2. A difference between horizontal and vertical deflection greater than about 25 mm (1 in.) is indicative of failure by yielding of inner cage reinforcement, or, more likely, by diagonal or radial tension.

The predominant failure was diagonal tension (shear) and slabbing in the invert region at about 5 or 7 o'clock. This failure consisted of failure of stirrup anchorage at the inside cage, diagonal cracking with radial displacement on the inside surface, and local delamination of inside concrete cover in the vicinity of the failure area. In some of the most distressed pipes, an additional diagonal tension failure occurred just beyond the end of the stirrups and reinforcing mat in the crown region at about 2 o'clock. These shear failures exhibited greater radial offsets than the shear failures in the stirrup-reinforced invert regions. The pipe with diagonal tension failures generally had measured differences between the shortened vertical diameter and lengthened horizontal diameter that were 38 mm (1.5 in.) or greater. Several pipe sections exhibited fine vertical cracking and flaking of concrete on the inside surface of the compression zone at the springline, indicative of the onset of a flexural compression failure at the springline.

SOIL-PIPE INTERACTION ANALYSIS AND DESIGN—SITE 1

Soil-pipe interaction analyses and design studies were performed using the computer program SPIDA (*1,2*) to analyze a representative installation with the 2850-mm (114-in.) inside diameter, 241-mm (9.5-in.) wall pipe used in a portion of the pipeline. The pipe-soil installation was modeled as shown in Figure 2, using two different soils to represent the existing in situ soil above the shale/sandstone foundation. In the first model, this soil was taken as a medium-to-soft silty clay soil, the condition most representative of the worst locations at the site, and was represented by standard 90 and 95 percent CL soils as equivalent to the silty clay in situ soils shown in certain borings located near the pipelines. In the second model, the in situ soil in Layers 2 and 3 of Figure 2 was taken as a very firm silty sand in situ soil and was repre-

TABLE 1 Site 1 Pipe Wall and Reinforcement Design

Inside Diameter mm (in.)	Wall Thickness mm (in.)	Concrete Stress f_c' MPa (psi)	Area of Circumferential Reinforcement			Welded Wire Fabric Reinforcement	Shear Stirrups (Invert and Crown Region)	
			Quadrant Location	Inner mm^2/m ($in.^2/ft$)	Outer mm^2/m ($in.^2/ft$)		Circular Spacing mm (in.)	Area/line $mm^2/m/line$ ($in.^2/ft/line$)
2700 (108)	254 (10)	41.4 (6000)	Crown & Invert	2411 (1.14)	1206 (.57)	50 mm x 200 mm (2 in. x 8 in.) (D9.5/W3.5)	117 (4.6)	360 (.17)
			Springline	1206 (.57)	1206 (.57)		NA	NA
2850 (114)	241 (9-1/2)	41.4 (6000)	Crown & Invert	2919 (1.38)	1460 (.69)	50 mm x 200 mm (2 in. x 8 in.) (D11.5/W4.5)	117 (4.6)	360 (.17)
			Springline	1460 (.69)	1460 (.69)		NA	NA
3000 (120)	279 (11)	41.4 (6000)	Crown & Invert	2665 (1.26)	1333 (.63)	50 mm x 200 mm (2 in. x 8 in.) (D10.5/W4.0)	117 (4.6)	360 (.17)
			Springline	1333 (.63)	1333 (.63)		NA	NA

NA = Not applicable

TABLE 2 Measured Differences Between Horizontal and Vertical Diameters

Pipe Diameter mm (in.)	No. of Section Measured	No. of Sections Within Ranges of Differences Between Measured Horizontal and Vertical Diameters, mm (in.)							
		0-19 (0-.74)	19-36 (.75-1.4)	38-48 (1.5-1.9)	51-74 (2-2.9)	76-99 (3-3.9)	102-125 (4-4.9)	127-150 (5-5.9)	152-175 (6-6.9)
2700 (108)	35	7	3	2	13	3	2	2	3
2850 (114)	8	1	0	1	2	3	1	0	0
3000 (120)	13	7	1	3	1	1	0	0	0

sented by standard 100 percent ML soils as equivalent to the in situ soil.

RESULTS OF SPIDA ANALYSIS AND DESIGN

The results of the soil-structure analyses for the pipe of 2850 mm (114 in.) inside diameter are given in Table 3 for each installation model. The maximum diagonal and radial tension strength of the pipe is governed by the maximum stirrup design factor, SDF, provided in the pipe design given in Table 1. SDF equals the area of stirrup reinforcing per foot of pipe length per line of stirrup times the maximum stirrup stress (yield or developable anchorage stress) divided by the stirrup spacing, circumferentially. The three edge bearing test results showed that the stirrups provided in the manufacturer's pipe design produced an SDF of approximately 1500 to 1650 N/mm/m (2,600 to 2,900 lb/in./ft) and a calculated stirrup stress of 483 to 517 MPa (70,000 to 78,000 psi).

The maximum height of fill that should have been placed on the pipe, on the basis of a SPIDA analysis and design using the load and resistance factors specified in Section 17 of the AASHTO Bridge Specification (*3*) and the ASCE SIDD Standard Practice (*4*), is about 3.7 m (12 ft). The AASHTO and SIDD load factors are 1.3, except that the load factor for thrust is taken as 1.0, for determining ultimate strength based on tensile yield strength and shear and radial tension strength.

A separate SPIDA analysis and design using load factors of 1.0 for failure by tensile yield and shear (diagonal tension) and radial tension and capacity reduction factors specified by AASHTO (*3*) shows that the maximum fill height that causes yielding of the stirrup reinforcement and failure of the stirrup anchorages at the invert is 5.5 to 6.1 m (18 to 20 ft).

If the natural soil in the regions below the shaped bedding had been a firm silty sand soil, instead of the medium to soft silty clay soils at Site 1, the maximum design height of fill for a pipe in the specified installation using the Section 17 design limits would have been 8 m (26 ft). The estimated fill height to cause failure would have been 12.2 to 13.7 m (40 to 45 ft). In this case, the installation meets the requirements for a SIDD Type 2 Installation (*4*). A design for this condition using the SIDD computer program (*5*) with a Type 2 installation indicates a maximum design depth of fill of 8 m (26 ft), as governed by stirrup yield strength, and a maximum depth of cover of about 12.2 m (40 ft) using load factors of 1.0 instead of 1.3, again governed by yield or anchorage failure of the stirrups at about the nominal 448 MPa (65,000 ksi) stirrup yield strength.

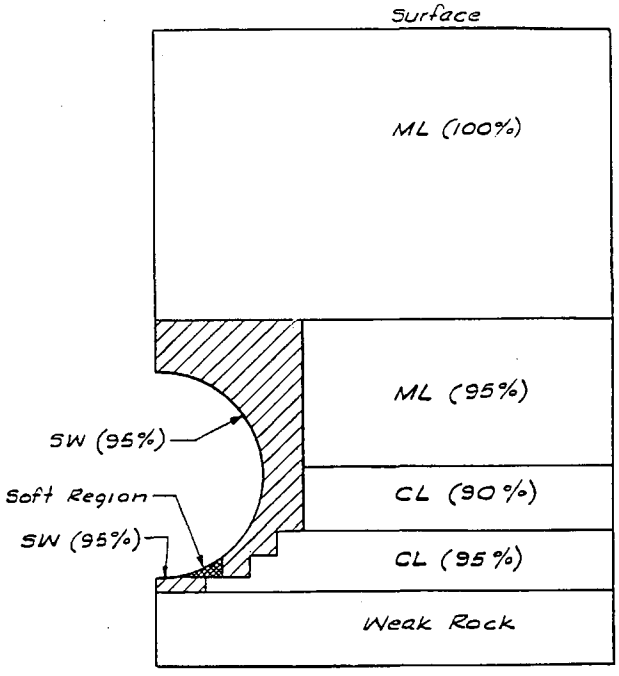

FIGURE 2 Finite element model of pipe-soil installation at Site 1.

DISCUSSION OF SOIL-PIPE INSTALLATION AT SITE 1

The SPIDA soil-pipe interaction analyses show that the specified Class 5 pipe design strength is completely inadequate for a pipe-soil installation with 15.3 to 19.8 m (50 to 65 ft) of backfill over the pipe regardless of the type of soil below and adjacent to the pipe (Cases 2 and 3 in Table 3). The results of the failure analysis for the actual installation (Case 1 in Table 3) shows why many of the pipes exhibited severe distress with major diagonal tension failures probably occurring when the backfill height was considerably less than the 12.2 to 13.7 m (40 to 45 ft) of backfill that was in place at the time that the failure was discovered. The results of the failure analysis for the same installation except that the soft soil is replaced with firm in situ silty sand (Case 4) shows that pipe in this type installation with 12.2 to 13.7 m (40 to 45 ft) of backfill, though very highly stressed, might not have reached a state of visible failure. Since natural soil conditions at the actual site were highly variable, as shown by the borings into original ground before construction, this analysis explains the existence of some pipe without visible evidence of failure.

A comparison of the soil-structure interaction results given in Table 3 for the soft-to-medium in situ clay and the firm in situ silty sand below and adjacent to the pipe shows the following significant characteristics of these installations:

- Vertical arching factor (VAF): The VAF is the ratio of total earth load on the pipe to the weight of a prism of earth directly over the pipe (prism load). Thus, it represents a nondimensional weight of earth on the pipe. In Installation Case 3, with firm silty sand in situ soil adjacent to the shaped bedding and below the subtrench, the VAF is 1.4, representing a magnitude of earth load that is typical of that found in many conventional designs of reinforced concrete pipe in embankment installations. However, in Installation Case 2, with the medium-to-soft silty clay soil below much of the shaped bedding (except near invert) and below the subtrench at the pipe haunch and adjacent side fill, the VAF increased to 1.65. This is because the firm support below the pipe invert causes the pipe to act as a hard object compared with the softer soil adjacent to it. The embankment soil over the pipe behaves as a "shear beam," receiving relatively greater support from the stiff pipe than from the soil adjacent to the pipe, which is underlain by a relatively thin layer of soft soils. As the depth of fill over the pipe in Installation Cases 1 and 2 is increased, as in the analysis for the depth causing failure in Case 1, the VAF increases still more from 1.65 for H = 3.7 m (12 ft) to 1.76 for H = 5.5 m (18 ft).
- Concentration of bearing reaction: The pipe in Installation Cases 1 and 2 with the stiff support below the invert and softer soil below the haunches is also subject to an increased invert moment and shear condition because of the more concentrated bearing reaction as well as the larger total load on the pipe. Because of the low stiffness of the in situ clay soil below the subtrench, the pipe receives little support from the compacted granular soil in the subtrench, and almost all of the bearing reaction is concentrated below the invert region. As a consequence, in spite of the highly compacted select granular embedment soil in the subtrench (see Figure 1), the bottom support reaction is concentrated near the invert instead of being uniformly distributed across the pipe width. This situation was no doubt compounded by the experience of the contractor that construction of the specified shaped bedding (a curved layer of sand) was a constant problem.
- Horizontal arching factor (HAF): The HAF is the ratio of total horizontal load on the pipe to the vertical prism load. The HAF of 0.42 for Installation Case 3 is a typical magnitude for embankment installations in firm, well-compacted granular embedments. The HAF of 0.45 for Installation Case 2 is increased somewhat compared with typical embankments because the very high vertical load and concentration of support near the invert produce a larger extension of the horizontal diameter into the soil embedment at the sides of the pipe, increasing the lateral support forces. The increased lateral support in Installation Case 2 is beneficial but only counteracts a very small portion of the detrimental effects from increased vertical load with this installation.

A review of the soil-pipe interaction analyses that are summarized in Table 3 indicates that an acceptable concrete pipe design for the 15.2- to 19.8-m (50- to 65-ft) height of fill over the culvert at this site requires the following basic design changes:

1. The soft in situ soils below the pipe and the subtrench should have been removed and replaced with select granular soil placed in layers compacted to at least 95 percent of standard Proctor density.
2. The soft in situ soils beneath the embankment for at least one pipe diameter on each side of the pipe section should have been removed and replaced with the same type of site backfill that was used in the main embankment, compacted to at least 95 percent of standard Proctor density.
3. The pipe strength should have been much greater than Class 5. A pipe wall thickness that is greater than the standard A, B, or C wall thicknesses should have been used together with sufficient stirrup reinforcement. An inner and outer circular cage with additional inner reinforcement in the form of mats at the invert and crown was a cost-effective arrangement for the required circumferential reinforcement.

PIPE AND SOIL INSTALLATION AT SITE 2

At Site 2, approximately 268 m (880 ft) of 1350-mm (54-in.) Class 5 concrete pipe was placed in a subtrench cut into the first 3-m (10-ft) height of embankment. This embankment was placed over the original ground surface without removing relatively shallow depths of varying soft soils that were present at most locations along the culvert alignment. However, when the pipe subtrench was cut to the specified depth through the first 3 m (10 ft) of placed embankment and underlying natural soil, any soft soil remaining below the bottom of the trench was removed by order of

TABLE 3 Results of SPIDA Soil-Structure Interaction Analyses for Site 1 Installation

Fill Height		Arching Factors		Governing Condition
Condition	H m (ft)	VAF	HAF	
1. Estimated Maximum H That Produces Pipe Failure (without Water or Live Load) with Actual Soil Conditions	5.5 to 6.1 (18 to 20)	1.76	.46	Shear-stirrup yield and anchorage failure
2. Design Maximum H (with Water + HS20 Live Load) with Actual Soil Conditions	3.7 (12)	1.65	.45	Shear-stirrup yield - SDF = 1500 N/mm/m (2600 lbs/in./ft)
3. Design Maximum H (With Water + HS20 Live Load) if Clay is Replaced with Firm Silty Sand Insitu Soil	7.9 (26)	1.40	.42	Shear-stirrup yield - SDF = 1500 N/mm/m (2600 lbs/in./ft)
4. Estimated Maximum H to Produce Pipe Failure (without Water or Live Load) if Clay is Replaced with Firm Silty Sand Insitu Soil	12.2 to 13.7 (40 to 45)	1.41	.45	Shear-stirrup yield and anchorage failure

the owner's inspectors and replaced with highly compacted natural soil (broken mica schist) from the site. The installation arrangement at Site 2 is shown in Figure 3.

After the embankment was completed to a maximum height of 18.3 m (60 ft) above the top of the pipe, extensive distress was discovered throughout the 1350-mm (54-in.) pipe culvert. A large number of sections of pipe with fill heights in excess of 12.2 m (40 ft) were observed with radial tension (slabbing) or shear (diagonal) tension failures, or both. In addition, many sections with fill heights between 9.5 and 12.2 m (31 and 40 ft), and a few in the range 6.4 to 9.5 m (21 to 31 ft), exhibited this type of failure.

The pipe was manufactured using the Packerhead process. The reinforced concrete pipe design 1350 mm (54 in.) in diameter was provided by the pipe manufacturer and was intended to meet ASTM C76 Class 5 strengths as required in the project specifications. The nominal wall thickness was 140 mm (5.5 in.) (B-wall) and contained inner and outer circular reinforcing cages with 25-mm (1-in.) nominal concrete cover thickness. The nominal area of each reinforcing cage was 1269 mm^2/m (0.60 $in.^2/ft$), and the design concrete strength was 41.4 MPa (6,000 psi). Since no three-edge bearing tests were required, or provided, the design was based on the manufacturer's empirical experience.

A minimum inner cage reinforcement area of 1544 mm^2/m (0.73 $in.^2/ft$) is specified in ASTM C76 for 1200-mm (48-in.), Wall B, Class 5 pipe, which is the largest Wall B Class 5 pipe diameter given in the table. Thus, the manufacturer's design appears to be questionable. The authors estimate that a minimum inside cage area of 1798 mm^2/m (0.85 $in.^2/ft$) is required for 1350-mm (54-in.) Wall B, Class 5 pipe with f'_c = 41.4 MPa (6,000 psi).

Observation of reinforcing in cores cut from a few pipes after the failure by one investigating agency indicates that the actual reinforcement may have been only 1015 mm^2/m (0.48 $in.^2/ft$) or less and that some pipe sections have concrete cover that exceeds the 25-mm (1-in.) specified cover plus the tolerance permitted in ASTM 76. Compressive tests of cores removed from two pipe sections after the distress described above was discovered show compressive strengths of 60.1 and 69.1 MPa (8,720 and 10,030 psi), respectively. Petrographic examinations of some cores show voids and disturbance of concrete structure, common characteristics of pipe made by older Packerhead machines.

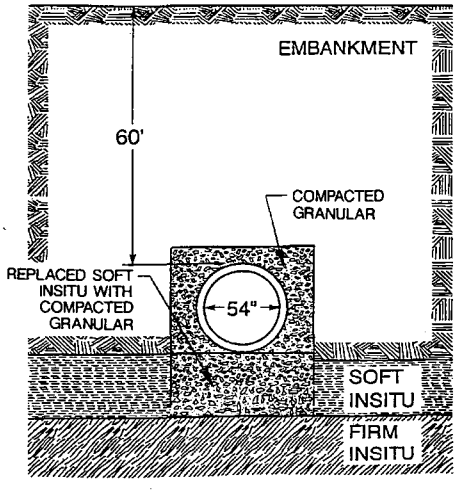

FIGURE 3 Idealization of typical installation at Site 2.

SOIL-PIPE INTERACTION ANALYSIS AND DESIGN—SITE 2

Soil-pipe interaction analyses and design studies were performed using the computer program SPIDA (*1,2*) to determine the maximum allowable height of earth fill that could be placed on a 1350-mm (54-in.) pipe with the nominal design properties given above and installed as shown in Figure 3. The pipe-soil installation was modeled as shown in Figure 4, using two different soils to represent soil conditions near the top of the original ground adjacent to the pipe bedding. In the first model, the soil in Layer 3 was taken as a soft silty sand or silty clay soil, the condition most representative of the worst locations at the site. This soil was represented by standard 80 percent ML soil as equivalent to the silty sand and silty clay in situ soils shown in certain borings located near the pipeline. In the second model, the soil in Layer 3 was taken as a firm silty sand in situ soil and was represented by standard 100 percent ML soil as equivalent to very firm silty sand in situ soil.

The SPIDA analysis and design studies give the results shown in Table 4 for the actual soil conditions (Cases 1 and 2). These indicate the following: allowable maximum fill height, 8.4 m (27.5 ft); calculated fill height at failure, 12.8 m (42 ft); and governing failure criterion, shear (diagonal tension) followed by radial tension.

Another SPIDA analysis was performed for the same pipe in an installation where the medium-to-soft silty sand layer on each side of the pipe bedding layer was replaced by a very firm in situ silty sand soil. The results of this study are also given in Table 4

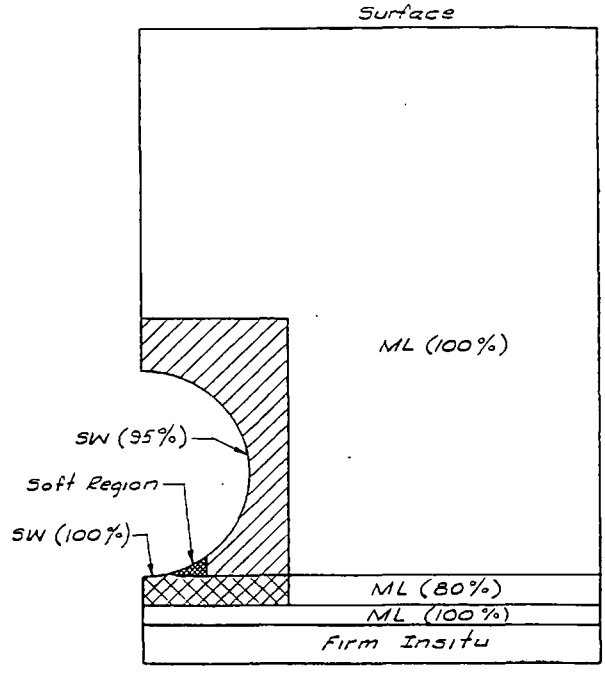

FIGURE 4 Finite element model of pipe-soil installation at Site 2.

TABLE 4 Results of SPIDA Soil-Structure Interaction Analyses for Site 2 Installation

Fill Height		Arching Factors		Governing Condition for Pipe Design
Condition	H m (ft)	VAF	HAF	
1. Estimated Maximum H That Produces Pipe Failure (without Water or Live Load) with Actual Soil Conditions	12.8 (42)	1.72	.44	Diagonal Tension
2. Design Maximum H (with Water + HS20 Live Load) with Actual Soil Condition	8.4 (27.5)	1.72	.43	Diagonal Tension
3. Design Maximum H (with Water + HS20 Live Load) if Soft Soil is Replaced with Very Firm Silty Sand Insitu Soil	13.7 (45)	1.35	.41	Diagonal Tension
4. Estimated Maximum H to Produce Pipe Failure (without Water or Live Load) if Soft Soil is Replaced with Very Firm Silty Sand Insitu Soil	22.2 (73)	1.35	.41	Diagonal Tension

(Cases 3 and 4). When the soft soil layer 600 mm (24 in.) thick is replaced by very firm silty sand in situ soil, the allowable maximum fill height increases to 13.7 m (45 ft). The height of fill that produces diagonal tension failure with load factors of 1.0 is about 22.2 m (73 ft).

When the soft silty soil layer below the embankment on each side of the pipe is replaced by a very firm in situ soil, the installation conforms to a SIDD Type 1 Installation (*4*). An analysis using the SIDD computer program for a Type 1 installation gives a maximum design fill height over the culvert of 12.4 m (40.5 ft). If the load factor is reduced from 1.3 to 1.0, a fill height of 18 m (59 ft) produces diagonal tension failure. These limits are about 11 and 24 percent more conservative than the comparable SPIDA results.

DISCUSSION OF PIPE AT SITE 2

The SPIDA soil-pipe interaction studies show that the subject pipe is overloaded by the specified maximum fill height of 18.3 m (60 ft), regardless of the stiffness of the soil below the embankment on either side of the pipe. However, the presence of soft soil below the embankment in a region adjacent to the pipe foundation on each side of the pipe greatly increases the overload. This is evident from a comparison of both the design maximum fill heights and the VAFs given in Table 4 for the installation cases with soft and firm soils adjacent to the pipe, respectively. The 1.35 VAF calculated for the pipe with firm in situ soil below the embankment adjacent to the pipe is typical of a normal embankment installation. The presence of a layer of soft soil 600 mm (24 in.) thick below the embankment on each side of a pipe that was placed on a firm soil foundation increases the load on the pipe by 27 percent.

The results given in Table 4 show that the capacity of the pipe is greatly enhanced if the 600-mm (24-in.) layer of soft soil below the embankment on each side of the pipe is replaced by firm in situ soil (or compacted granular soil) for about one diameter beyond the pipe. However, a review of the soil-structure interaction analyses shows that even with the improved installation without soft soil, an adequate pipe design that meets the direct design limits given in Section 17 of the AASHTO bridge specification requires either a thicker wall or stirrup reinforcement and greater circumferential reinforcement for the maximum fill height of 18.3 m (60 ft) at this site.

The results of the failure analyses (Cases 1 and 4 in Table 4) show that pipes that have soft soil under the adjacent embankment are expected to have failed in diagonal tension under 18.3 m (60 ft) of fill, whereas pipes with firm in situ soil or compact granular soil in this region may not have reached the failure state in diagonal tension or radial tension. Since the site conditions were variable, this is consistent with observations that not all pipe sections had visible evidence of diagonal tension failure.

CONCLUSIONS

Investigation of the unsatisfactory performance of the concrete pipe in the Site 1 and the Site 2 installations described in this paper leads to the following general conclusions:

1. The SPIDA soil-pipe interaction analyses predict the observed failures for cases with soft soils below the pipe haunches or below the embankment adjacent to the pipes. They also indicate that the pipe at both sites, though overstressed, may not exhibit failure by diagonal and radial tension if soft soils are not present in these regions. Since conditions at both sites are variable, the SPIDA analyses provide valuable insight that corroborates the observed pipe behavior at each of the sites described in the paper.
2. After the improperly designed pipes at Sites 1 and 2 had essentially failed in diagonal and radial tension, they continued to remain intact as they deflected downward vertically and outward horizontally up to 1 to 3 percent of their diameters without collapse. Because of these large deflections, sufficient vertical load was relieved and sufficient lateral load mobilized to enable support of the remaining earth load by ring compression.
3. The design of rigid pipe under high embankments should be based on an adequate investigation of existing soil conditions and consistent with the specified compaction for embankment soils and the embankment subgrade. The design should include a soil-structure interaction analysis to establish the earth load and pressure distribution resulting from the in situ soil conditions and specified embankment soil conditions. The pipe designs at Sites 1 and 2 were based on erroneous and grossly inadequate assessments of the required pipe strength for these sites, installation conditions, and heights of backfill over the pipes.
4. Before placing soils for an embankment, soft soils should be removed in the vicinity of culvert alignments for a distance of at

least one diameter beyond each side of the culvert outside diameter. At both Sites 1 and 2, the embankments were constructed without removing soft in situ soils, but the pipe was founded on firm soil, leading to substantial increases in earth load on the pipe compared with a pipe in a normal embankment installation.

5. Ideally, the stiffness of the bedding or foundation of a rigid culvert should be low under the middle one-third of the pipe diameter (invert region) and sufficiently high under the outer thirds of the pipe diameter to support the full load on the pipe. The reverse condition, in which a stiff foundation or bedding is provided below the invert and soft soil is permitted below the haunches or below a subtrench in the haunch region (the condition that existed at Site 1), greatly increases the bending moment and shear stress resultants on the pipe wall in the critical invert region, leading to premature distress and potential failure.

6. The extreme failure of the pipes with diameters of 2700 mm (108 in.), 2850 mm (114 in.), and 3000 mm (120 in.) at Site 1 resulted from failure to recognize the criteria summarized in Conclusions 3, 4, and 5. The failure of the pipe 1350 mm (54 in.) in diameter at Site 2 resulted from failure to recognize the criteria summarized in Conclusions 3 and 4.

7. It is feasible to design cost-effective precast concrete pipe to provide adequate performance for the backfill heights and general installation conditions at Sites 1 and 2 on the basis of a proper soil-structure interaction analysis and recognition of the interdependence of the design requirements for the embedment and embankment soils and the pipe walls. The traditional method of estimating the pipe loads does not account for the effect of soft soil supporting the embankment adjacent to the pipe and, hence, underestimates the earth load on the pipe.

REFERENCES

1. *Concrete Pipe Technology Handbook.* American Concrete Pipe Association, 1993.
2. Heger, F. J., A. A. Liepins, and E. T. Selig. SPIDA: An Analysis and Design System for Buried Concrete Pipe. *Proc., International Conference on Advances in Underground Pipeline Engineering,* American Society of Civil Engineers, New York, 1985, pp. 143–154.
3. *Standard Specifications for Highway Bridges.* American Association of State Highway and Transportation Officials, 1992.
4. *Standard Practice for Direct Design of Buried Precast Concrete Pipe Using Standard Installations (SIDD).* ASCE 15-93. American Society of Civil Engineers, New York, 1993.
5. *PIPECAR Version 2.0—User Manual.* FHWA-IP-89-019. FHWA, U.S. Department of Transportation, 1994.

Publication of this paper sponsored by Committee on Subsurface Soil-Structure Interaction.

Ultimate Load Analysis of Prestressed and Reinforced Concrete Box Culverts

N. MEAMARIAN, T. KRAUTHAMMER, AND JOHN O'FALLON

The effects of compressive membrane forces on the analysis and design of prestressed/reinforced concrete box culverts are considered. Box culvert panels are modeled as one-way slab strips with restrained edges, and the theory of plasticity is applied to find the ultimate load and support reactions for the model. Modified compression field theory is used to relate the sectional forces to internal stress, strain, and angle of diagonal cracks at each specified location and to the total deflection. A direct solution of the equations obtained is not possible. Therefore, numerical methods are used in developing a computer program to perform the calculations. The output results for 16 one-way slab strips are compared with test results. Reasonable agreements are found for load, deflection, and support reactions at the ultimate load conditions. Load enhancement is obtained by considering the ratio of calculated ultimate load to Johansen's load and is found to be between 1.8 and 2.9 for the slabs tested.

Culverts are transverse drains under highway, railroad, and other embankments, made from a variety of materials including reinforced concrete, corrugated metal, plastics, wood, and stone. Cast-in-place or precast reinforced concrete box culverts are very common nationwide. Single or multicell box culverts often provide a cost-effective alternative to short-span low-rise bridges. Box culverts have several advantages over bridges, including lower initial and maintenance expense, less construction time, and simplicity of construction. Precast reinforced concrete box culverts offer additional advantages such as enhanced quality control, use of higher-strength concrete, lower cost because of mass production, shorter installation time, and fewer construction problems related to bad weather.

Several investigations (*1–4*) suggested that culverts are overdesigned. Although applied soil pressure on the culverts has been increased in the latest editions of AASHTO specifications, soil-structure interaction and the effects of compressive membrane forces on structural behavior are still ignored. Current practice for analysis and design of prestressed and reinforced concrete slabs and box culverts is based on elastic methods of analysis and the strength method of design (*5*; ACI 318-89, ASTM C789-90, ASTM C850-90). Other acceptable methods of analysis and design are not fully developed by standard codes of practice. The standard design tables, based on elastic analysis and ultimate strength design (ASTM C789-90 and ASTM C850-90), are the most widely used method for box culvert design.

Current reinforced concrete models are unable to predict the behavior of cracked concrete members. Most current codes of practice are based on the empirical equations obtained for specific conditions. Furthermore, the artificial division of concrete members into prestressed concrete and conventionally reinforced concrete makes the codes more complicated and less consistent. There is a need for a rational model to predict the behavior of prestressed/reinforced concrete flexural members under the combined effects of transverse loads and membrane forces induced by edge restraints at the ultimate load condition. Considering the amount of money spent annually for culvert construction, any improvement in design could have a large impact on the annual costs of highway culverts.

N. Meamarian and J. O'Fallon, Federal Highway Administration, 6300 Georgetown Pike, McLean, Va. 22101. T. Krauthammer, Civil Engineering Department, Pennsylvania State University, University Park, Pa. 16802.

MEMBRANE FORCES IN SLABS

Compressive membrane forces, resulting from the lateral support restraints, enhance the flexural strength of slabs (*6*). A typical load-central deflection curve for an edge-restrained uniformly loaded slab is shown in Figure 1.

There are no membrane forces if no edge restraints are provided, and the slab will fail theoretically at the Johansen's yield line load, as indicated by the dashed line. Compressive membrane forces increase the load capacity of the slab up to Point D on the curve, which will be referred to as the ultimate load of the slab from now on. The ultimate load (also called collapse load) in this paper refers to the nominal load strength of the slab. Provisions of ACI 318-89 Chapter 9 and concept of strength reduction factor, ϕ, must be used to satisfy the design requirements for practical design.

$$\phi(\text{nominal load strength}) \geq \text{factored load, U}$$

Increasing the deflection beyond Point D will cause a sharp decline in the capacity because of the reduction of compressive membrane forces. Starting from Point E, all the membrane forces in the slab change from compression to tension. Tensile membrane forces are carried largely by the reinforcing steel acting as a tensile membrane. The slab will experience large deflections and extensive cracks over the yielded sections in the tensile membrane domain until complete collapse due to reinforcement rupture or debonding of the bars at Point F.

The length of a reinforced concrete box culvert is considerably greater than its width or rise for most practical cases; therefore, each culvert panel can be modeled as one-way slab strips or beams spanning the supports. Considering the preceding rationale, Krauthammer et al. (*8*) used the Park and Gamble (*6*) approach for a fixed-end one-way slab strip with four plastic hinges and developed a computer program to obtain a relationship between the normalized central deflection of culvert panels (central deflection/strip depth) and normalized load, with respect to the Johansen's load for different surrounding stiffness values as shown in Figure 2.

1. The ultimate load of a culvert panel is not very sensitive to the exact value of its central deflection.
2. Stiffness of surrounding members need not be very large to provide membrane action.
3. Load enhancement due to membrane action could be more than 50 percent compared with Johansen's yield line theory.

APPROACH

Global Load-Deflection Relationship

Culvert panels can be modeled as one-way slab strips spanning between other panels as the supports (Figure 3). Lateral stiffness of supports and surrounding soil provides the restraint required to develop in-plane forces. Generally, two major steps are required for analysis of this model. First, external analysis is needed to find support reactions, deflections, and applied load. In the second step, reactions and external loads are related to internal stresses of concrete and steel at different locations. Classical methods of analysis are not applicable for this case, since load and support reactions are dependent on material properties, vertical deflection, lateral stiffness of supports, and long-term deformations.

Perhaps the most commonly accepted approach for considering the membrane forces in reinforced concrete slabs is the one presented by Park and Gamble (*6*), which has been the basis for many other research studies. Four plastic hinges are assumed for the general case to develop a collapse mechanism condition in this method (Figure 4).

Considering the theory of plasticity, equilibrium, and compatibility, Park and Gamble presented an equation to relate the load capacity of the slab strip to its geometry, material properties, lateral shortening, central strip defection, and lateral stiffness of supports. Park and Gamble's equations can be modified to consider the effects of prestressing force and long-term deformations (*9*). The free body diagram of Segment 1-2 at and after yielding is considered (Figure 5). Forces applied by each component of the concrete section including reinforcing bars, prestressing tendons, and concrete are shown.

It is assumed that the slab segments between the plastic hinges remain straight after collapse and that there is complete symmetry regarding geometry, reinforcement, loading, and deformations. The supports are assumed to be fixed against rotation and partially

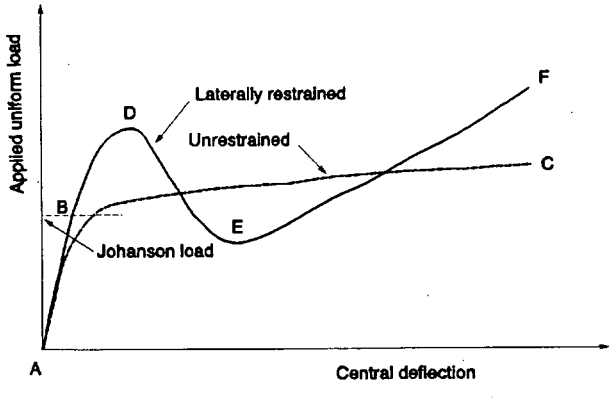

FIGURE 1 Typical load-deflection curve for edge-restrained slabs (*7*).

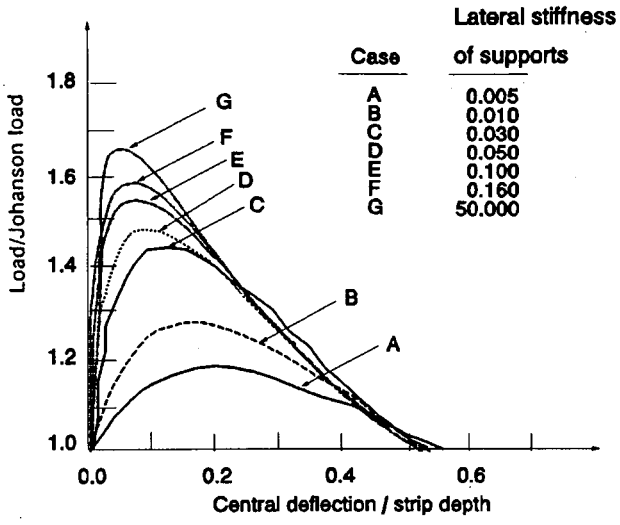

FIGURE 2 Analytical results for ultimate load of bottom slab in a reinforced concrete box culvert (*8*).

restrained against lateral movements at each end. However, there will be some provision to consider measured rotations as input for the computer program developed herein. Both mild steel reinforcement and prestressing tendons are assumed to have a definite yield point beyond which no extra strength is demonstrated due to strain hardening. Therefore, forces provided by steel at plastic hinges are simply equal to reinforcement areas multiplied by their yield strength. The concepts of Whitney's rectangular stress block (ACI 318-89) for a reinforced concrete section at the ultimate load condition is used to define the sum of the concrete compressive forces at each plastic hinge. It is further assumed that the axial strain, ϵ, is constant along the length of the strip. Application of the equations of equilibrium to the free body diagram shown in Figure 5 will result in the following equation (*9*):

$$
\begin{aligned}
M_u' + M_u - N_u\delta = 0.85 f_c' \beta_1 hb \Bigg[& \frac{h}{2}\left(1 - \frac{\beta_1}{2}\right) \\
& + \frac{\delta}{4}(\beta_1 - 3) + \frac{\beta L^2}{4\delta}(\beta_1 - 1)\left(\epsilon + \frac{2t}{L}\right) \\
& + \frac{\delta^2}{8h}\left(2 - \frac{\beta_1}{2}\right) + \frac{\beta L^2}{4h}\left(1 - \frac{\beta_1}{2}\right)\left(\epsilon + \frac{2t}{L}\right) \\
& - \frac{\beta_1 \beta^2 L^4}{16 h \delta^2}\left(\epsilon + \frac{2t}{L}\right)^2 \Bigg] - \frac{1}{3.4 f_c' b}(T' + R' - T \\
& - R - C_s' + C_s)^2 + (C_s' + C_s)\left(\frac{h}{2} - d' - \frac{\delta}{2}\right) \\
& + (T' + T)\left(\frac{h}{2} - d' + \frac{\delta}{2}\right) \\
& + R'\left(d_r' - \frac{h}{2} + \frac{\delta}{2}\right) + R\left(d_r - \frac{h}{2} + \frac{\delta}{2}\right) \qquad (1)
\end{aligned}
$$

where

M_u, M_u' = positive and negative plastic moments, respectively;
N_u = axial force at ultimate load condition;
δ = deflection of the middle slab segment;

f'_c = 28-day concrete uniaxial compressive cylinder strength;
β_1 = ratio of the equivalent stress block depth to neutral axis depth;
h = member thickness;
b = beam or slab strip width;
β = ratio of the positive hinge distance form support to the member span length;
L = length of span;
ϵ = axial short-term strain;
t = outward lateral movement of each support;
T, T' = steel tensile forces at positive and negative hinges, respectively;
R, R' = prestressing tensile forces at positive and negative hinges, respectively;
C_s, C_s' = compressive steel forces at positive and negative hinges, respectively;
d' = concrete cover to the center of mild steel reinforcement;
d_r, d_r' = top and bottom cover to the center of prestressing steel at positive and negative hinges, respectively; and
c, c' = depth of neutral axis at positive and negative hinges, respectively.

The term $\epsilon + 2t/L$ on the right-hand side of Equation 1, which is the total axial strain, can be found as shown below (*9*), where S is the support lateral stiffness per unit width of the slab strip or beam at each end [e.g., load per unit of outward displacement of the support in units of (lb/in.)/in], E_c is the concrete modulus of elasticity, and K is the ratio of long-term to short-term deformations. Note that the Park and Gamble equations may be obtained by inserting the values of $b = 1$ and $R' = R = K = 0$.

$$\epsilon + \frac{2t}{L} = \frac{\left(\frac{1+K}{hE_c} + \frac{2}{LS}\right)\left[0.85f'_c\,\beta_1\left(\frac{h}{2} - \frac{\delta}{4} - \frac{T' + R' - T - R - C'_s + C_s}{1.7f'_c\,\beta_1 b}\right) + \frac{C_s - T - R}{b}\right]}{1 + 0.2125\frac{f'_c\,\beta_1\beta L^2}{\delta}\left(\frac{1+K}{hE_c} + \frac{2}{LS}\right)} \quad (2)$$

A relationship can be found between the external loads and sum of the internal moments about Point 2 in Figure 5 (interior hinge)

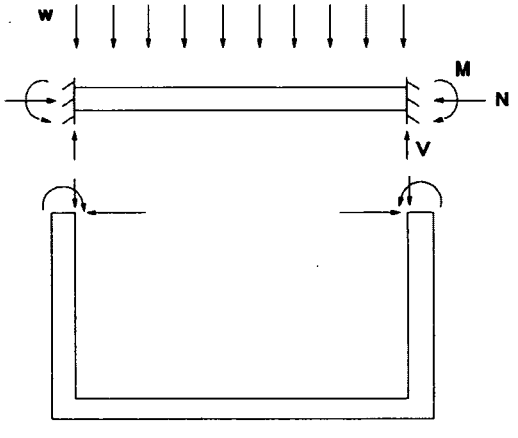

FIGURE 3 Modeling of box culverts.

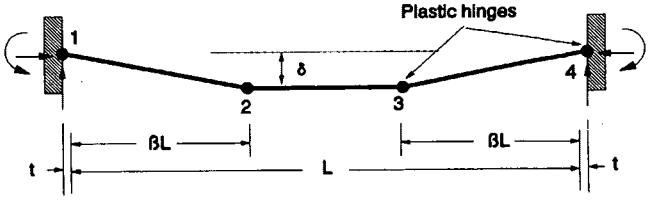

FIGURE 4 Plastic hinges in restrained slab strip (*6*).

by using the principles of virtual work. The internal virtual work done by Segment 1-2 of the slab strip due to a virtual rotation of θ about Point 1 is equal to $(M_u + M'_u - N_u\delta)\theta$. Equating the external and internal virtual work for Segment 1-2 leads to Equation 3 for a uniformly distributed load and Equation 4 for two concentrated loads of P and βL from each end:

$$\left(\frac{w}{2}\right)(\beta L)^2 = M_u + M'_u - N_u\delta \quad (3)$$

$$P(\beta L) = M_u + M'_u - N_u\delta \quad (4)$$

A direct solution of Equations 3 or 4 is not possible, since there is only one equation with two unknowns (w or P and δ). An iterative numerical solution is adopted in which the value of δ is increased gradually. For each value δ_i, the corresponding value of the applied load, w_i or P_i, is obtained by using Equations 1, 2, and 3 or 4 according to the loading type. The iteration process continues until an appropriate ultimate load and the corresponding deflection are obtained (Point D in Figure 1). Then support reactions can be found by applying equations of equilibrium and strain compatibility (*9*). Sectional forces at any point between the supports can be calculated by using equilibrium equations when the end reactions are obtained.

Consideration of Internal Conditions

The recently developed modified compression field theory, fully explained by Vecchio and Collins (*10–12*) and Collins and Mitchell (*13*), provides a unified approach for the analysis of reinforced concrete sections under combined effects of shear, moment, and axial loads. Modified compression field theory is applicable to reinforced and prestressed concrete flexural members at different stages of loading and cracked concrete condition. It is assumed that shear forces are resisted by a field of diagonal compressive stress, f_2 (Figure 6), with angle of θ, in combination with a field of diagonal tensile stress, f_1. Mohr's circle relates the principal strains to the angle of inclination of the cracks, θ, and to the longitudinal and transverse strains (strain compatibility). Material stress-strain relationships are used to relate strains in each material to stresses, and equilibrium equations are applied to find the relationship between the internal stresses and sectional forces resulting from the external loads (*13*). Equations of the modified compression field theory are not suitable for direct solution without more simplification. Therefore, an iterative method of solution is adopted in this study by using numerical solution techniques and computer programming (*9,13*). This method involves three major nested loops (iterating loops) based on concrete tensile strain, ϵ_1, shear force, V, and crack inclination angle, θ.

Material Constitutive Laws

Material constitutive laws will be satisfied by considering the stress-strain relationship for steels and concrete. Mild steel reinforcement is assumed to act as an elastic-plastic material in tension or compression. In practice, the stress-strain curve for prestressing steel is linear before the elastic limit, at about $0.7f_{pu}$. This relationship is approximated by a Ramberg-Osgood curve, as defined below (*14*):

$$f_p = E_p \epsilon_p \qquad f_p \leq 0.7f_{pu} \tag{5}$$

$$f_p = \frac{E_p' \epsilon_p}{\left[1 + \left(\frac{E_p' \epsilon_p}{f_{pu}}\right)^m\right]^{1/m}} \qquad f_p > 0.7f_{pu} \tag{6}$$

where E_p' is the tangential modulus of the Ramberg-Osgood curve and m is the shape parameter (taken as 4).

The compressive stress-strain curve for concrete is usually obtained from the standard cylinder compressive test, but stress conditions in a cracked concrete section are quite different from the cylinder test. Vecchio and Collins (*10*) found that the principal compressive stress of concrete, f_2, depends not only on the principal compressive strain, ϵ_2, but on the principal tensile strain, ϵ_1, as well. They suggested the following parabolic stress-strain relationship for normal strength [$f_c' < 6{,}000$ psi (41.38 MPa)] cracked concrete:

$$f_2 = f_{2max}\left[2\left(\frac{\epsilon_2}{\epsilon_c'}\right) - \left(\frac{\epsilon_2}{\epsilon_c'}\right)^2\right] \tag{7}$$

$$\frac{f_{2max}}{f_c'} = \frac{1}{0.8 + 170\epsilon_1} \leq 1.0 \tag{8}$$

where

f_{2max} = cracked concrete compressive strength,
ϵ_c' = concrete cylinder strain at compressive strength,
ϵ_1 = concrete tensile strain, and
ϵ_2 = concrete compressive strain.

An equation for concrete of higher strength has been suggested by Thorenfelt et al. (*15*). The equation is a generalization of two of the expressions recommended by Popovics (*16*). This equation

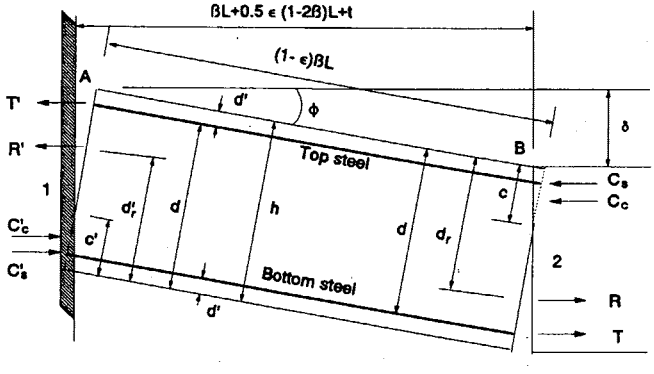

FIGURE 5 Deformed shape and forces for a slab segment between the plastic hinges (*6*).

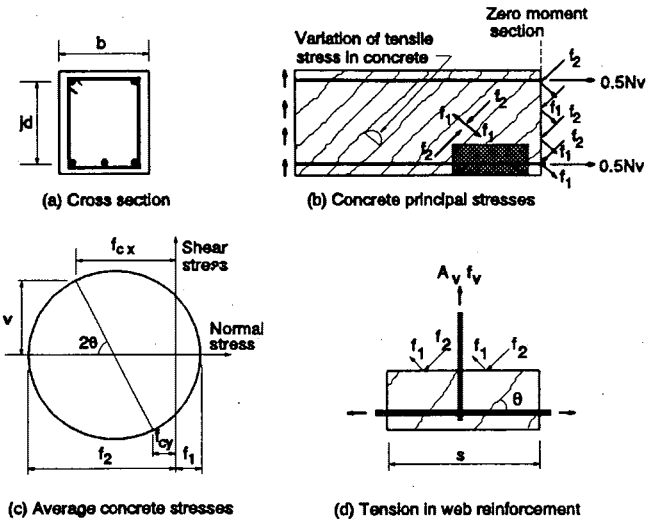

FIGURE 6 Equilibrium conditions for modified compression field theory (*13*).

relates the concrete stress, f_c', to concrete strain, ϵ_2, as follows:

$$\frac{f_c}{f_c'} = \frac{n_f\left(\frac{\epsilon_2}{\epsilon_c'}\right)}{n_f - 1 + \left(\frac{\epsilon_2}{\epsilon_c'}\right)^{n_f k_d}} \tag{9}$$

where

ϵ_c' = concrete cylinder strain at compressive strength $\approx (f_c'/E_c) \times [n_f/(n_f - 1)]$,
n_f = curve-fitting factor = $E_c/(E_c + E_c') \approx 0.8 + f_c'/2{,}500$ (f_c' in psi),
E_c = concrete tangent modulus of elasticity when $\epsilon_c = 0$,
$E_c' = f_c'/\epsilon_c'$, and
k_d = factor to increase the stress decay after the ultimate strength, taken as 1 for $\epsilon_2/\epsilon_c' < 1$ and $k_d \approx 0.67 + f_c'/9{,}000$ for $\epsilon_2/\epsilon_c' > 1$ (f_c' in psi).

Collins and Mitchell (*13*) modified the recommended average tensile stress curve for concrete, given by Vecchio and Collins (*11*), to account for the effects of steel bond and loading type (Equations 10 and 11):

$$f_1 = E_c\epsilon_1 \qquad \epsilon_1 \leq \epsilon_{cr} \tag{10}$$

$$f_1 = \frac{\alpha_1\alpha_2 f_{cr}}{1 + \sqrt{500\epsilon_1}} \qquad \epsilon_1 > \epsilon_{cr} \tag{11}$$

where

ϵ_1 = average concrete principal tensile strain between the diagonal cracks,
f_1 = average concrete principal tensile stress between the diagonal cracks,
ϵ_{cr} = concrete cracking strain,
f_{cr} = concrete cracking strength,
α_1 = reinforcement bond characteristics factor, and
α_2 = loading type factor.

Shear capacity of a concrete member may be limited to the forces transmitted along the cracks. Local shear forces transmitted by aggregate interlock are dependent on the crack width. Collins and Mitchell (*13*) suggested a simplified form of the equation given by Vecchio and Collins (*11*) for the limiting value of the local shear stresses along the cracks, v_{ci}, as below (in psi), where ω is the crack width calculated according to CEB-FIP code (in.) (*17*) and a = maximum aggregate size (in.).

$$v_{ci} = \frac{2.16\sqrt{f'_c}}{0.3 + \dfrac{24\omega}{a + 0.63}} \tag{12}$$

Since the two sets of forces shown at Sections 1-1 and 2-2 in Figures 7b and 7c must be statistically equivalent, they have the same sum of vertical components. With the assumption of shear reinforcement yielding at cracks, the equality mentioned above yields Equation 13:

$$f_1 = v_{ci} \tan \theta + \frac{A_v}{sb}(f_{vy} - f_v) \tag{13}$$

where f_{vy} and s are shear reinforcement yield strength and spacing, respectively. The smallest value from Equations 10, 11, and 13 is considered to be the concrete principal tensile strength.

Stress and strain conditions become more complex after the section is cracked. The presence of concrete tensile stresses between the cracks stiffens the member. This phenomenon, which is called tension stiffening, is accounted for by using the average tensile stress given by Equation 11 and is considered to exist only around the tensile reinforcement in an area called the effective embedment zone (*12*). The effective embedment zone is assumed to be extended 7.5 d_b in each direction parallel to the sides of the section around each longitudinal tensile reinforcing bar, where d_b is the bar diameter (*17*).

Numerical Implementation

A computer program has been developed for IBM-PC and compatible computers based on a 20-step iterative solution technique (*9*). A condensed flowchart for the program is shown in Figure 8. Geometry, material properties, reinforcement area, loading type, and so forth are given as input data. Support reactions, deflection, and load at ultimate conditions are then calculated by using an iterative procedure for incremental deflection values (Equations 1 and 2). In the next step, equations of equilibrium are applied to find the sectional forces at any specified section between the supports, after which the principles of the modified compression field theory are applied by using a numerical solution method (*9,13*) to find all the unknown parameters including stresses and strains in concrete and steel, angle of diagonal cracks, total deflection, and crack width at the ultimate load conditions. The output of the computer program can be used to check the adequacy of a reinforced/prestressed concrete member for structural strength and serviceability. The member geometry or reinforcement area need to be revised if strength or serviceability requirements are not satisfied.

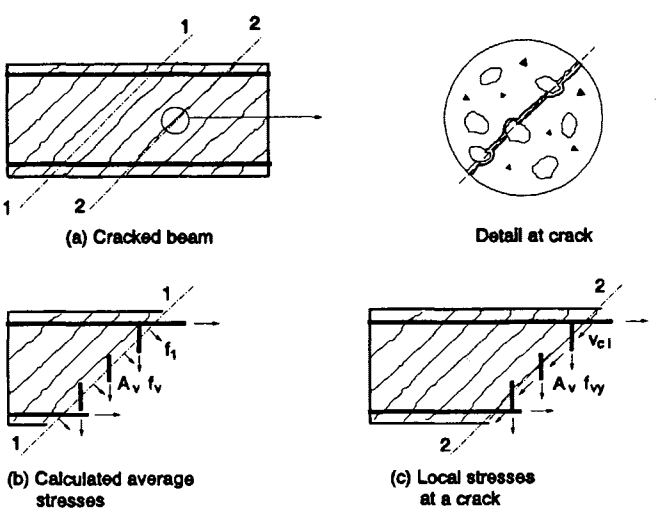

FIGURE 7 Stress transmission across the cracks (*13*).

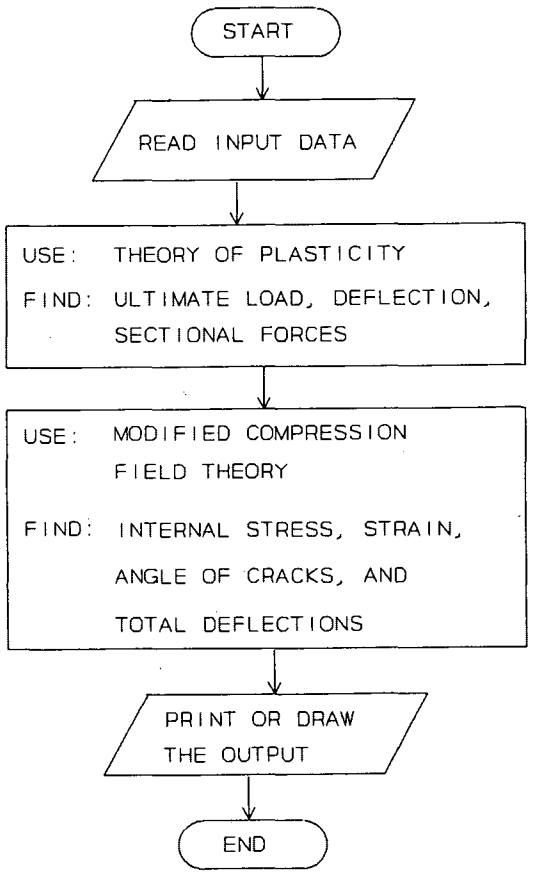

FIGURE 8 Condensed flowchart.

COMPARISON WITH EXPERIMENTAL RESULTS

A series of 16 slab panels 36 in. (914 mm) long by 24 in. (610 mm) wide were tested by Guice (*18*). Two sets of equal numbers of slab specimens were cast with thicknesses of $2^5/_{16}$ in. (59 mm) and $1^5/_8$ in. (41 mm). The area of main reinforcement was the same for the midspan and the supports but differed from one slab to another. Small-diameter deformed wire was used for both tem-

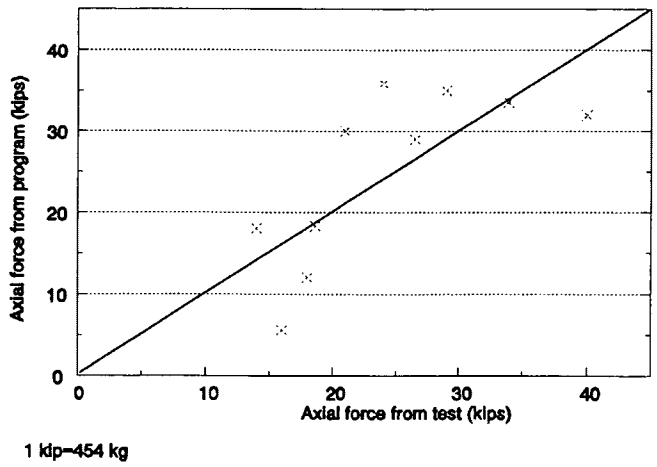

FIGURE 9 Computer program versus test (axial force).

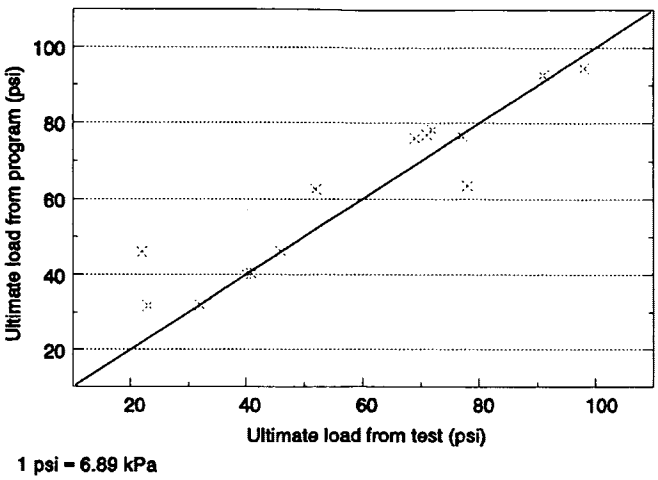

FIGURE 11 Computer program versus test (ultimate load).

perature and shear reinforcements. Pin-shaped shear reinforcement was used at each location of longitudinal and transverse reinforcement contact. The important fact about the testing assembly is that the steel supports for the slabs were designed to allow partial lateral movement and rotation of the supports. Support rotation was not originally considered in the equations obtained from the theory of plasticity for external analysis, but the required provisions were added to the computer program to consider the effects of given support rotations on the external analysis. The values obtained from the computer output for axial force, support moment, load, and deflection/thickness ratio (δ/h) at the ultimate load condition are plotted against the corresponding results from the test data in Figures 9 through 12. The average, standard deviation, and coefficient of variance for the ratio of calculated to test results are given in Table 1.

PRESENT APPROACH VERSUS YIELD LINE APPROACH

The yield line theory approach (*19*) is used to compare the ultimate load of the slab specimens to those resulting from the application of the computer program developed in this study. Membrane force is not considered in the yield line theory; thus it does not contribute to the ultimate load capacity obtained by the yield line theory. The ratios of computed load/Johansen's load are plotted against the reinforcement percentage ratio for each group of slab thicknesses in Figure 13. The solid line is for the thicker slabs [$H = 2^5/_{16}$ in. (59 mm)], and the dashed line is for the thinner slabs [$H = 1^5/_8$ in. (41 mm)].

DISCUSSION OF RESULTS

Evaluation of the results in Table 1 and Figures 9 through 12 indicates that program outputs are reasonably close to test results. The average ratio of theoretical load to tested load is only 4 percent higher than 1 with a standard deviation of 0.13. The average values for the ratios of calculated to tested axial force and moment at the supports are 7 percent higher than 1. Whereas the deviations are small and reasonable, they may be due to several factors including support rotation, initial gap between the slab and support

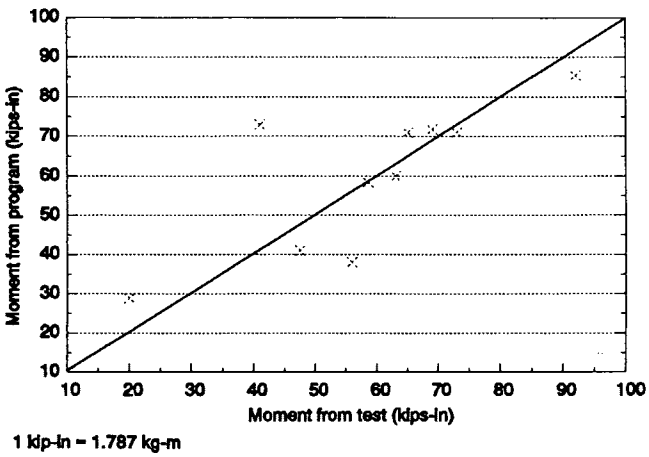

FIGURE 10 Computer program versus test (support moment).

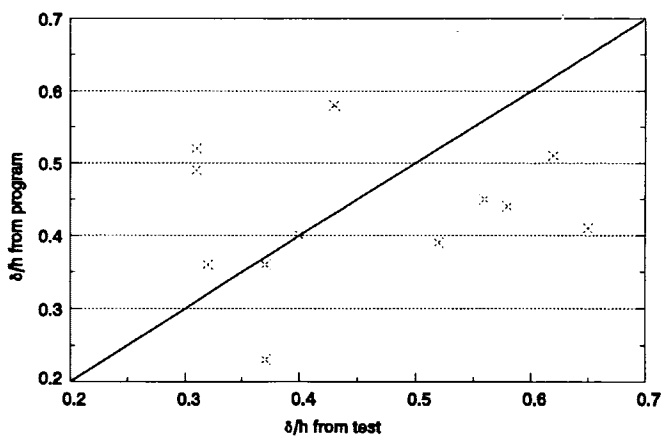

FIGURE 12 Computer program versus test (deflection/thickness).

TABLE 1 Calculated Values and Test Results (Statistical Parameters)

Parameter	Axial Force	Moment	Load	Deflection
Average	1.07	1.07	1.04	1.00
Std. Deviation	0.38	0.29	0.13	0.33
Coefficient of Variance	35%	27%	12%	33%

rack, and debonding. The average theoretical deflection is the same as the average test results. It appears that despite the very close results, theoretical deflections are less than the tested values for higher deflection/thickness ratios due to the same problems discussed above. Evaluation of Figure 13 indicates a considerable load enhancement as expected due to membrane forces, especially for low reinforcement ratios (calculated load/Johansen's load = 1.7 to 2.9). Figure 13 also shows that the load enhancement is higher for thinner slabs with moderate reinforcement ratios (0.007 to 0.012), but it is the same for slabs with low reinforcement ratios (0.005).

Effects of support rotation complicate the analysis. It was assumed that top steel at the supports yields even after the introduction of compressive strains at the top steel level because of support rotation. This assumption is necessary to find the ultimate load from the collapse mechanism; however, this might not be representative of the actual conditions. Testing may have been terminated because of large deflections due to support rotations, before the top support rebars yielded (*18*). The other problem observed in the test procedure was related to uneven support rotations and forces. This violates the assumption that was made for a symmetrical geometry.

CONCLUSIONS

It was shown that the combined application of the theory of plasticity and the modified compression field theory provides a rational method for prediction of structural response of one-way slabs with laterally restrained edges. The formulations satisfy conditions of equilibrium, compatibility, and plane section theory and give a realistic consideration of cracked concrete behavior. Several critical factors such as strain softening, tension stiffening, repeated load, reinforcement type, and long-term shortening are considered in this approach. This analytical model incorporates the theoretical relationships between parameters in easy-to-use computer software on the basis of numerical iteration methods. Application of the software to 16 reduced-scale one-way reinforced concrete slab panels and comparison with actual test results shows that, overall, the program outputs regarding the forces at the supports, load, and deflection of mid-span at ultimate load condition are reasonably close to test results.

The study considered the membrane forces and arching action for one-way prestressed and reinforced concrete flexural member analysis and design in a rational manner, leading to significant load enhancement and saving of reinforcement and concrete materials in addition to more accurate prediction of member behavior at cracked condition. The results are also applicable to any structure that can be modeled as a one-way member with restrained edges. For example, the strip method can be used to model a two-way slab or box culverts as a series of one-way strips that can be analyzed easily by the software.

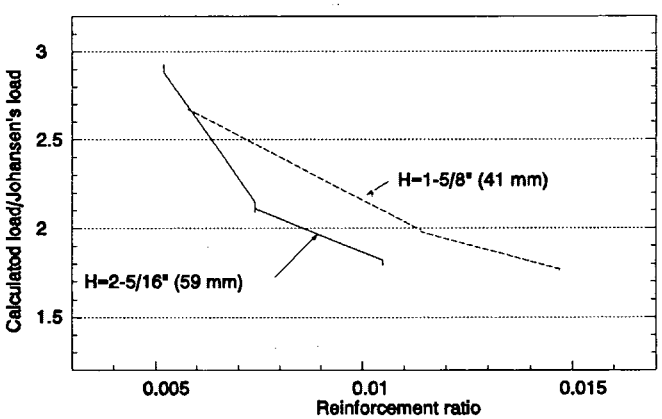

FIGURE 13 Computer program versus yield line theory for tested slabs.

RECOMMENDATIONS

It was demonstrated that the presence of compressive membrane force enhances the flexural strength of concrete members considerably; therefore, it is recommended that membrane forces be considered in the analysis and design of flexural prestressed and reinforced concrete structural members with laterally restrained edges, such as box culverts and interior slab panels. The required provisions regarding the consideration of such forces for design purposes need to be included in the prestressed and reinforced concrete design codes. A uniform approach for prestressed and reinforced concrete members and higher values for load factors are recommended until further study, especially for sustained loads. Axial shortening resulting from long-term deformations and outward lateral movement of the supports could reduce the membrane force considerably. Therefore, careful consideration of support lateral stiffness and long-term axial deformation is important to prevent overestimation of flexural enhancement provided by membrane forces.

There is a need for more testing to obtain a better definition of structural behavior and to verify the software output results for stresses and strains and for prestressed elements. It is also desirable to model the D-regions (disturbed regions where stress trajectories are not smooth) at and around plastic hinges and implement this model in the computer program to have a more complete and accurate analysis of the structure. A possible method for modeling D-regions is using the strut-and-tie method (*20*). The boundary loads and deformations for D-regions can already be obtained from the current program output. Combined application of the present software and proper modeling of D-regions would provide a consistent method of analysis and smooth transition from B-regions to D-regions. The analysis in this study is valid only for symmetrical slabs with regard to reinforcement, geometry, and end restraints. Further study to consider unsymmetrical cases is necessary.

ACKNOWLEDGMENT

This study was sponsored by FHWA. The authors gratefully acknowledge the sponsorship of this organization.

REFERENCES

1. Tadros, M. K., C. Belina, and D. W. Meyer. Current Practice of Reinforced Concrete Box Culvert Design. In *Transportation Research Record 1191*, TRB, National Research Council, Washington, D.C., 1988, pp. 65–72.
2. Katona, M. G., P. D. Vittes, C. H. Lee, and H. T. Ho *CANDE-1980: Box Culverts and Soil Models*. Report FHWA-RD-89-172. Federal Highway Administration, 1981.
3. Frederick, G. R., C. V. Ardis, K. M. Tarhini, and B. Koo. Investigation of the Structural Adequacy of C 850 Box Culverts. In *Transportation Research Record 1191*, TRB, National Research Council, Washington, D.C., 1988, pp. 73–80.
4. Tadros, M. K., J. V. Benak, A. M. Abdel-Karim, and K. A. Bexten. Field Testing of a Concrete Box Culvert. In *Transportation Research Record 1231*, TRB, National Research Council, Washington, D.C., 1989, pp. 49–55.
5. *Standard Specification for Highway Bridges* (15th edition). AASHTO, Washington, D.C., 1992, pp. 124–326.
6. Park, R., and W. L. Gamble. *Reinforced Concrete Slabs*. John Wiley and Sons, 1980, pp. 562–565.
7. Iqbal, M., and A. T. Derecho. *Design Criteria for Deflection Capacity of Conventionally Reinforced Concrete Slabs, Phase I*. State-of-the-Art Report, Naval Construction Battalion Center, Port Heuneme, Calif., May 1979.
8. Krauthammer, T., J. J. Hill, and T. S. Fares. Enhancement of Membrane Action for Analysis and Design of Box Culverts. In *Transportation Research Record 1087*, TRB National Research Council, Washington, D.C., 1986, pp. 54–61.
9. Meamarian, N. *Compressive Membrane Effects on the Behavior of One-Way Structural Concrete Members with Application for Analysis and Design of Box Culverts*. Thesis. The Pennsylvania State University, University Park, 1993.
10. Vecchio, F. J., and M. P. Collins. *The Response of Reinforced Concrete to In-Plane Shear and Normal Stresses*. Publication 82-03. Department of Civil Engineering, University of Toronto, Toronto, Ontario, Canada, 1982.
11. Vecchio, F. J., and M. P. Collins. The Modified Compression Field Theory for Reinforced Concrete Elements Subjected to Shear. *ACI Structural Journal*, Vol. 83, No. 2, March–April 1986, pp. 219–231.
12. Vecchio, F. J., and M. P. Collins. Predicting the Response of Reinforced Concrete Beams Using Modified Compression Field Theory. *ACI Structural Journal*, May–June 1988, pp. 258–268.
13. Collins, M. P., and D. Mitchell. *Prestressed Concrete Structures*. Prentice-Hall, Inc., 1991.
14. Hsu Thomas, T. C. Nonlinear Analysis of Concrete Membrane Elements. *ACI Structural Journal*, Vol. 88, No. 5, Sept.–Oct. 1991, pp. 552–561.
15. Thorenfelt, E., A. Tomaszewicz, and J. J. Jensen. Mechanical Properties of High-Strength Concrete and Application in Design. *Proc., Symposium on Utilization of High-Strength Concrete*, Stavanger, Norway, June 1987., pp. 149–159.
16. Popovics, S. A Review of Stress-Strain Relationships for Concrete. *ACI Journal*, Vol. 67, No. 3, 1970, pp. 243–248.
17. *Model Code for Concrete Structures* (3rd. edition). Comité Euro-International du Béton, Paris, 1978.
18. Guice, L. K. *Behavior of Partially Restrained Reinforced Concrete Slabs*. Technical Report SL-86-32. Structures Laboratory, U.S. Army Engineer Waterways Experiment Station, Vicksburg, Miss., Sept. 1986.
19. Johansen, K. W. *Yield Line Formulae for Slabs*. Cement and Concrete Association, London, 1972.
20. Schlaich, J., K. Schäfer, and M. Jennewein. Toward a Consistent Design of Structural Concrete. *PCI Journal*, May–June 1987, pp. 75–150.

Publication of this paper sponsored by Committee on Culverts and Hydraulic Structures.

PART 2

Trenchless Technology

Case History: Horizontal Directionally Drilled Pipeline Crossing of the Atchafalaya River at Melville, Louisiana

CHARLES W. HAIR III AND NANCY W. SCHULTZ

Development of horizontal directional drilling (HDD) design procedures is examined by detailing a state-of-the-art (at the time of execution in 1987) trenchlessly placed river crossing: a high-pressure natural gas pipeline 976 m (3,200 ft) long and 915 mm (36 in.) in diameter installed beneath the Atchafalaya River in south central Louisiana. The pipeline was near an existing pipe suspension bridge and numerous conventionally placed lines, most of which had been affected by river scour. Unique project features are the crossing's large diameter and length coupled with its being the first subdrilling (in the United States) of a major, publicly owned flood protection levee. The site history and river channel/subsurface conditions are described. These factors led to selection of the crossing's implementation methodology and geometry and the decision to subdrill the levee. Development of the installation's design is reviewed, and efforts inherent to construction permitting are highlighted. The actual construction is described, with concentration on solutions to problems encountered. An analysis of the effects this installation has had and is having on HDD design and construction is then presented in conjunction with recommendations for improving future HDD engineering.

Since its inception in early 1972, the horizontal directionally drilled (HDD) method of trenchlessly constructing pipeline river crossings has evolved to the extent that such procedure is often preferred over more traditional installation means [i.e., the conventional (cut-and-cover trenching) and aerial (suspension bridge) placement techniques (*1*)]. When in situ conditions and construction economics are amenable for crossing a river or other, similar obstacle in the range of 200 to 1800 m (700 to 6,000 ft) in width, HDD offers a more rapidly placed, potentially longer-lived, virtually maintenance-free installation having greatly reduced environmental effects.

HDD METHODOLOGY AND DESIGN

The standard process first entails using a small-diameter nonrotating drill stem to forward thrust bore and/or jet a pilot hole controlled to the crossing's specific geometry (vertical penetration and horizontal run). Afterwards, pullback reaming of the pilot hole to a diameter sufficient for carrier pipe installation—usually 300 mm (12 in.) in excess of the production pipe diameter—is performed. Pull-in of the previously assembled and pressure-tested production pipe string is then accomplished to complete the operation.

C. W. Hair, Louis J. Capozzoli and Associates, Inc., 10555 Airline Highway, Baton Rouge, La. 70816. N. W. Schultz, Civil Design Technical Services, Transcontinental Gas Pipe Line Corporation, 2800 Post Oak Boulevard, P.O. Box 1396, Houston, Tex. 77251-1396.

In the technology's early developmental stages, the planning of HDD crossings was largely empirical and mostly performed by the drilling contractors themselves. Now, however, a rational design approach, stemming from an understanding of in situ geotechnical/potamological conditions, is evolving for the engineering of more efficient and economical HDD placements (*2,3*). This site characterization–based design methodology embodies definitions of (*a*) passive site conditions [i.e., the crossing location's geology, topography, and subsurface stratigraphy as well as the obstacle's characteristics (a river's dimensions and meander/scour potential, a highway or levee embankment's subsidence possibilities, an encapsulation site's subsurface contaminate migration plume, etc.)] and (*b*) active site conditions [i.e., the various responses of and to the HDD construction process (drilling mud seeps, torque/pull force requirements, pipe stress generation, etc.)]. Not only does this methodology offer a greater chance of HDD installation success, but it also allows for extension of such construction technique to a much broader array of applications. To rationally design an HDD river crossing, the requisite site characterization must therefore define the in situ conditions' effects on the constructed facility—both during and after placement—while delineating the constructed facility's effects on the preexisting (and, in some cases, future) conditions.

In accomplishing this engineering procedure, the site's geology, topography, hydrography, potamology, and geotechnology must be established. Using such data as the design basis, the drilled installation's geometry and execution details can then be planned. The placement's effects on the site may be forecast to allow development and timely implementation of any necessary construction or postconstruction actions. Following promulgation of the project's detailed design, construction permits may be acquired and the work can be bid. Actual execution, including in-progress inspections to ensure design accomplishment, may then proceed. Follow-up work can provide certification of both the project's conduct and the site's integrity refurbishment.

PROJECT DESCRIPTION

Although it has since been eclipsed by longer, larger-diameter installations, the 1987 pipeline river crossing evaluated in this paper has laid much of the groundwork for engineering future HDD placements.

New Construction

The intent of the project was to install a high-pressure natural gas pipeline 915 mm (36 in.) in nominal diameter across the Atcha-

falaya River just north of Melville, Louisiana. The general project location is the upstream (northern) end of south central Louisiana's Atchafalaya River Basin (see Figure 1). The impetus for construction was periodic exposure and destruction by the river, mainly through vertical scouring, of cut-and-cover dredged pipelines belonging to the crossing's owner, Transcontinental Gas Pipe Line Corporation (TGPL). The new alignment was also intended to parallel TGPL's existing pipeline suspension bridge supporting two lines 760 mm (30 in.) in nominal diameter across the Atchafalaya.

HDD was tentatively selected as the crossing methodology because of the finished product's potential insulation from future river activity (meandering and scouring). Cost of the as-constructed HDD installation—exclusive of material (pipe) purchase—approached $4.25 million. In comparison, the projected expense of a similar conventional crossing of similar extent was $2.75 million, whereas installation of another aerial placement was forecast to cost $6.5 million. The demonstrated lack of longevity precluded further consideration of the conventional technique. On the basis of construction costs and follow-on maintenance expenses, another aerial crossing was ruled out.

River Channel Conditions

In general terms, the leveed, partially flow-managed Atchafalaya River is a north-south oriented distributary of the Mississippi and Red rivers. Flow volume management (30 percent of the Mississippi's water volume is congressionally mandated for diversion down the Atchafalaya) is accomplished by the U.S. Army Corps of Engineers through a series of hydraulic structures positioned 40 km (25 mi) north of Melville. From the point of parent stream/distributary stream divergence to the Gulf of Mexico, the Atchafalaya's channel is roughly 40 percent as long as the Mississippi's course. Consequently, the Atchafalaya has a higher hydraulic gradient (flow slope) resulting in a faster current and a less convoluted (i.e., straighter) channel.

At the crossing site's latitude, the Atchafalaya is situated in the western third of the Mississippi River's floodplain: a mostly sediment-filled alluvial valley approximately 65 km (40 mi) wide and 60 to 90 m (200 to 300 ft) deep. TGPL's existing pipelines essentially bisect a gently curving, convex eastward, 5-km (3-mi) river reach. Upstream, the channel describes an approximate 20-degree bendway from the northwest. Downstream, sequential bendways varying between 30 and 110 degrees, interspersed with straight reaches 1.5 km (1 mi) long, are present. Articulated concrete mattresses revet both sides of the river at selected points. In addition to being longitudinally discontinuous, these "erosion inhibitors" do not transversely extend much beyond the underwater toe of the protected bank's slope.

At TGPL's site, the river's width approximates 410 m (1,350 ft), and its roughly U-shaped cross section features a minimum bottom elevation (i.e., a thalweg) of about −52 ft, National Geodetic Vertical Datum (NGVD). Water depth at "normal" stage slightly exceeds 21 m (70 ft). During the crossing study's conduct in mid-1985, the eastern bank was caving (ablating/sloughing) at and downstream of TGPL's pipeline crossings. Conversely, the western bank, which until shortly before the investigation had also been a caving bank, exhibited slight building (accreting) tendencies.

Site Surface Conditions

The 1930s-vintage flood protection levees bounding both sides of the channel were, during the 1950s, incorporated as guide levees into two emergency flood relief spillways: the Morganza Floodway on the east and the West Atchafalaya Floodway to the west. The distance between the opposing levees' riverside toes at the crossing site is roughly 840 m (2,765 ft). The comparatively narrow western batture (land between the levee's riverside toe and the water's edge) is about 85 m (280 ft) wide, with a surface elevation varying between 35 and 32 ft, NGVD. The eastern batture is almost 345 m (1,135 ft) wide and features several large, water-filled borrow pits. Surface elevation on that side ranges between 38 and 33 ft, NGVD. Crests of both sides' levees are nominally at elevation 52 ft, NGVD. Landward of either levee, the ground surface gently slopes to elevation 25 ft, NGVD, because of the presence of "natural levees" (course-paralleling, shallow-sloped ridges of sediment deposited by the river during prehistoric flooding).

Site Subsurface Conditions

Extracted from site-specific on-land and in-river borings performed for the crossing study, the soil profile consists of two types of alluvial sedimentation, locally termed topstratum and substratum, overlying marine (saltwater sea-deposited) clay. Generalized stratification is given in Table 1.

The marine clay, constituting a coastal prairie terrace formation, defines the Mississippi River valley's horizontal as well as vertical limits: the coastal prairie terrace "uplands" to the east and west consist of such material. The salient feature is that the marine clay has never been penetrated by the river. Figure 1 shows details.

Site Groundwater Conditions

The river's stage defines the groundwater level at the channel edges. By approximately 90 m (300 ft) landward, the water table is within 0.9 m (3 ft) of the site surface as evidenced by the eastern batture borrow pit water levels. On the levees' landsides, free water can fluctuate between the ground surface and the approximate 1.5-m (5-ft) depth: this will depend primarily on rainfall amounts.

Significantly, the phreatic surface (i.e., the pressure head) in the substratum sand responds to stages of the Mississippi's main channel located approximately 56 km (35 mi) to the east. The import of this is that the Mississippi's water level at the crossing site's latitude can rise approximately 3 m (10 ft) above the Atchafalaya's flood protection levee crests. Consequently, maintaining hydraulic integrity of both the topstratum clay and the Atchafalaya's channel edge levees is an important factor in preventing flooding.

River Regimen

On the basis of the site conditions described, the Atchafalaya River's potential for reconfiguring/relocating itself—through horizontal meandering and vertical scouring—was assessed (*4*). Figure 1 shows the findings.

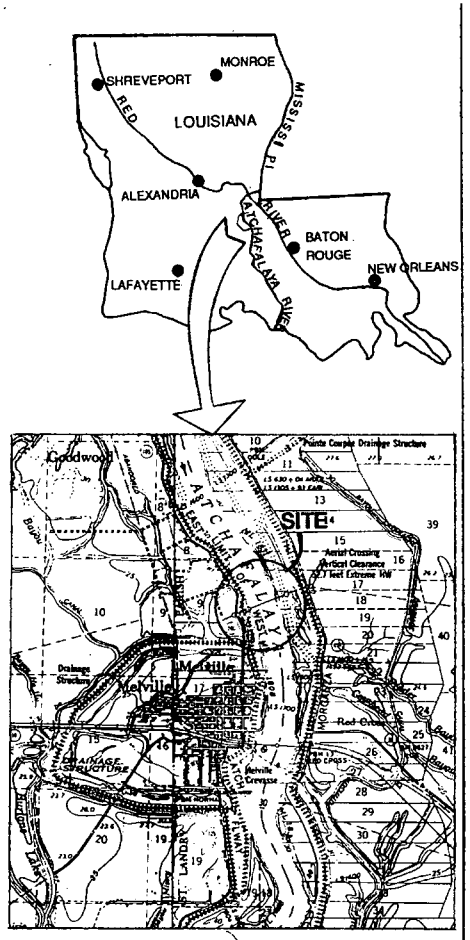

SITE LOCATION

SCALE: 1 : 62,500

NOTE:

SITE LOCATION TAKEN FROM USGS
15 MINUTE SERIES QUADRANGLE MAPS:
FORDOCHE, LOUISIANA - 1959
PALMETTO, LOUISIANA - 1959.

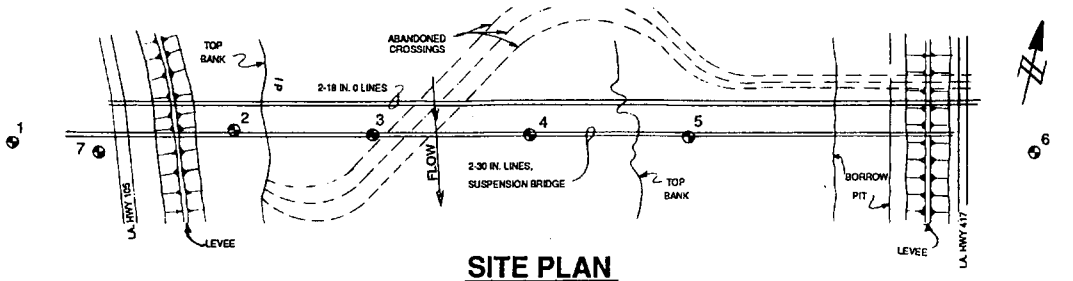

SITE PLAN

SCALE: 1 IN. = 200 FT.

⊕ = BORE HOLE LOCATION

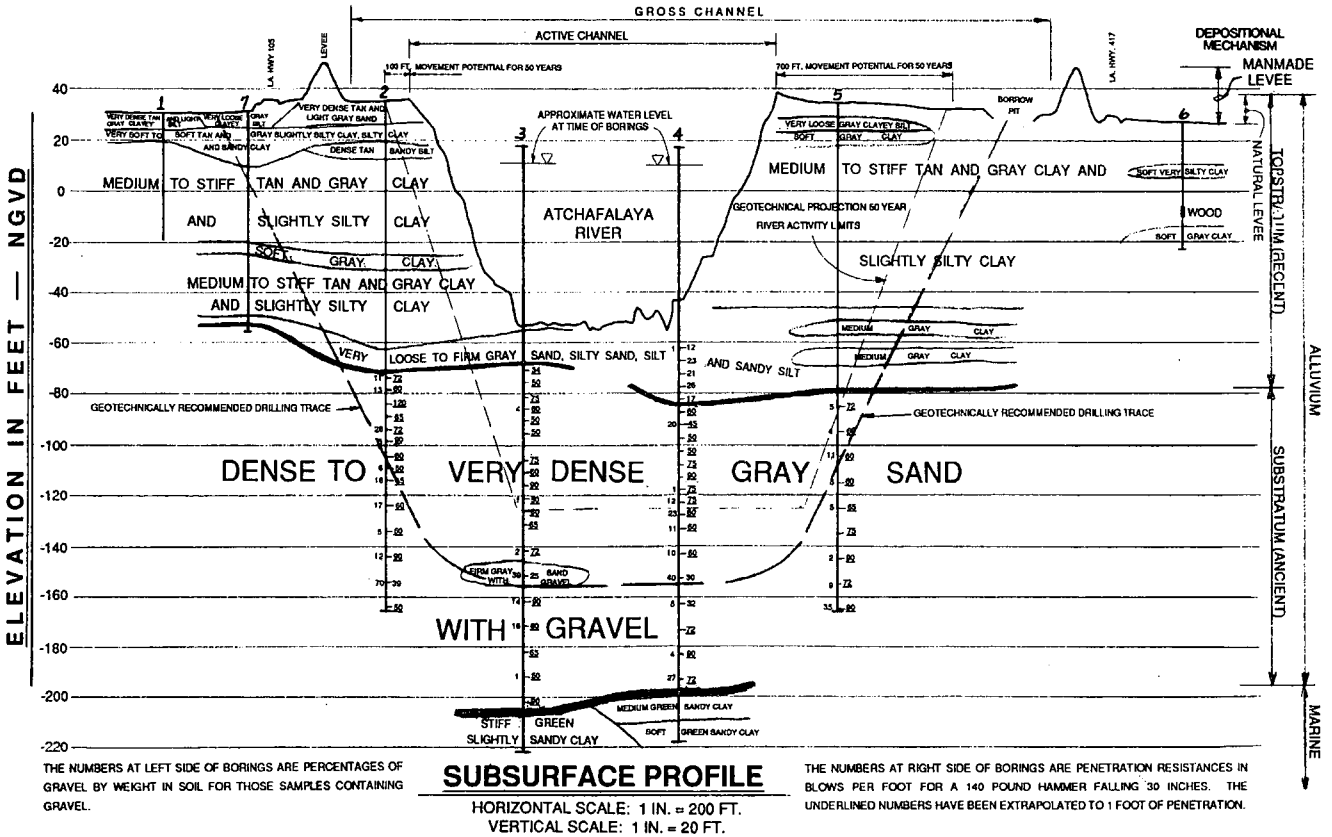

THE NUMBERS AT LEFT SIDE OF BORINGS ARE PERCENTAGES OF GRAVEL BY WEIGHT IN SOIL FOR THOSE SAMPLES CONTAINING GRAVEL.

SUBSURFACE PROFILE

HORIZONTAL SCALE: 1 IN. = 200 FT.
VERTICAL SCALE: 1 IN. = 20 FT.

THE NUMBERS AT RIGHT SIDE OF BORINGS ARE PENETRATION RESISTANCES IN BLOWS PER FOOT FOR A 140 POUND HAMMER FALLING 30 INCHES. THE UNDERLINED NUMBERS HAVE BEEN EXTRAPOLATED TO 1 FOOT OF PENETRATION.

FIGURE 1 Site conditions.

The limits of short-term horizontal activity were judged to be the historically mapped 1808 and 1831 bank lines. Such data indicate that the Atchafalaya has essentially been confined to its present-day channel during the period in question. These channel limits are now mostly defined by the in-place flood protection levees, whose locations were necessarily adjusted to compensate for minor course shifting. The most recent such levee relocation was a 1984–1985 "setback" on the western bank just upstream of the crossing site.

The present-day ground surface landward of the levees features no evidence of significant meandering (oxbow lakes, meander scrolls, etc.). Consequently, prehistoric channels had to be divined from published studies (*5*). They indicated that a trace of the Mississippi-Ohio River system approximately 3,000 years old and a 4,000- to 5,000-year-old Arkansas River system course had once traversed the area. This information indicates that these ancient channels and the modern Atchafalaya are independent of one another. Further discussion of the factors driving the Atchafalaya's horizontal alluviation is beyond the scope of this paper.

In terms of vertical river activity, the topstratum's loose to firm silt and sand above elevation −85 ft, NGVD, is indicative of normal river penetration (i.e., seasonal scouring). The substratum's dense to very dense sand, as evidenced by its in situ density, has probably not been as recently disturbed by alluvial activity. However, hydrographic charts of the Atchafalaya show that localized "holes" can extend below elevation −100 ft, NGVD. The closest such "permanent" penetrations are located approximately 29 km (18 mi) upstream and 24 km (15 mi) downstream.

Vertical scour should naturally be restricted by the substratum's zone of gravel-bearing sand between elevations −90 and −150 ft, NGVD. By requiring a higher velocity for entrainment, the graveled material will probably not be extensively penetrated under presently existing flow conditions. Prehistoric river courses, possibly the ancient Arkansas channel mentioned earlier, are likely responsible for the sand's gravel constituency, as opposed to post-flood "fall-back" into "recent" scour holes of the present-day Atchafalaya.

Future River Configuration

In view of the foregoing analysis, the Atchafalaya River was deemed likely to continue its established behavior during the 50-year design life of the new crossing. The major potential for regimen change hinges on "capture" of the Mississippi by the hydraulically more efficient Atchafalaya. Although potamological forces presently at work will someday cause this, such an event was assessed as being unlikely within the next half century.

Bank shifts of 215 m (700 ft) eastward and 30 m (100 ft) westward from present-day locations were projected for the 50-year design period. Scour penetration as deep as elevation −130 ft, NGVD—midway into the substratum's graveled sand zone—was also forecast for the same period. These alluviation limits served as the basis for selecting the HDD installation geometry.

CROSSING DESIGN

On the basis of results of the site characterization, TGPL elected to install the HDD river crossing from a point landward of the western flood protection levee to a location on the opposite side's batture near the eastern levee's riverside toe (see Figure 1). Place-

TABLE 1 General Stratification

Nomenclature	Approximate Inclusive Stratum Elevations Feet, NGVD	Material Description
Topstratum. Deposition in/from the present day Atchafalaya/Mississippi Rivers.	Surface (38/25) to 22/10	Natural levees: dense clayey silt and sand in the western bank, mostly medium strength clay with silt pockets in the higher eastern bank.
	From The Above to -50/-68	Medium to stiff strength clay containing pockets of soft clay and (infrequently) wood. The stronger clay strata feature "slickensides": desiccation induced cracks which have subsequently "healed". The wood represents buried cypress forests.
	From The Above to -70/-85	Loose to firm silt and sand. This layer is slightly thicker in the eastern bank.
Substratum. Deposition in/from previous courses of the Mississippi River or its predecessors.	From The Above to -198/-210	Dense to very dense sand containing a zone of up to 25%, by weight, gravel between elevations -90 and -150 feet, NGVD.
Marine. Deposition onto a Miocene (late Tertiary) age saltwater seabed.	From The Above to The Extent Of The Exploration	Soft to stiff strength sandy clay. In general, this material is highly overconsolidated and slickensided.

ment depths were to be between 52 and 55 m (170 and 180 ft) below the bank/batture surfaces. In essence, the western levee and its adjacent narrow batture were scheduled for subdrilling both to avoid potential river activity encroachment (onto the new line) and to prevent the short-radius curve (for this large-diameter pipe) necessary to reach the desired HDD elevation. Installation depth was selected to circumvent both river scour and the more extensive gravel concentrations of the substratum sand. The marine clay, an ideal material for HDD, was not selected as an installation medium because of its extreme depth.

Planned drilling dimensions were about 976 m (3,200 ft) horizontally with a penetration to approximately elevation −145 ft, NGVD. Entrance/exit angles were designed to vary between 10 and 14 degrees from the horizontal. Sagbend curve minimum radius was set at 1100 m (3,600 ft) on the basis of the rule of thumb that 25 mm (1 in.) of carrier pipe diameter requires 30 m (100 ft) of curvature radius to limit induced bending stress to an inconsequential magnitude (although some flexural stress is generated by even a large-radius curve, the magnitude is considered so small as to be trivial; thus the term "stress-free" bend is commonly applied). The pipe itself was to be 15.875 mm (0.625 in.) wall thickness, high yield strength (X-65 steel with a fusion bonded epoxy coating).

CROSSING PERMITTING

This rather straightforward design required an 18-month-long follow-up effort for acquiring permits. Two items of information were necessary to satisfy local (Levee Boards), state (Louisiana's Office of Public Works), and federal (U.S. Army Corps of Engineers) agencies then having an interest in the project: (*a*) proof that harmful levee subsidence (settlement) or instability (landsliding) would not occur and (*b*) a methodology to positively restore integrity of the topstratum clay penetrated by the HDD bore landward of the western flood protection levee.

The overriding objective was to provide assurance that the pipe's levee crossings—especially the subdrilled one—would not unduly affect integrity of either flood protection embankment or noticeably disturb the adjacent roads. For the subdrilled case, such assurance was sought through a scheme, described more fully later, to grout the soil-pipe annulus beneath and landward of the western bank's levee. Beneficially, subdrilling this levee precluded a "heavy" surface crossing's inducement of traditional adversities: slope instability and embankment settlement.

Satisfying concerns about HDD's effects on the site and the site's effects on the HDD placement involved conducting slope stability and embankment subsidence determinations. On the basis of soil data developed in the original exploration and information extracted from subsequent studies and preexisting records, these evaluations included limiting equilibrium factor-of-safety analyses together with finite element/consolidation/long-term creep foundation soil deformation assessments. Figures 2 and 3 show the input soil data/parameters and the detailed analytical results.

Levee Stability/Subsidence

For the line's crossing of the eastern levee's surface, the embankment's 5.8-m (19-ft) existing height was increased by 2.1 m (7 ft) to account for the weight of the pipe and the requisite earthen bedding/covering. The intent was to determine both the effect on slope stability (the safety factor reduction) and the settlement to be generated by the newly placed pipeline. Requirements were that the postconstruction safety factor be greater than 1.30 and that the pipe not settle into the design (i.e., net) levee section.

Computational details and the critical stability surfaces derived from a wedge analysis are shown in Figure 2. Following standard practice, only the two-dimensional case was evaluated; stability augmentation due to three-dimensional effects was not considered. Also, the embankment portion containing the pipe was treated as a solid soil mass of uniform unit weight. The outcome was that for all failure modes (wedges) evaluated, the safety factor exceeded the required minimum.

Settlement of the crest due to imposition of the pipeline crossing was projected to be only 76 mm (3 in.) during the ensuing 50 years. Therefore, the earthen pad 305 mm (12 in.) thick beneath the pipe was judged sufficient to prevent pipeline encroachment into the embankment's net section.

Subsoil Deformation

For the western levee's subdrilling, the joint objectives were demonstration of the facility's future watertightness and assessment of embankment-induced settlement effects on the pipeline. These studies were conducted because of concerns about installation efficiency, long-term viability of the soil-pipe annulus seal, and design of the pipe's wall thickness to accommodate subsoil deflections/loadings. In addition, the material for grouting the soil-pipe annular space required design and testing. The intent of the latter efforts was production of a grout material that could also serve as the "drilling fluid" during the carrier pipe's pull-in and thereby help to ensure a complete annular plug.

Since the dense to very dense substratum sand is virtually incompressible, analysis of the levee's effects on the pipe involved determining the topstratum clay's initial (undrained elastic-plastic deflections), primary consolidation (settlement), and secondary consolidation (time-dependent creep) deformations. Computed values for these movements in the various clay substrata beneath selected locations of the levee cross section are shown as the "strain field" of Figure 3. This accounts for residual settlement stemming from the original (1932 through 1935) construction and deflections caused by a newly built embankment setback.

Because half of the pipe below the western levee was scheduled for embedment in incompressible sand and deflection magnitudes experienced by the pipe are proportional to the underlying thickness of compressible clay, flexure of the line due to the levee's present position was projected to be 3 mm (1/8 in.) in 50 years. With respect to stress effects on the pipe, this is inconsequential.

Of much greater concern was the pipe flexure possibly generated by a future levee setback. To assess this, the strain field of Figure 3 was used to predict embankment-induced deflections should the levee be relocated onto pristine foundation soils containing the HDD placement. Fortunately, as with the soil deformations beneath the existing levee's position, the projected deflections from such a setback were judged unlikely to affect integrity of the HDD installed pipeline.

Grout Design

Consisting of bentonite clay, portland cement, and a proprietary set retardant, the grout mixture was a key design element in this

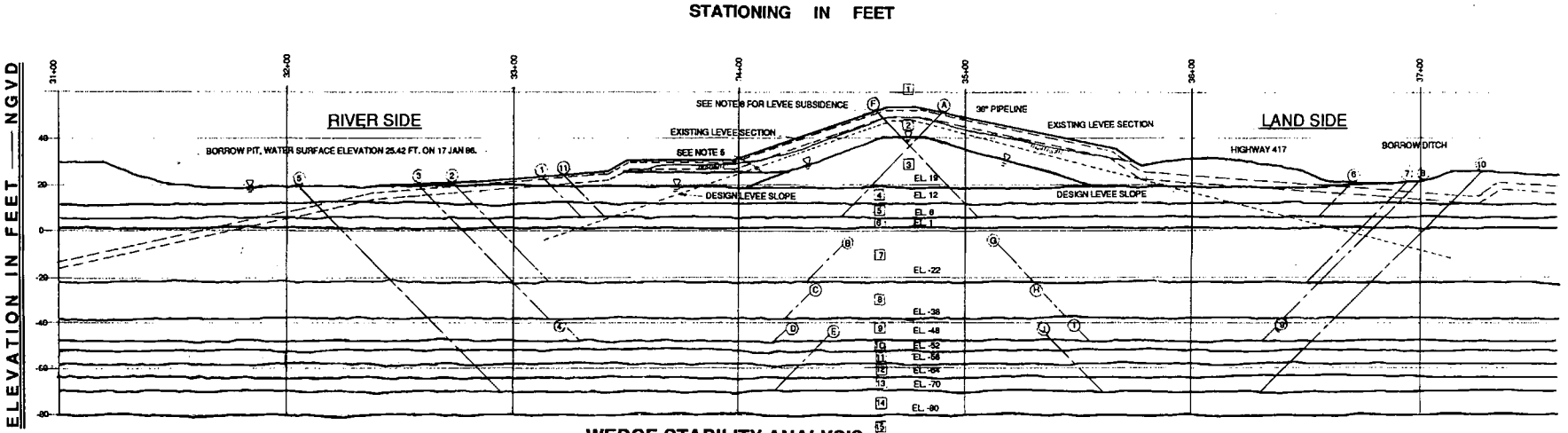

WEDGE STABILITY ANALYSIS

LOCATION	SLIP SURFACE NUMBER		ELEV.	DRIVING $+D_A$	DRIVING $-D_p$	$\sum D$	RESISTING $+R_A$	RESISTING $+R_B$	RESISTING $+R_p$	$\sum R$	SAFETY FACTOR
RIVERSIDE	A	1	6	389.28	59.81	329.47	220.41	153.52	98.17	472.10	1.43
	B	2	-22	816.32	230.96	585.36	367.52	281.46	242.88	891.86	1.52
	C	3	-38	1108.12	388.13	719.99	456.90	308.38	334.97	1100.25	1.53
	D	4	-48	1311.32	539.18	772.14	534.95	347.99	417.44	1300.38	1.68
	E	5	-70	1845.91	804.36	1041.55	714.11	325.74	627.07	1666.92	1.60
(SEE NOTE 5)	A	11	6	388.68	41.08	347.60	220.41	140.18	101.70	462.29	1.33
LANDSIDE	F	6	6	394.84	41.03	353.81	221.92	200.25	89.33	511.50	1.45
	G	7	-22	829.10	230.92	598.18	375.70	293.70	247.35	916.75	1.53
	H	8	-38	1124.67	420.31	704.36	468.59	280.35	342.74	1091.68	1.55
	I	9	-48	1326.77	579.01	747.76	550.47	307.05	424.62	1282.14	1.71
	J	10	-70	1861.48	978.42	883.06	728.95	190.01	675.71	1594.67	1.81

SOIL DATA NO.	γ_t or γ'	$\bar{c}$	$\bar{\phi}$
1	18850.50	23.95	0
2	18065.06	23.95	0
3	8325.64	23.95	0
4	7697.29	47.90	0
5	7540.20	14.37	0
6	7226.03	47.90	0
7	5969.33	26.35	0
8	5969.33	31.61	0
9	6597.68	44.07	0
10	9425.25	9.58	15
11	8482.73	46.94	0
12	8011.46	9.58	15
13	7540.20	29.22	0
14	9425.25	0.00	25
15	9425.25	0.00	35

LEGEND:

γ_t = TOTAL SOIL UNIT WEIGHT IN N/m^3

γ' = SUBMERGED SOIL UNIT WEIGHT IN N/m^3

$\bar{c}$ = SOIL COHESION IN kPa.

$\bar{\phi}$ = ANGLE OF INTERNAL FRICTION IN DEGREES.

▽ = WATER SURFACE.

$\bar{c}$ BASED ON UNCONFINED AND UNCONSOLIDATED/UNDRAINED COMPRESSION TESTS.

$\bar{\Phi}$ BASED ON SPT BLOW COUNTS AND UNCONSOLIDATED/DRAINED COMPRESSION TESTS.

NOTES:

1. SAFETY FACTOR = $\dfrac{R_A + R_B + R_p}{D_A - D_p} = \dfrac{\sum R}{\sum D}$
2. TWO DIMENSIONAL ANALYSIS, WEDGE METHOD USED FOR SAFETY FACTOR COMPUTATIONS.
3. DEPICTED LOW WATER STAGE WITH GROUND WATER MOUND.
4. SOIL PROFILE FROM:
   LJC&A BORINGS
   USACE BORINGS
5. SAFETY FACTOR AFTER RAPID DRAWDOWN OF BORROW PIT (FULL BORROW PIT WATER SURFACE ELEVATION 26 FEET, NGVD).
6. MAXIMUM LEVEE SUBSIDENCE OF 5 INCHES AT THE CENTER DUE TO PIPELINE CROSSING'S ADDITIONAL WEIGHT. THIS GRADES TO ZERO AT THE TOES. SUBSIDENCE OCCURS IN 50 YEARS.

FIGURE 2 Eastern levee stability/subsidence.

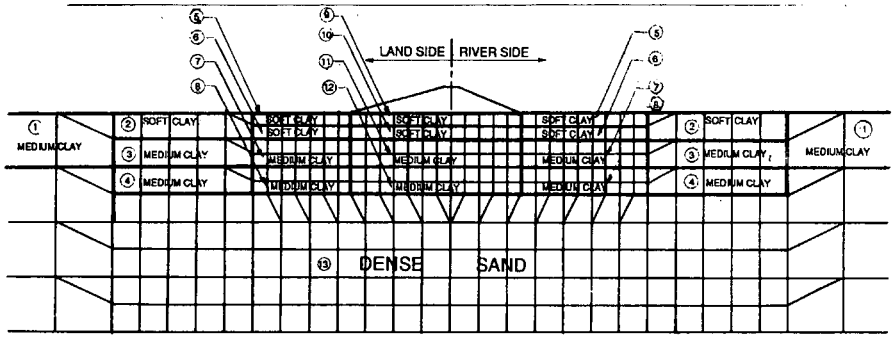

WEST LEVEE SOIL SYSTEM

FINITE ELEMENT MODEL PRIOR TO LOADING

Eu = YOUNG'S STRESS-STRAIN MODULUS IN kPa
u = POISSON'S RATIO
SOIL PARAMETERS BASED ON:
-ANISOTROPICALLY CONSOLIDATED TRIAXIAL COMPRESSION LOADING/UNLOADING TESTS WITH PORE PRESSURE MEASUREMENTS.
-INCREMENTAL AND CONSTANT RATE-OF-STRAIN CONSOLIDATION TESTS.

NO.	Eu	u	NO.	Eu	u
1	3830	0.45	8	7180	0.45
2	2870	0.45	9	4790	0.45
3	4790	0.45	10	7180	0.45
4	7180	0.45	11	10770	0.45
5	2390	0.45	12	14360	0.45
6	3590	0.45	13	478800	0.20
7	4790	0.45			

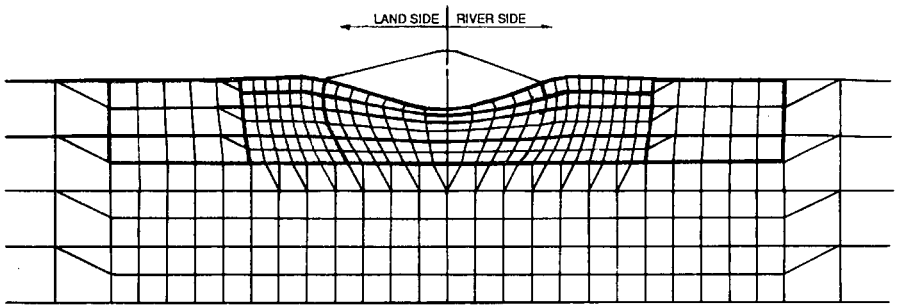

UNDRAINED DEFORMATIONS

HORIZONTAL DISPLACEMENTS AMPLIFIED BY A FACTOR OF 130.
VERTICAL DISPLACEMENTS AMPLIFIED BY A FACTOR OF 55.

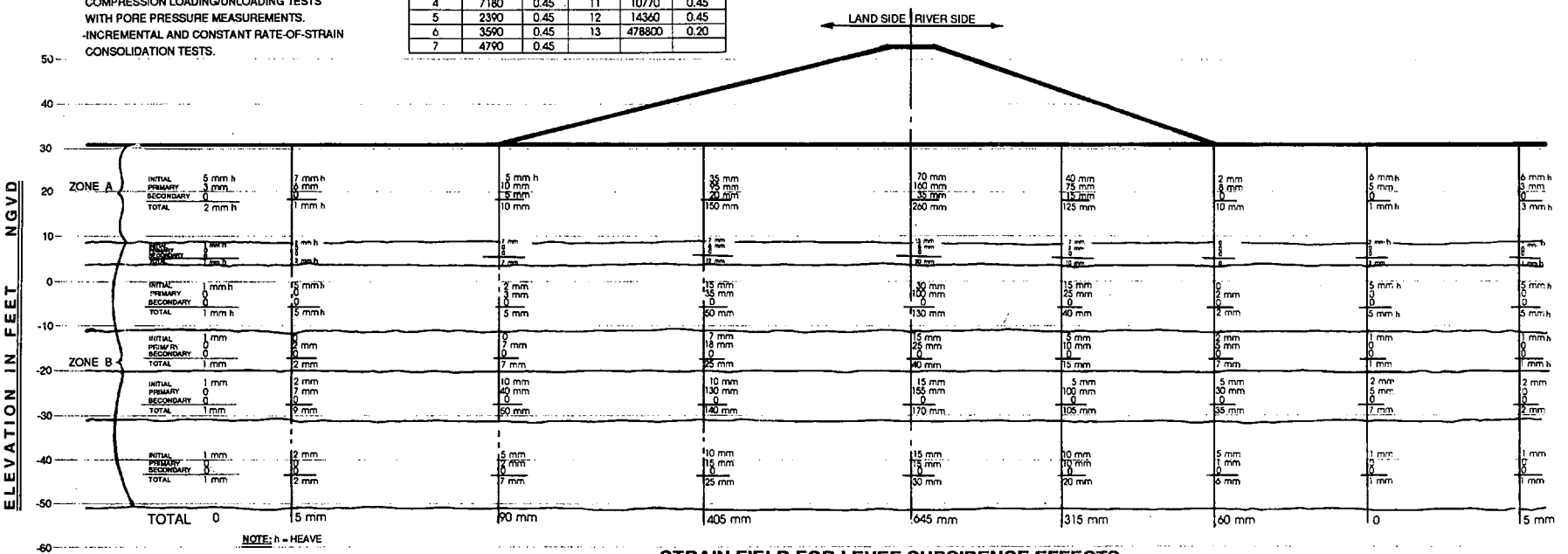

STRAIN FIELD FOR LEVEE SUBSIDENCE EFFECTS

ZONE A PRIMARY IN 6 MONTHS CREEP RATE: 40 MM SETTLEMENT PER SECONDARY CYCLE
ZONE B PRIMARY IN 50 YEARS CREEP RATE: 60 MM SETTLEMENT PER SECONDARY CYCLE
EXISTING LEVEE: ZONE A HAS BEEN THROUGH 2 CYCLES OF SECONDARY CONSOLIDATION.
ZONE B JUST COMPLETED PRIMARY CONSOLIDATION.

FIGURE 3 Western levee subsoil deformations.

project. Developed by the Halliburton Company, the grout had four crucial characteristics:

- Effectiveness of the retardant in delaying the cement's initial set (14 days was required by the HDD contractor),
- Compressive strength development 30 days subsequent to setting [1380 kPa (200 psi), that is, four times the topstratum clay's maximum compressive strength, was mandated],
- Impermeability (a coefficient of permeability, k, less than 1×10^{-7} cm/sec was stipulated), and
- Shrinkage potential [no volume reduction (shrinkage) of the in-place grout plug was permissible].

The requirement for annulus grouting was driven by the need to counter HDD's site-specific effects, particularly the possible compromise of the subdrilled levee's/topstratum clay's watertightness. Since the Mississippi is capable of generating a substratum sand phreatic head exceeding the Atchafalaya's levee crest elevations, any unplugged penetration in the topstratum clay adjacent to the latter stream's flood protection embankments could cause sand boils leading to crevasse (levee breach) development. Furthermore, the grout's planned injection during carrier pipe pull-in generated the need for a cement set delay to allow time for both normal construction and unforeseen delays.

For reasons discussed later, the annulus sealing procedure envisioned by the design phase did not produce the now in-place plug. Consequently, a complete discussion of the grout's development will not be provided. Rather, since the grouting constituted a major aspect of this project, two general comments are appropriate. First, the developmental process revealed that detailed testing procedures are not available in a unified/coordinated set of standards. Therefore, various methodologies from the American Petroleum Institute (API) and American Society for Testing Materials (ASTM) were used in concert to quantitatively prove the grout design. Second, and more important, the detailed testing showed that the grout mixture was capable of performing as both the final stage drilling fluid and the agent for restoring the levee foundation's/topstratum clay's integrity.

Permit Acquisition

On the basis of combined results of the site characterization and grout evaluation programs, the HDD crossing design was judged to be feasible. Therefore, it was permitted by the local levee boards having jurisdiction. The process included detailed technical input from Louisiana's Office of Public Works and the U.S. Army Corps of Engineers, New Orleans District.

INSTALLATION

After permit receipt, the installation contractor was engaged: Inarc Horizontal Drilling, Inc. (the successor firm to Reading & Bates Horizontal Crossing Division, an early industry leader in HDD applications). Actual construction—involving two attempts at carrier pipe pullback—took place during the second half of 1987. Site restoration was finalized in late 1988.

First Attempt

Work began in early July 1987. The site's setup is shown in Figure 4. HDD rig positioning was on the western bank approximately 150 m (500 ft) landward of the flood protection levee. Halliburton supplied a barge-mounted "mud plant"—anchored in the river against that same bank—to deliver the various drilling fluids, particularly the delayed-set grout. The Atchafalaya's opposite side, the eastern batture/bank, then became the pipe make-up side: the HDD bore's ground penetration was in a borrow pit just riverward of the levee's toe. The assembled carrier pipe was placed in a flotation trench perpendicular to and landward of the levee. During the pullback process, a dragline-suspended cage roller was used to lift the pipe string over the roadway adjacent to the levee's landside toe. Rollers and/or side-boom dozers situated directly on the levee helped guide the carrier pipe into the directionally bored hole.

During pilot hole establishment, inadvertent drilling fluid returns (mud seeps) were noted at the ground surface on both the eastern and western sides of the river (*6*). These seeps were positioned no more than 10 ft, laterally, from the HDD trace's surface projection and were discrete (i.e., readily definable in terms of their appearance on the ground). Significantly, one such seep penetrated upward through the western bank flood protection levee to exit within 1 m (3 ft) of that embankment's crest. Another surfaced in a crack in the asphalt-paved highway paralleling that same levee's landside toe. Also of significance is that the mud seeps did not occur while directional drilling was transiting the substratum sand. Interestingly, the contractor reported that this phenomenon was common in the soft clays of northwestern Europe.

After much evaluation, the seeps were attributed to passage of pressurized drilling fluid through preexisting anomalies in the topstratum clay (slickensided prefractures, tree roots, etc.). Downhole mud pressurization was possibly initiated by clay cuttings sealing the soil-pilot stem annular space and thereby preventing return of fluid to the drill rig. The rig's mud pump was capable of producing pressures in excess of 6900 kPa (1,000 psi), with roughly 1725 kPa (250 psi) of pressure needed to operate the downhole drill motor. Penetration of the substratum sand allowed the trapped mud to flow radially into the pervious formation rather than intrude into the impermeable topstratum clay's comparatively well-defined planes of weakness. Hence, mud seeps were not prevalent while the bore penetrated sand. On the basis of these premises, regulatory authorities, principally the U.S. Army Corps of Engineers, allowed pilot hole construction to continue. However, such permission was made contingent on the western bank's levee section intruded by the returns being rebuilt immediately after the crossing's completion.

Subsequent to pilot hole installation, pullback reaming was accomplished in the standard manner. This opened the bore to a nominal diameter of 1400 mm (56 in.). Preexisting mud seeps did not cause significant problems during this operational phase. Although some flow was noted, drilling fluid appearance on the ground surface was not significant.

The first attempt at pullback began in mid-September, a dummy (short section) pull having been completed earlier in the month. For this initial try, the "very large" diameter steel casing being drawn downhole contained two smaller-diameter polyethylene lines. Their purpose was to allow selective water injection for control of the carrier pipe's buoyancy. Rough computations indicated that the empty pipe string generated approximately 2900 N/m (200 lbf per lineal foot) of positive buoyancy when immersed in the drilling slurry. Despite this precaution, after a little more than 300 m (1,000 ft) of the pipe assembly had been drawn be-

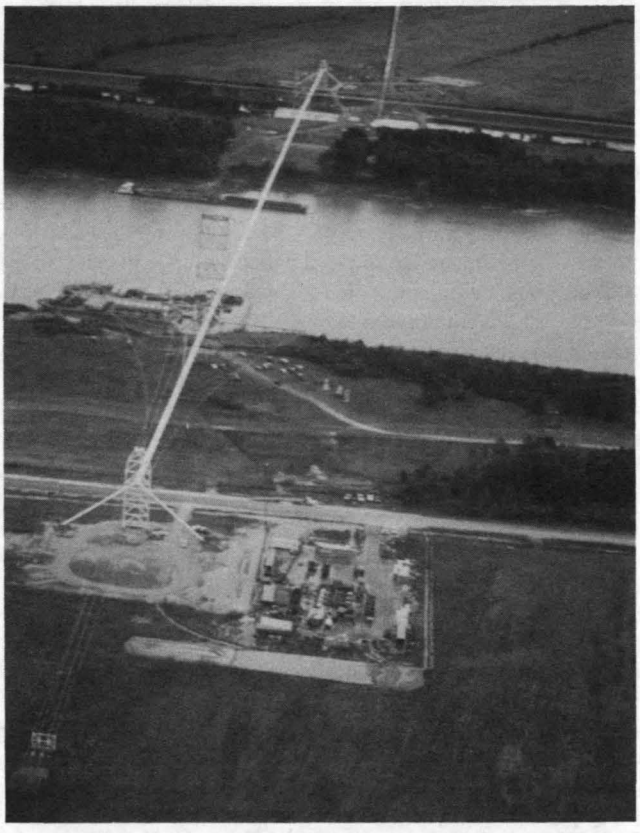

FIGURE 4 Eastward-looking views of the crossing construction. *Top*, detail of pipe side penetration point during final pullback; *bottom*, overall perspective of project as seen from above the HDD drill rig during the first pull-in attempt. Drilling mud seeps on and landward of the levee together with Halliburton's barge-mounted drilling mud/grout plant are shown in bottom photograph. In the top photograph, note how the carrier pipe is handled as it is tailed over the levee.

neath the eastern batture, forward progress was halted near the end of the eastern side's sagbend curve. At this point the pipe appeared to be stuck. Efforts to free it, which lasted almost $1^1/_2$ weeks and included buoyancy adjustments and the use of a vibratory hammer in the hope of "liquifying" sand surrounding the line, were unsuccessful. As a result, an explosive charge was placed downhole to within 30 m (100 ft) of the pullhead/reaming assembly. Detonation allowed the separated pipe segment/pullhead to continue across the river. The remaining 270 m (900 ft) of carrier pipe that could not be withdrawn was then filled with concrete and abandoned in-place.

Failure of the initial attempt at carrier pipe pull-in was attributed to a variety of factors. Two appear paramount. First, an obstruction downhole could have been caused by an undecayed cypress log or gravel fallback—phenomena common throughout the area's geotechnical profile (in fact, "wood" was encountered in the eastern bank's topstratum clay by both the initial exploration's borings and the pilot hole drill). A pilot bore geometrical aberration may have resulted from the bit being deflected by such an obstruction. Subsequent reaming possibly accentuated this borehole jog into a small-radius curve in the HDD geometry (*2,3*). Second, the large diameter, thick-walled, and relatively stiff (high section modulus) carrier pipe required substantial pulling force just to negotiate the planned sagbend (*7*). Combining this with the pull force necessary to draw the carrier pipe around the borehole's geometrical anomaly produced a total exceeding the HDD rig's 4480-kN (650,000-lbf) nominal line pull capacity. The consequent halting of the pull-in thus allowed time for the bored hole to fully collapse around the in-place casing. The result was that the pipe became inextricably stuck.

Second Attempt

After loss of the initial attempt, the pilot bore was partially redrilled using a midcourse offset from the original trace. Extreme care was taken this time to produce a cleanly reamed, smooth hole (one free from geometrical aberrations) that strictly conformed to the design geometry. Significantly, no obstruction was encountered during redrilling, nor were appreciable amounts of wood fragments noted in the drilling fluid returns.

The refurbished hole was ready for carrier pipe pullback by the middle of November. Additional carrier pipe had been secured and placed, and Halliburton's barge-mounted mud plant had been returned to the site to mix and deliver delayed-set grout.

Carrier pipe pullback operations requiring approximately 90 hr to complete were begun on November 18, a Wednesday. The planned point of delayed-set grout injection, between 150 and 215 m (500 and 700 ft) from the HDD drill rig, was reached by the pullhead assembly late Saturday evening. At that time, high pull forces, sometimes approaching 2760 kN (400,000 lbf), and unacceptably slow progress—occasionally at the rate of one 10-m (33-ft) pull-pipe joint in 60 min—indicated that grout injection might halt the operation. The reasoning was that the resultant change in drilling fluid lubricity could induce a total force requirement exceeding the HDD rig's line pull capacity. Although the pullback rate steadily and substantially increased after the pullhead assembly approached to within 140 m (460 ft) of the HDD drill rig, intermittently high pull forces continued until the pullhead was about 90 m (300 ft) from exiting the ground surface. As a consequence, it was not until the final 60 m (200 ft) of carrier pipe pullback that the delayed-set grout was injected. In essence, the pullback's successful completion lacked extensive placement of the planned annulus grout.

Also of note was that flow from the previously established drilling mud seeps steadily increased throughout the pullback's course. Copious amounts of drilling slurry and the delayed-set grout mixture covered the site subsequent to carrier pipe pull-in (see Figure 5).

Postconstruction Activities

Several days after pull-in completion, the contractor attempted to seal the topstratum clay by inserting a drill stem section down the soil-pipe annular space. Using this as an injector, an approximate 165-m (540-ft) length of annulus was grouted. Unfortunately, Halliburton's barge-mounted plant had moved off site the day after carrier pipe pull-in. Consequently, even though the actual material injected featured much the same formula as the original grout, the mixing facility was far less sophisticated. As subsequent events showed, the injected material did not perform as planned.

Concurrent with postconstruction grout injection, the western levee section, which experienced the drilling mud seep, was removed and rebuilt to Corps of Engineers design standards. In addition, to further enhance levee water tightness, its attendant seepage retardation berm (between the embankment's landside toe and the side ditch of LA Highway 105) was substantially augmented. On balance, these efforts were fortunate since the original embankment segment, during its more than 50 years of existence, had settled close to its net section geometry.

Grout Evaluation

Samples of the grout mixture injected after pull-in were obtained in the field for evaluation. The procedure was similar to the ASTM standard used in concrete work (i.e., molding/curing/breaking of cylinders) since an applicable API specification could not be identified.

Observation of the recovered specimens showed the material to be mechanically unstable. Rather than setting up, the slurry separated into its bentonite, portland cement, and water components. Later evaluation by an independent chemical testing laboratory indicated that this was due to an insufficient percentage of bentonite.

To compensate for the in-place seal material's unsatisfactory performance, a jet-installation procedure (pressure mixing of a portland cement/soil/water grout through vertical holes drilled to intercept the soil-pipe annulus) was used. Accomplishment was from the surface of the seepage retardation berm and extended for roughly 85 ft along the pipe. The work, shown in Figure 5, was performed in October and November 1988, about 1 year after successful pull-in of the carrier pipe.

During the jet-grout construction, samples of the mixture were molded. After curing, time phase testing indicated that the requisite strength, impermeability, and volumetric constancy had been achieved. Most important, the jet-grout material's mechanical stability indicated that it would form an impermeable plug.

Crossing Completion

On the basis of findings of the jet-grout evaluation program, and after the contractor had rigorously cleaned up the construction site

FIGURE 5 Westward-looking views of the HDD drill rig setup site after carrier pipe pull-in. *Top*, drilling mud seeps mixed with grout returns from the directional borehole immediately after completion of the crossing. *Bottom* (foreground), jet grouting through the levee's seepage retardation berm. The purpose of the grouting, completed almost 1 year after line pull-in, was to help ensure viability of the soil-pipe annulus plug. Note effectiveness of site surface cleanup efforts (*bottom*, background).

(see Figure 5), the installation was judged complete. The integrity of the overall placement and, in particular, restoration of the top-stratum clay's integrity, has subsequently been proved through several cycles of high water, including the long-duration Mississippi River flooding of 1993.

PROJECT SIGNIFICANCE

Experiences and features of this project have materially affected the investigation, planning, and implementation of subsequent HDD construction (*2–4*).

Site Characterization

Greater consideration is now being given to determining a crossing site's geology, potamology, and geotechnology. In essence, site investigations are now "looking" for active as well as passive conditions:

- The limits, both present and future, of the obstacle to be crossed;
- The surface/subsurface conditions beneficially and adversely affecting HDD routing; and
- The physical and statutory obstructions to HDD conduct.

Site-specific studies are now being relied on to foretell features such as cypress logs (where a modern river distributary is cutting through buried backswamp forests generated by an ancient, independent, stream) and gravel pockets (at locations and elevations formerly subject to hydraulic gradients/entrainment capacities significantly different from such parameters of the present day waterway). The potential for these and other factors now determines the spacing of exploration boreholes as well as the necessity and applicability for detailed geophysical investigative techniques. Finally, heightened regard for both natural features (wetlands, etc.) and man-made facilities (levees, highways, existing pipelines, etc.) calls for a more comprehensive site characterization than has been the case in the past.

Crossing Design

Closer attention is now being paid to defining the mutually interactive effects of the site features and the construction methodology. In essence, detailed considerations inherent to levee stability and subsidence and prediction and remediation of drilling mud seeps have been identified and are being addressed. Further studies on pull force requirements in regard to pipe bending radius and stiffness, downhole buoyancy, and detailed borehole geometry are being performed. Finally, the necessity for designing specialized drilling fluids (from the standpoints of cuttings entrainment, carrier pipe pull-in lubricity, corrosion-coating protection, pipe buoyancy, and occasionally annulus sealing) is being recognized. In all these areas, much research still remains to be accomplished. Site integrity restoration requirements and the increasingly rigorous permitting processes at local, state, and federal levels add impetus to continuing such crossing design improvements.

Crossing Execution

The manner in which construction adversity is handled is now more rational. Geometrical aberrations caused by contact with obstructions can be identified through various types of downhole surveys and eliminated or reduced before their effects are magnified later in the installation. This points up the need for establishing as smooth a pilot bore as possible to help ensure successful pull-in of the larger-diameter carrier pipes. Furthermore, the recognition that inadvertent drilling mud returns are always possible when impervious (i.e., clay) soils are drilled is the key to addressing this and other such phenomena. Finally, potential problems associated with customized grout demonstrate that pre- and post-construction testing procedures for these materials and other such "speciality" drilling fluids specific to HDD need to be standardized.

SUMMARY

Successful installation of this HDD pipeline river crossing has shown that the construction technology can now be engineered. When utilized in applicable situations,the procedure will produce economical, minimally disruptive, and long-asting pipeline placements. Project-pecific feasibility of the method should be established through comprehensive site characterization. Existing geological and geotechnical conditions must be defined together with the dynamic (time dependent) nature of the obstacle to be negotiated. Furthermore, the installation methodology must be planned and executed with regard to existing site features and the interactive effects of those features and the construction. Physical phenomena and material behavior are key factors. This project has shown HDD to be a viable construction option in instances where a thorough site investigation, installation design, and economic assessment program so indicate. In this respect, enhanced HDD utility and continued reduction of the technology's few drawbacks will result from increased emphasis on procedural engineering.

REFERENCES

1. Hair, J. D., and C. W. Hair, III. Considerations in the Design and Installation of Horizontally Drilled Pipeline River Crossings. *Proc., Pipeline Infrastructure Specialty Conference,* American Society of Civil Engineers, Boston, Mass., 1988, pp. 10–22.
2. Hair, C. W., III. Subsurface Conditions Affecting Horizontal Directional Drilling. *Proc., Trenchless Technology: An Advanced Technical Seminar,* Trenchless Technology Center, Louisiana Tech University, 1993, pp. 217–236.
3. Hair, C. W., III. Site Characterization for Horizontal Directional Drilling. *Proc., Second Annual Spring Symposium,* Directional Crossing Contractors Association, Brownsville, Tex., 1993.
4. Hair, C. W., III. Obstacle Evaluation as the Basis for Crossing Design. *Proc., Pipeline Crossings Specialty Conference,* ASCE, Denver, Colo., 1991, pp. 59–70.
5. Fisk, H. N. *Fine-Grained Alluvial Deposits and Their Effects on Mississippi River Activity.* Waterways Experiment Station, U.S. Army Corps of Engineers, Vicksburg, Miss., 1944–1947.
6. Hair, J. D. Analysis of Subsurface Pressures Involved with Directionally Controlled Horizontal Drilling. *Proc., Pipeline Crossings Specialty Conference,* ASCE, Denver, Colo., 1991, pp. 1–12.
7. Langlinais, J. Required Pulling Forces for Bored Pipeline. *Pipeline and Utilities Construction,* Vol. 47, No. 12A, Dec. 1992, pp. 28–29.

Publication of this paper sponsored by Committee on Soil and Rock Properties.

Auger and Slurry Microtunneling Tests Under Controlled Ground Conditions

DAVID BENNETT, EDWARD J. CORDING, AND TOM ISELEY

Microtunneling tests using auger and slurry machines were performed at a test facility that was constructed by first excavating a trench 104 m (340 ft) long, 5 m (16 ft) wide, and 3 to 4 m (10 to 13 ft) deep into which six types of soils were placed and compacted in sections approximately 18 m (60 ft) long. The soil profiles included a lean silty clay (loess), a dry sand, highly plastic buckshot clay, wet sand, clay gravel, and silt. The interfaces between soil profiles were sloped to simulate mixed-face conditions and to provide challenges to ground control and alignment and grade control during these transitions. Moisture and density tests were performed to ensure uniformity. Horizontal inclinometers and settlement plates together with surface survey points provided data to evaluate settlement and heave along the test section. Penetration resistance was measured in each section of the completed test bed. Strain gauges were installed in eight of the centrifugally cast, fiberglass-reinforced polyester resin pipes 600 mm (24 in.) in diameter (supplied by Hobas Pipes USA) to measure strains in the pipe as it was being jacked into place. Steering jack loads, jacking thrust loads, and cutterhead torque were also measured during the drives. The results of these tests will be used together with other information to develop guidelines for conducting feasibility studies and selecting proper methods compatible with anticipated ground conditions and project requirements. Preliminary guidance for microtunneling and pipe jacking projects, including the effects of overcut and lubrication on jacking loads and ground deformations, is offered on the basis of test results and related studies.

The microtunneling test program is one of three main elements of the research project "Trenchless Construction: Evaluation of Methods and Materials To Install and Rehabilitate Underground Utilities." The other elements of this project include an evaluation and demonstration of horizontal directional drilling technology and pipeline rehabilitation systems. These elements of the research program have been described elsewhere (*1–4*). The research is a U.S. Army Corps of Engineers and industry cost-shared project funded under the Construction Productivity Advancement Research (CPAR) program. The laboratory partner is the U.S. Army Engineer Waterways Experiment Station (WES) Geotechnical Laboratory. The industry partner is Louisiana Tech University's Trenchless Technology Center. Industry participants are contributing more than half the total cost of this research. The objective of the CPAR program is to improve productivity in the U.S. construction industry.

The process of microtunneling is well understood in the United States and especially in Japan and Europe, where it originated and was refined and developed. However, the factors that govern successful performance or that can lead to catastrophe on microtunneling projects are not as clearly understood. This situation is especially critical in the United States, where this technology is just beginning to emerge. It is true that more than 83 km (50 mi) of microtunneling have been driven in the United States and there have been many successful projects. However, most of this experience has been gained in one metropolitan area in the southern United States, within a relatively narrow range of ground conditions. Microtunneling practice has evolved in this area to be a highly successful alternative to open trench construction when experienced, knowledgeable contractors, engineers, and owners are involved. As this technology spreads to other regions of the United States, some with very different ground conditions and design constraints, it is unclear how much of this experience can be directly transferred. The microtunneling research was intended to help bridge these knowledge and experience gaps.

The construction of the microtunneling test bed and the chronology of events during the tests of both the auger and slurry machines have been described in detail elsewhere (*5*) and are only summarized here. In this paper, the results of these tests and some of the implications for microtunneling are described. The final product of this element of the research program will be a set of guidelines based on the results of these tests, project case studies, and other information that owners and engineers can use to evaluate and select trenchless methods appropriate to project requirements and site conditions. Specific objectives of the microtunneling tests included the following:

- Development of reliable methods for predicting jacking loads for various ground conditions,
- Development of methods for predicting and controlling ground deformations associated with microtunneling, and
- Verification of alignment and grade control capabilities.

DEFINITION OF MICROTUNNELING

There is no universally accepted definition of microtunneling, but it can be described as a remotely controlled, guided, pipe-jacking process. The guidance system usually consists of a laser mounted in the jacking pit as a reference with a target mounted inside the microtunneling machine's articulated steering head. The microtunneling process does not require personnel entry. Since the same type of system can be used to install almost any size pipe from 250 mm (10 in.) to 3 m (10 ft) in diameter, no arbitrary size constraint should be placed on the definition. The process can be successfully used under a variety of ground conditions ranging from soft soils to rock, including mixed-face conditions and boulders, both above and below the water table.

D. Bennett, USAE Waterways Experiment Station, 3909 Halls Ferry Road, Vicksburg, Miss. 39180–6199. E. J. Cording, Department of Civil Engineering, University of Illinois, 1106 Newmark Laboratory, 208 N. Romine Street, Urbana, Ill. 61801. T. Iseley, Trenchless Technology Center, Louisiana Tech University, P.O. Box 10348, Ruston, La. 71272-0046.

DESIGN AND CONSTRUCTION OF TEST BED

The design objectives for the experiment and test bed were to

1. Provide realistic but challenging ground conditions to test the limits of microtunneling capabilities (ground conditions were intended to be increasingly challenging from the drive pit to the end of the test bed);
2. Provide ground conditions that varied in a controlled fashion and minimized boundary effects so performance could be correlated with known ground conditions;
3. Allow measurements to be made for evaluation of machine-ground interaction, including cutterhead torque, jacking thrust, effects of lubricants on pipe loads, stresses, and strains, and ground settlement and heave; and
4. Allow evaluation of two types of microtunneling systems (auger and slurry systems) under the same ground conditions.

The microtunneling demonstrations and evaluations were performed during September and October 1992 at a specially constructed test facility built at WES in Vicksburg, Mississippi. Figures 1 and 2 show an end view and a profile view, respectively, of the test facility, which was constructed by first excavating a trench 104 m (340 ft) long, 5 m (16 ft) wide, and 3 to 4 m (10 to 13 ft) deep into which six types of soils were placed and compacted in sections approximately 18 m (60 ft) long. The various backfill materials were placed and compacted in thin lifts, and moisture and density tests were performed on all materials in each lift to ensure uniformity. The soil profiles included a lean silty clay (loess), a dry sand, highly plastic buckshot clay, wet sand, clay gravel, and silt. Select backfill properties are summarized in Table 1. As shown in Figure 2, the interfaces between soil profiles were sloped to simulate mixed-face conditions as the machines exited one zone and entered another and provided challenges to ground control and alignment and grade control during these transitions. Horizontal inclinometers and one level of settlement plates were installed 0.6 m (2 ft) above the crown of the centerline of each tunnel. A second level of settlement plates was installed 1.2 m (4 ft) above the crown. Additional backfill was then placed to provide a berm 1.2 m (4 ft) high over original ground level so that at least 2.4 m (8 ft) overburden was provided over the tunnels, for proper operation of the slurry microtunneling machine. A third level of settlement rods was then installed with the anchors approximately 15 cm (6 in.) from each planned tunnel springline. Figure 1 is an end view of the test bed showing the relative locations of all instrumentation. The settlement plates and rods and the horizontal inclinometers, together with surface survey points, provided data to evaluate settlement and heave along the test section. Penetration resistance was measured in each section of the completed test bed, and these values are summarized in Table 1. Strain gauges were installed in eight of the 600-mm (24-in.) ID Hobas jacking pipes to measure strains along the tunnel length and around the pipe circumference. Jacking loads generated in the drive pit are resisted by soil shear stresses along the pipe string and soil pressure against the face of the microtunneling machine. Consequently, the thrust at the face of the machine is only a fraction of the force generated by the jacks in the drive pit. The strain gauges were installed in the first two pipes that were to be installed behind the steering head for each tunnel, in a third pipe to be installed at approximately the midpoint of each drive, and in a fourth pipe to be installed near the end of each drive. This arrangement was intended to provide continuous strain data on a given pipe as it was pushed from the drive pit and to provide measurements of strain at key points between the drive pit and steering head. These data would allow evaluation of the pipe stresses and loads along the length of the tunnel and evaluation of the resistive soil shear stresses in the different soil profiles. In addition, the strain gauges were installed at three locations 120 degrees apart inside each of the instrumented pipes. This arrangement provided information about eccentric loads applied to the jacking pipe or those that might develop because of steering corrections. The multiple gauge locations also provided a measure of redundancy in case of failure of one or more gauges. This scheme was followed for both tunnel drives.

The gauges were installed in a full bridge circuit at each location using two active gauges to measure axial strains. The two gauges positioned to measure hoop strains in the bridge were mounted on "dummy blocks" isolated from the pipe with a bonding material that would not transmit strains to these gauges. This arrangement allowed net axial strains to be measured and accounted for temperature and cable length effects. The arrangement worked remarkably well, and excellent quality strain data were

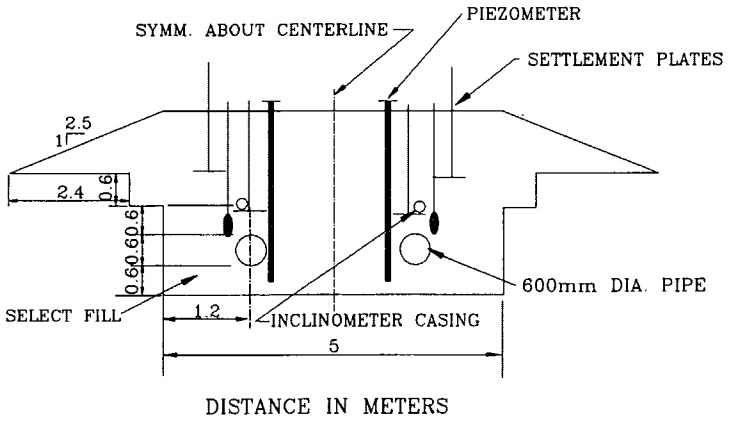

FIGURE 1 End view of test bed showing location of microtunnels and instrumentation.

obtained during both tunnel drives. Only 1 of the 24 gauge installations was destroyed during the microtunneling tests. Strain data were recorded continuously during each tunneling operation using a computer data acquisition system. Zero and check readings were made with a Vishay strain indicator.

MICROTUNNELING TESTS AND RESULTS

Auger Microtunneling Test

The auger microtunneling tests were conducted using a Soltau RVS 250A machine, furnished by American Microtunneling, South Daytona Beach, Florida, with an outer diameter of approximately 670 mm (26.3 in.) resulting in an overcut of 13 mm (0.5 in.) on the diameter. The reader is referred to the manufacturer's specifications for a full description of this machine. The control panel was set up adjacent to the drive shaft and fitted with a computerized data acquisition system to monitor and record machine performance parameters, including position of the steering head, torque, thrust, and steering jack pressures. This data acquisition system was set up to record data at 3-min intervals, keyed to time, date, and distance. The jacking frame was fitted with jacks of capacity 2225 kN (250 metric tonnes). The jacking pipe used was 3.05 m (10 ft) long, 600 mm (24 in.) inside diameter by 655 mm (25.8 in.) outside diameter standard Hobas GRP, rated at 1025-kN (115-U.S. ton) design load with a factor of safety of 2.5. Four of the jacking pipes were strain-gauged as discussed previously. Strain data were recorded continuously during the jacking operation. A separate computer data acquisition system read all strains 60 times per minute, and the average of the peak strains over that minute for each channel was recorded. This setup was intended to correlate peak jacking thrusts with strains while avoiding extraneous data from unloading cycles with the jacking system.

A plywood spacer ring was placed between the pushing plate and the pipe to distribute loads more evenly and minimize point loads. Plywood spacer rings were also placed between each pipe as the job progressed.

During the auger microtunneling trials, approximately 95 m (312 ft) of tunneling was performed over 12 days, which includes 11 days of tunnel boring, for an average of 8.5 m (28 ft) per day. Mobilization and installation required 6 working days. Demobilization and site cleanup required 3 working days. These production rates were affected by the research nature of this project and may not be typical of commercial projects.

Slurry Microtunneling Test

The slurry microtunneling tests were conducted using an Iseki Unclemole Z TCZ furnished by Iseki, Inc., San Diego, California, with an outer diameter of 660 mm (26.0 in.), resulting in an overcut of only 5 mm (0.2 in.) on the diameter. The reader is referred to manufacturer's specifications for a complete description of this machine. The control panel was set up adjacent to the drive shaft. Machine performance data were displayed on gauges on the control panel and recorded manually as each pipe was pushed. Recorded data included penetration rate, torque, thrust, slurry flow rates, and position of the steering head. The jacking frame was fitted with three stage Molemeister jacks of 1430 kN (150 metric tonnes) capacity. The jacking pipe was 2.44 m (8 ft) long, 600 mm (24 in.) inside diameter by 655 mm (25.8 in.) outside diameter standard Hobas GRP, rated at 1025 kN (115 U.S. tons) design load. Four of the pipes had strain gauges installed as described previously. As with the auger machine test, strain data were recorded continuously during the jacking operation.

During the slurry machine test, approximately 66 m (216 ft) of tunneling was performed over 21 days, including 17 days of actual tunneling, for an average of 4 m (13 ft) per day. Mobilization and installation required 6 working days, whereas demobilization and site cleanup required 4 working days. Again, these production rates may not be typical of commercial projects because of the research aspects involved.

TEST RESULTS

Alignment and Grade Control

The computerized data acquisition system used with the auger machine recorded and plotted the position of the steering head in

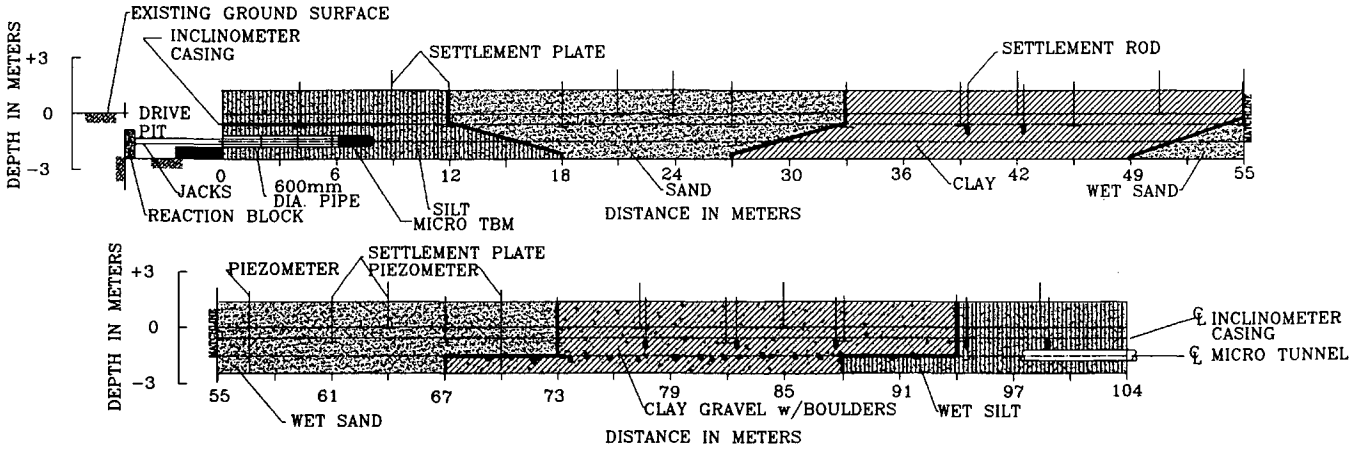

FIGURE 2 Profile along test bed showing location of microtunnels, instrumentation, and various zones of select backfill.

relation to the position of the laser at 3-min intervals during the drive. These measurements indicated that maximum horizontal and vertical deviations were less than 32 mm (1.25 in.). In fact, deviations were typically less than 12 mm ($^1/_2$ in.). The position of the steering head was surveyed at the end of the test and was within 12 mm ($^1/_2$ in.) of its intended location, both vertically and horizontally.

The slurry machine deviations from the laser beam to the actual position of the steering head were monitored continuously by closed circuit television. The positions were recorded manually at least twice as each pipe was jacked. The deviations from planned line and grade were less than 25 mm (1 in.) in all cases and typically less than 12 mm ($^1/_2$ in.). The position of the steering head, when excavated, was within 12 mm ($^1/_2$ in.) of its intended position, both vertically and horizontally.

Ground Movements

Ground movements were measured after each pipe was pushed during both the auger and slurry tunneling machine tests, using the settlement plates at three levels, the horizontal inclinometers 0.6 m (2 ft) above the crown of each tunnel, and surface survey points.

For the slurry machine test, measured ground movements were less than 6 mm ($^1/_4$ in.) throughout the 66-m (216-ft) drive, as measured at all levels, and were typically within the level of measurement precision. These insignificant ground movements were due in part to the very small overcut but primarily to the careful control of slurry face pressures to balance the earth pressure. For the auger machine test, ground heaves of 12 to 38 mm ($^1/_2$ to $1\ ^1/_2$ in.) or more were measured at a few locations, and large settlements were observed in the flooded sand section as shown in Figure 3. The large settlements measured in the flooded sand (approximately 200 mm at Station 0+55 and approx. 145 mm at Station 0+70) during the auger machine tests were due primarily to outside events. The large settlement at Station 0+55 was due to a $1^1/_2$-hr storm shutdown and high groundwater levels, which resulted in sand being carried into the face of the machine with uncontrolled inflowing water. This event could have been prevented by sealing off the auger casing in the jacking shaft, which is normal practice, to prevent water and sand from flowing through the auger casing, or by use of compressed air at the face to dry the soil and stabilize the wedge of sand between the face of the shield and the cutter disk. After this event, compressed air was used and satisfactory ground control was maintained. At Station 0+70 the compressor failed momentarily, and another large settlement occurred, approximately 0.6 m (2 ft) from a piezometer that had been installed the previous day by jetting the tip down to tunnel level. This installation practice created a loose saturated pocket of sand adjacent to the planned pipe location and was a major contributing factor in the subsequent ground movement.

The large apparent heave shown near Station 0+55 in Figure 3 is believed to be an upward buckling of the inclinometer casing and is not an actual ground heave. No surface heave was observed at this location. The smaller ground heaves observed may have been partly caused by pushing the machine too hard and too fast (i.e., the face pressure exceeded the passive earth pressure). However, shearing dilation of the dense sand and swelling in the buckshot clay may have contributed to the measured heaves.

In general, slurry microtunneling machines are capable of more precise ground control because of the ability to balance earth pressures with slurry face pressures. However, with proper auger machine setup and operation based on the manufacturer's recommendations, a skilled operator can usually maintain satisfactory ground control. The auger machine has recognized limitations with regard to ground control, especially if high groundwater levels and wet flowing sands or silts are encountered. When difficult ground conditions are expected, advice should be sought from machine manufacturers or other competent, experienced persons.

TABLE 1 Select Backfill Properties

Test Bed Section	USCS Soil Classification	Max. Density (kN/m^3)	Optimum Moisture Content (w%)	Liquid Limit (LL)	Plastic Limit (PL)	Plasticity Index (PI)	Standard Penetration Test Blow Counts (N)	Other Test Data and Comments
1	Silty Clay (CL)	17	19.1	39	25	14		
2	Sand, medium to fine, poorly graded (SP)	18 16	-	-	-	-	54 to 58	
3	Plastic Clay (CH)	15	23.2	66	22	44	7 to 15	UC = 141 to 154 kN/m^2 Su_{vane} = 60 to 73 kN/m^2 Swell Press. = 48 to 96 kN/m^2 Swell Volume = 7.9%
4	Sand, poorly graded (SP)	(<----------same as Section 2----------->)						
5	Gravelly Clayey Sand (SC)	20	9.2	20	12	8	28 to 56	Presence of gravel makes interpretation of SPT values problematic
6	Clayey Silt (ML)	(<-----essentially same soil as Section 1------>)					9 to 17	

Jacking Loads and Pipe Performance

As mentioned, strains were continuously monitored at three locations in four pipes for each microtunneling machine test. The strain-gauged pipes included the first and second pipes behind the steering head, a third pipe near the middle of the drive, and the fourth pipe near the end of the drive. Excellent quality data were obtained to determine soil resistance at the face of the machine and along the sides of the pipe in each type of soil. A typical strain data plot is shown in Figure 4, with strain in microns measured in Pipe 23 plotted against time in minutes required to push Pipe 23 during the slurry machine tests. For both the auger and slurry machine tests, the strain measurements indicated that the jacking loads on the pipe were eccentric at the point of application in the jacking pit and elsewhere along the pipe string, especially in the first pipe behind the steering head. At this location, measured strains varied widely as steering corrections were made. The effects of steering corrections were also evident in the second pipe behind the steering head, though to a lesser extent. Misalignment between the pipe string and the jacking plate and flexibility in the jacking system contributed to the eccentric strains measured in the jacking pit. These strain data are being used with additional data to improve methods for estimating jacking loads under various ground conditions for the different types of machines evaluated and for the machine setup and operating practices.

Jacking loads of more than 1070 kN (120 U.S. tons) were measured toward the end of the 95-m (312-ft) drive with the auger machine. The overcut was 6 mm ($^1/_4$ in.) on the radius, and no bentonite or other lubrication was used. These factors contributed to the relatively high jacking loads, though these loads were not considered abnormally high for the ground conditions by the machine manufacturer or operator.

The jacking loads exceeded 1160 kN (130 U.S. tons) toward the end of the 66-m (216-ft) drive with the slurry machine. The overcut was only 2.5 mm (0.1 in.) on the radius, and bentonite was used intermittently. These factors undoubtedly contributed to the high jacking loads, but time was also an important factor on both drives, especially with regard to the buckshot clay, which exhibited swelling tendencies. Heavy rainfalls during both tests may have also contributed to the high jacking loads by causing the density of the sands to increase further.

Predicted and actual jacking loads for both the auger and slurry machine tests are shown in Figure 5. The actual and predicted loads generally show good agreement. The largest discrepancies occurred in the transition or mixed-face zones between soil sections, which emphasizes the difficulty in reliably estimating shear stresses in mixed ground.

The jacking loads measured with the slurry machine were higher than with the auger machine throughout every soil section. This result was partly caused by the use of the much smaller overcut and may be partly due to the difference in operating principle of the slurry machine, especially in clay, where the soil must be mixed with slurry and squeezed through the cutterhead openings. The slurry machine test also required more time than the auger machine test. A complicating factor in this comparison is that no lubricant was used during the auger machine test, whereas bentonite lubricant was used intermittently during the slurry machine tests.

The high jacking loads and eccentric pipe stresses resulted in the pipe capacity being exceeded on four occasions during the

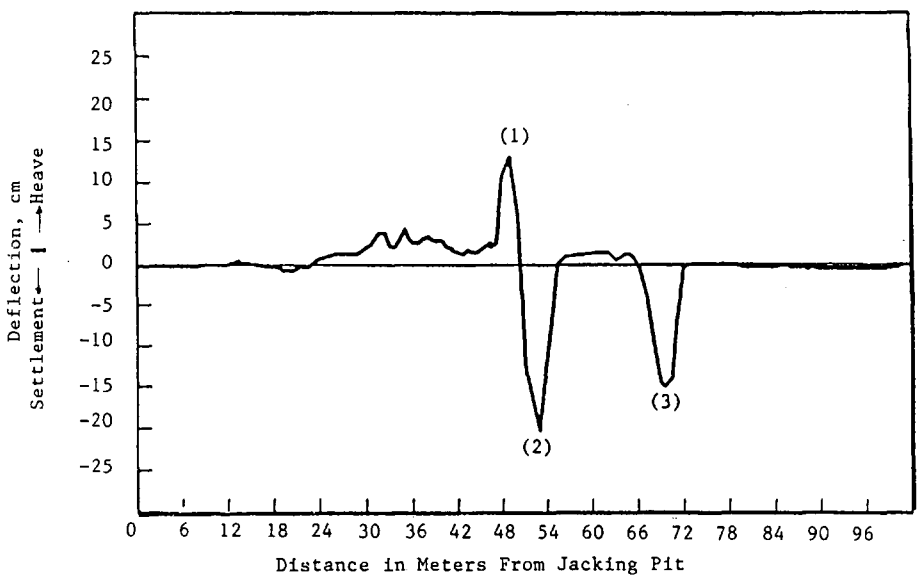

Notes: (1) Large apparent heave most likely upward buckling of inclinometer casing related to large adjacent settlement.
(2) Large settlement occurred after 1-1/2 hr. storm shutdown. Water carried sand into face & through auger casing. Used compressed air after this event for ground control in flooded sand.
(3) Large settlement occurred adjacent to piezometer jetted into place when air compressor momentarily quit. See text for further explanation of these events.

FIGURE 3 Vertical deflections of inclinometer casing 0.6 m above tunnel crown measured during auger microtunneling machine tests.

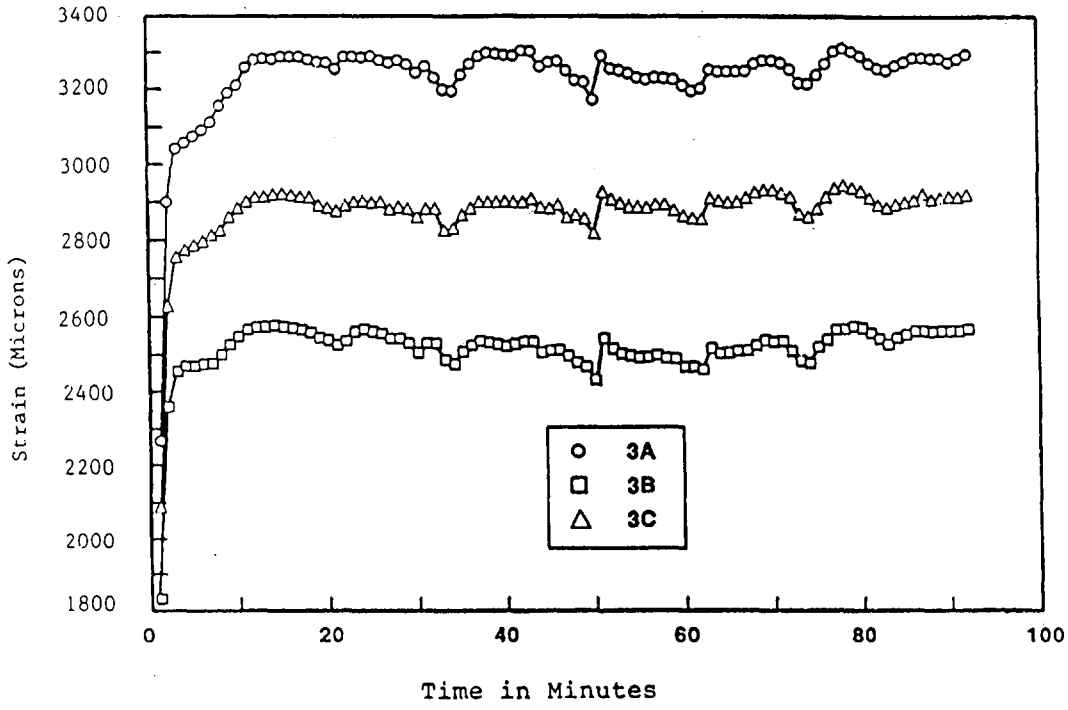

FIGURE 4 Strains in Pipe 23 versus time required to push Pipe 23 during slurry machine tests. Gauge locations A, B, and C correspond to 12, 8, and 4 o'clock, respectively.

auger machine tests and on eight occasions during the slurry machine tests.

Specimens were obtained from unfailed portions of the damaged pipe sections and tested in uniaxial compression to failure. Unconfined compressive strengths from three tests ranged from 9,220 to 10,100 psi. The average pipe stresses at failure during the field tests were 3,850 to 4,500 psi during the auger machine tests and 3,495 to 4,765 psi during the slurry machine tests.

The measured jacking loads, if distributed more uniformly, would not have caused pipe stresses high enough to result in pipe failure. However, because of the eccentric nature of the applied loads, as well as bending stresses and point loads that resulted

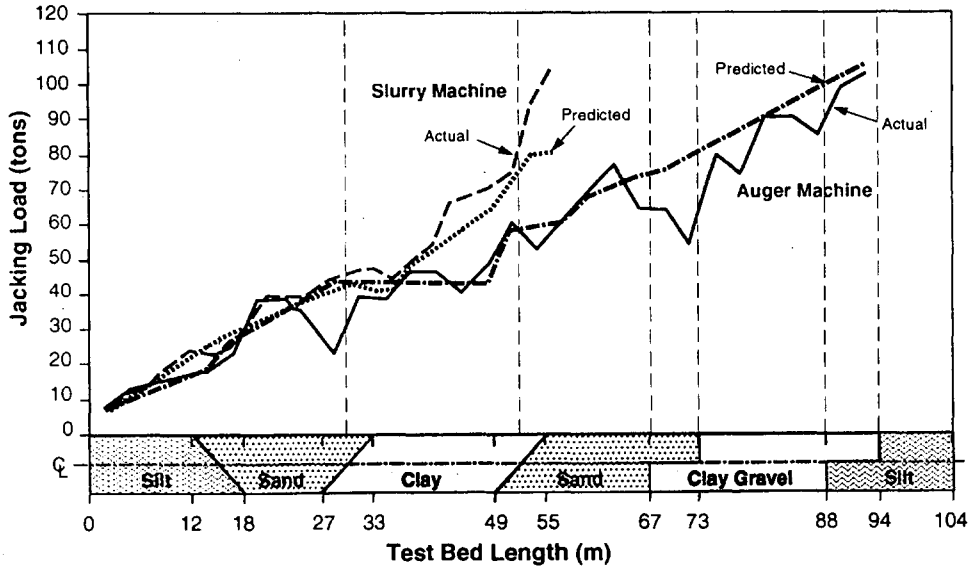

FIGURE 5 Actual and predicted jacking loads for auger and slurry microtunneling tests at WES.

from steering corrections and initial misalignment, the actual pipe stresses exceeded ultimate pipe capacity. The pipe was not defective, but a higher load capacity pipe should have been specified.

CONCLUSIONS AND RECOMMENDATIONS

The microtunneling tests provided a unique opportunity for an impartial documentation of performance of both auger and slurry systems in ground conditions that varied in a controlled manner, to provide increasing challenges from the beginning to the end of the test bed. Properties of the various soil profiles in the test bed were well documented, and the experiment was designed to allow correlations to be developed between the known ground conditions and machine performance. Even though some problems were encountered in the execution of the tests (*5*), a great deal was learned. Extensive measurements and observations were recorded and will form the basis for developing these correlations and predictive methods. Credible case history data will be sought to complement and verify these observations and correlations. Research and reliable case history data from Japan and Europe can provide valuable insights, and this information will be used to complement U.S. experience and these tests.

The results of the field evaluations underscore the need for better understanding of the interrelationships among machine characteristics, setup and operation, and the jacking loads and ground deformations that can be expected for given ground conditions. Some insights developed from the tests and complemented by review of other projects and conversations with microtunneling experts are given in this section.

It is unrealistic to assume that jacking loads are ever uniformly distributed around the pipe circumference and end-bearing area. Eccentric loads should be considered the norm, not the exception. All reasonable measures should be taken to keep maximum jacking loads within allowable levels and to minimize the eccentricity of the loads and resultant pipe stresses. These measures should include the following:

1. Ensure that pipes are straight and uniformly dimensioned, ends are square, and joints are designed to allow efficient load transfer from pipe to pipe.
2. Use a pipe joint spacer or packer that is highly compressible to aid in distributing axial stresses uniformly. The packer material should have uniform dimensions and should have a low Poisson ratio [i.e., the ratio of lateral (radial) to longitudinal (axial) strain] to minimize the development of tensile radial stresses at the joints. Research carried out at the University of Oxford (*6–8*) has shown the importance of selecting proper packer materials to reduce eccentric loads.
3. Ensure that the jacking frame, jacks, and steering head are correctly aligned along the planned line and grade and that the thrust block is square and true. The jacking frame must be robust to minimize flexibility under load, and the frame must be adequately supported so that it does not settle or shift during the jacking operations. The steering head and pipe must be supported in the jacking pit so that initial misalignment and settlement are minimal.
4. Make steering corrections gradually to minimize abrupt misalignment angles between adjacent pipes and resultant eccentric stresses. The University of Oxford research (*6–8*) and these tests have clearly established the adverse impact on pipe capacity of misalignment between adjacent pipes and resulting stress concentrations.
5. Provide adequate overcut space around the pipe to allow steering corrections to be made and to allow lubricant, when used, to more completely coat the pipe exterior. This measure also reduces the maximum expected jacking loads.

The amount of overcut between the cutterhead shield outside diameter and the pipe outside diameter can have an enormous influence on jacking loads, especially in relatively stable soils such as stiff clays. A smaller but still significant influence can be seen in dense sands. These soils, if given enough overcut space, dilate as the shield passes through the soil, reducing density and shear resistance along the trailing pipe string. This behavior is analogous to the behavior observed during direct shear tests on initially loose and initially dense sands. At constant normal loads, loose sands show a volume decrease during shear. Dense sands tend to dilate (i.e., show a volume increase) during shear under constant normal loads. If there is no annular space for this dilation to occur, normal loads increase and the shear resistance increases. The sand grains may be sheared through, which requires more jacking (shear) load than if the grains have sufficient space to dilate and roll over each other.

In addition, the beneficial effects of lubricants are enhanced with the use of a larger overcut because the lubricant more completely surrounds the pipe and promotes a stable opening, reducing frictional stresses along the pipe string. With a small overcut the lubricant cannot as easily coat the circumferential area of the pipe string and more mixing with the host soil occurs, as verified by excavations performed after the field tests. These excavations showed that there was no continuous annular ring of lubricant surrounding the pipe in any of the test bed soils. In some locations the soil to pipe interface was dry. In others (e.g., sands) the lubricant had migrated and mixed with the soil. These observations may also indicate the need for more than one lubricant injection point on the circumference of the tail shield portion of the steering head.

Typically, overcut ranges from approximately 6 to 12 mm ($^1/_4$ to $^1/_2$ in.) on the radius for pipes of diameter 750 mm (30 in.) or less. The concern usually expressed with using a large overcut [say 25 mm (1 in.) on the radius] has been that surface settlements may be unacceptably large. However, analytical studies and comparisons with studies of settlements around larger-diameter soft ground tunnels (*9–13*) suggest that large settlements should not be an undue concern for any reasonable amount of overcut as long as ground conditions are well defined, sound operating principles are followed, and the machine is set up properly. This is especially true for deeper installations and smaller-diameter pipes. The general relationships among surface settlement, pipe diameter, and depth are shown in Figure 6, which is intended to show general trends only. Actual settlements would depend on ground conditions, stabilization measures, and other factors. Indeed, catastrophic settlements almost always can be traced to improper machine setup or operation or unexpected ground conditions coupled with the inability to quickly implement corrective actions, rather than to amount of overcut.

A problem experienced in the slurry machine tests that may have occurred as a result of using a very small overcut is that some of the coupling bells or sleeves that seal adjoining pipes were damaged or destroyed, compromising the watertightness of the installation. This problem may be minimized by ensuring that

pipe sleeves are flush (i.e., no protrusions exist) and through the use of a more robust sleeve design. At the very least, if the contractor plans to use a small overcut [less than 6 mm ($^1/_4$ in.) on the radius], the pipe manufacturer or supplier should be made aware of this intent, because more care may be required in installing the sleeves to avoid protrusions and a more robust pipe or coupling may be required. This problem was not observed with the auger machine that used a 6-mm ($^1/_4$-in.) overcut on the radius.

Finally, steering corrections can be more easily accomplished when a reasonable amount of overcut or annular space is allowed for articulating the steering head, especially in hard ground or rock.

In the light of these observations, an overcut of less than 12 mm ($^1/_2$ in.) on the radius is not generally recommended. However, the selection of proper overcut should take into consideration pipe diameter, straightness and roundness, manufacturing tolerances on these characteristics, the design jacking load capacity, depth and length of the installation, ground conditions, and allowable ground movements as well as machine characteristics and steering requirements. For example, larger overcut is usually required for hard ground or rock for proper steering. Larger overcuts are also required for larger-diameter pipe.

The use of pipe lubricants is generally recommended. The lubricants should be injected continuously from the very beginning of the job. If use of lubricants is delayed until jacking loads have escalated to dangerous levels, it is usually too late to obtain any meaningful benefit. The inconvenience of this additional operation is offset in most cases by the reduction in jacking loads and reduction of risk of damage to the installed pipe string.

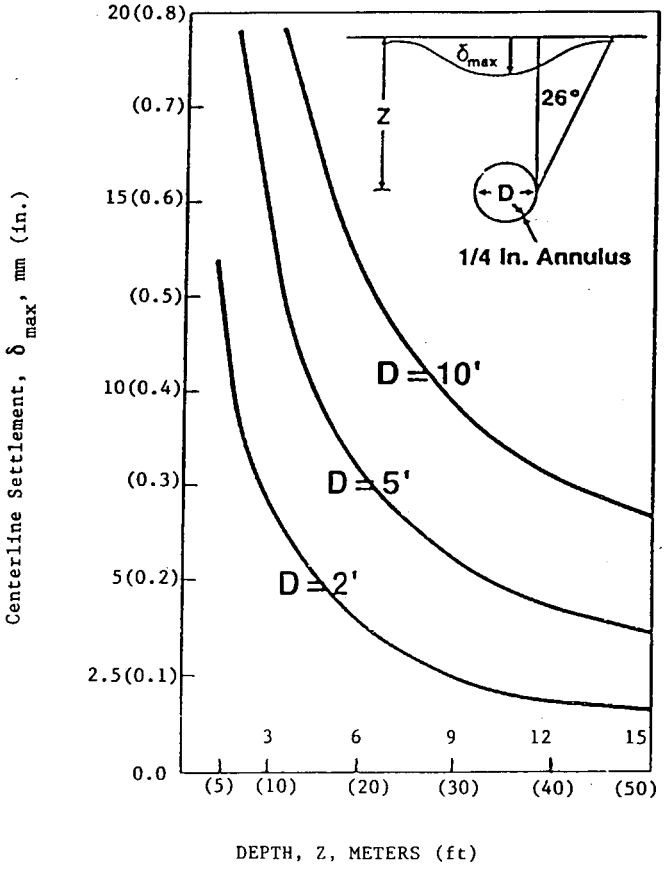

FIGURE 6 Estimated settlement versus depth for various diameter tunnels. Figure shows only general trends. Actual settlements would depend on ground conditions, stabilization measures, and other factors.

ACKNOWLEDGMENTS

The work reported herein resulted from research conducted under the CPAR research program by the U.S. Army Corps of Engineers Waterways Experiment Station and Louisiana Tech University. Permission was granted by the chief of engineers to publish this information.

The authors express their appreciation to the industry participants for their support of this research, particularly Hobas Pipes, USA, Inc., Houston, Texas; Iseki, Inc., San Diego, California; Soltau Microtunneling, Charleston, South Carolina; and American Microtunneling, South Daytona Beach, Florida. These companies and their principals are commended for their participation in these impartial tests. It is through the efforts of individuals and groups such as these that real progress can be achieved in this exciting technology.

REFERENCES

1. Iseley, D. T., M. Najafi, and R. D. Bennett. Trenchless Construction: Evaluation of Methods and Materials To Install and Rehabilitate Underground Utilities. *Proc., International NO-DIG '92*, Washington, D.C., 1992, pp. D1–D17.
2. Iseley, T., M. Najafi, and D. Bennett. Small Drilled Crossings: Mini-HDD Method; Overview and Case Study. *Pipeline Digest*, Aug. 1993.
3. Guice, L. K., and C. Norris. Description of the CPAR Field Testing: Long-Term Hydrostatic Pressure Testing of Liner Materials. *Proc., Trenchless Technology: An Advanced Technical Seminar*, Vicksburg, Miss., Jan. 1993, pp. 69–84.
4. Najafi, M., D. T. Iseley, and D. Bennett. Corps, Industry Evaluate Trenchless Construction Methods. *The National Utility Contractor*, Vol. 16, No. 3, March 1992.
5. Bennett, D., and P. A. Taylor. Construction of Microtunneling Test Facility at WES and Preliminary Test Results. *Proc., Trenchless Technology: An Advanced Technical Seminar*, Vicksburg, Miss., Jan. 1993.
6. Ripley, K. J. *The Performance of Jacked Pipes.* Ph.D. dissertation. University of Oxford, United Kingdom, 1989.
7. Norris, P. *The Behaviour of Jacked Concrete Pipes During Site Installation.* Ph.D. dissertation. University of Oxford, United Kingdom, 1992.
8. Milligan, G. Pipejacking Research. *World Tunneling and Subsurface Excavation*, Oct. 1993, pp. 343–346.
9. Peck, R. B. Deep Excavations and Tunneling in Soft Ground. State of the Art Report. *Proc., 7th International Conference on Soil Mechanics*, Mexico City, 1969, pp. 225–290.
10. Peck, R. B., A. J. Hendron, Jr., and B. Mohraz. State of the Art of Soft Ground Tunneling. *Proc., 1st North American Rapid Excavation and Tunneling Conference*, AIME, 1972, Vol. 1, pp. 259–286.
11. Hansmire, W. H., and E. J. Cording. Performance of a Soft Ground Tunnel on the Washington Metro. *Proc., 1st North American Rapid Excavation and Tunneling Conference*, AIME, 1972, Vol. 2, pp. 371–389.
12. Cording, E. J., and W. H. Hansmire. Displacements Around Soft Ground Tunnels. *Proc., 5th Pan American Congress on Soil Mechanics and Foundation Engineering*, Buenos Aires, Argentina, 1975.
13. Hansmire, W. H., and E. J. Cording. Soil Tunnel Test Section: Case History Summary. *Journal of Geotechnical Engineering*, ASCE, Vol. 111, No. 11, Nov. 1985.

Publication of this paper sponsored by Committee on Subsurface Soil-Structure Interaction.